Stability analysis of transmission systems with high penetration of distributed generation

PROEFSCHRIFT

ter verkrijging van de graad van doctor
aan de Technische Universiteit Delft,
op gezag van de Rector Magnificus prof.dr.ir. J.T. Fokkema,
voorzitter van het College voor Promoties, in het openbaar te verdedigen op
donderdag 21 december 2006 om 10:00 uur

door

Muhamad REZA
elektrotechnisch ingenieur

geboren te Bandung, Indonesië.

Dit proefschrift is goedgekeurd door de promotoren:
Prof.ir. W. L. Kling
Prof.ir. L. van der Sluis

Samenstelling promotiecommissie:

Rector Magnificus,	voorzitter
Prof.ir. W. L. Kling,	Technische Universiteit Delft, promotor
Prof.ir. L. van der Sluis,	Technische Universiteit Delft, promotor
Prof.dr. J. A. Ferreira	Technische Universiteit Delft
Prof.dr.ir. J. H. Blom	Technische Universiteit Eindhoven
Prof.ir. M. Antal	Technische Universiteit Eindhoven (emeritus)
Prof.dr.ir R. Belmans	Katholieke Universiteit Leuven, België
Prof.dr. M. J. O'Malley	University College Dublin, Ierland

This research has been performed within the framework of the research program 'Intelligent Power Systems' that is supported financially by SenterNovem, an agency of the Dutch Ministry of Economic Affairs.

Stability analysis of transmission systems with high penetration of distributed generation.
Dissertation at Delft University of Technology.

ISBN: 91-628-7039-4

Cover: A miniature of transmission lines tower in Madurodam, The Hague, photographed and modified by Muhamad Reza, and used for this thesis with permission from Madurodam B.V.

To Bapak, Ibu, Novi and Rifqi.

Summary

Stability analysis of transmission systems with high penetration of distributed generation

Nowadays, interest in generating electricity using decentralized generators of relatively small scale is increasing. Such generation is known as 'distributed generation' (DG). Many of the prime movers of such DG technologies are based on renewable energy sources resulting in an environmentally-friendly power generation.

It is well-known that the implementation of DG influences the technical aspects of the distribution grids. The impact of a small amount of DG connected to the grid on the power system transient stability has not been treated so often. When the penetration level of DG increases, its impact is no longer restricted to the distribution network but begins to influence the whole system.

This work deals with the impact of implementing DG on the transmission system transient stability, with the emphasis on a potential transition from a 'vertical power system' to a 'horizontal power system' (Chapter 1).

For this purpose, it is important to examine characteristics of DG that influence the dynamic stability behavior of a transmission system (Chapter 2). Therefore, DG units are classified based on the primary (both conventional and renewable) energy sources. To a large extent, the type of primary energy source determines the output power characteristics of DG and the type of grid connection applied. It also determines the utilization of power electronic interfaces. Based on the DG classification, basic models of DG technology to be used in the transient stability simulation of a large power system can be derived, presented in Chapter 3.

A problem in power systems is maintaining synchronous operation of all (centralized) synchronous machines. The stability problem associated is called *rotor angle stability*. In this work, the impact of the DG implementation on this is investigated. Therefore, in Chapter 3, the phenomena of the rotor dynamics of synchronous machines, that determine the rotor angle stability of a power system, are explained by means of the *swing equation*, the *power-angle curve* and the *equal area criterion* concepts. Indicators for assessing the stability performance of a power system derived from these concepts are the *maximum*

rotor speed deviation and *oscillation duration* of the (centralized) synchronous machines. For simulation purposes, the widely known *39-bus New England* dynamic test system is used with minor adjustments. The basic setup of the test system is described, while details are listed in Appendices B and C. Several software packages suitable for the transient dynamic simulation of DG in a large system are highlighted. The representations of different DG technologies within the software packages are discussed, with the emphasis on the representation of *power electronic interfaced (converter connected)* DG units.

The investigation of the impact of a high DG (penetration) level on power system transient stability, is presented in Chapter 4. The impact of increasing DG penetration levels, DG grid-connection-strength, different DG technologies, and DG protection schemes of *converter-connected* DG are simulated and discussed. It is found that DG influences the system transient stability differently depending on the factors above. However, there is no significant stability problem observed up to about 30% DG penetration level regardless the technology. This is logical when all centralized generators remain in the system – as well as their active and their reactive power control and the inertia of their rotating masses – along with the increasing DG levels. Furthermore, implementing DG is a natural way of 'limiting' the power flows on the transmission lines. It improves the transient stability of a transmission system, since large power flows may have a detrimental effect on the damping of the oscillations: the heavier the lines are loaded, the weaker the coupling between generators and loads becomes, and the larger the oscillations of the centralized generators may be, especially with long lines.

In Chapter 5, the investigation is focused on the impact of DG levels on the system transient stability when the increasing DG level is followed by a reduction of centralized generators in service resulting in a 'vertical to horizontal' transformation of the power system. The emphasis is on the use of converter connected DG units to supply active power. Therefore, different from the preceding Chapter 4, the increasing DG level implies a reduction in rotating masses (inertia) and reactive power control ability in the system. In some cases, power system transient instabilities with very high DG levels (more than 50%) are found. Several solutions are proposed for these problems by means of *rescheduling centralized generators* and *optimizing the power flow*. In some cases, a minimum number of centralized generators has to remain in the system to avoid system instabilities.

The results discussed in Chapters 4 and 5 are merely based on a deterministic approach, where the parameters of the test system are set to the typical values. Beside the deterministic approach, a stochastic analysis can also be used to study the transient stability of the power systems, as presented in Chapter 6. The study is focused on the impact of the stochastic behavior of DG. The results show that including the stochastic behavior of DG leads to a more complete and detailed view of the system performance.

Finally, Chapter 7 investigates the situation when the power system is pushed towards a scenario, where DG penetration reaches a level that covers the total load of the original power system (100% DG level). The DG units are im-

plemented via power-electronic converters within so called "*active distribution systems*" (ADS) connected to the transmission system also via power-electronic interfaces. The power system is still connected to a source that provides a constant 50 Hz voltage that is meant to give a (system) frequency reference for the generators but generates no power at steady state. Therefore, any power imbalance in the system must be compensated by generators in the ADS. However, due to the power-electronic interfaces, the output power of the DG units (and the ADS) are decoupled from the grid frequency. Therefore in this chapter, the voltage is used to detect and maintain the power balance. For this purpose, specific control concepts are developed. The simulation results show that by applying such control systems, the power balance in the power system can be maintained by the ADS.

The research performed in this work indicates that from the transmission system stability point of view, if higher DG penetration levels are coming up, sufficient inertia and voltage support must be installed. Furthermore, one should be aware of the fact that the system behaves stochastically, especially with DG. To a certain extent regional balancing of power can be performed by local voltage control.

Samenvatting in het Nederlands

Stabiliteitsanalyse van een transmissienet met een hoge penetratiegraad van decentrale opwekking

Tegenwoordig neemt de interesse in het produceren van elektriciteit met relatief kleine decentrale eenheden toe. Deze manier van elektriciteitsopwekking wordt ook wel 'distributed generation' (DG) genoemd. Veel aandrijfsystemen van DG technologieën zijn gebaseerd op hernieuwbare energiebronnen wat resulteert in een milieuvriendelijke energieopwekking.

Het is bekend dat de toepassing van DG de technische aspecten van de distributienetten beïnvloedt. De invloed van kleine hoeveelheden DG aangesloten op het net, op de transiënte stabiliteit van het transportnet is nog niet vaak onderzocht. Wanneer het penetratieniveau van DG stijgt, is het effect niet meer beperkt tot het distributienet, maar wordt het gehele systeem beïnvloed.

Dit proefschrift onderzoekt de effecten van de toepassing van DG op de transiënte stabiliteit van het transmissienet, met de nadruk op een potentiële overgang van een 'verticaal gericht systeem' naar een 'horizontaal gericht systeem' (Hoofdstuk 1)

Met dit doel is het belangrijk om de kenmerken van DG te onderzoeken, die het dynamische stabiliteitsgedrag van een transmissiesysteem beïnvloeden (Hoofdstuk 2). Daarom worden DG eenheden geclassificeerd op basis van de primaire energiebronnen (zowel conventionele als hernieuwbare). Het soort primaire energiebron bepaalt in grote mate de kenmerken van de energie-output van DG en het type netaansluiting dat wordt toegepast. Ook bepaalt het of vermogenelektronische interfaces worden gebruikt. Gebaseerd op de DG classificatie kunnen basismodellen afgeleid worden voor de DG technologieën om te gebruiken in de transiënte stabiliteitssimulatie van een transmissienet, wat in Hoofdstuk 3 behandeld wordt.

Een probleem in elektriciteitsvoorzieningsystemen is het handhaven van synchrone werking van alle (centrale) synchrone machines. Het stabiliteitsprobleem dat daarmee samenhangt heet de *rotorhoek stabiliteit*. In dit proefschrift worden de effecten van de toepassing van DG daarop onderzocht. Daartoe

worden in Hoofdstuk 3, de fenomenen van de rotordynamica van een synchronische machine verklaard, die de rotorhoek stabiliteit van een transmissienet bepalen, middels de *bewegingsvergelijking*, de *vermogen versus hoek* curve en het *gelijke oppervlakte criterium* concept. De indicatoren voor het beoordelen van het stabiliteitsgedrag van een transmissienet afgeleid uit deze concepten zijn de *maximumafwijking van de rotorsnelheid* en de *duur van de slingering* van de synchrone machines. Voor simulatiedoeleinden wordt het bekende *39-knooppunten New England* dynamisch testsysteem gebruikt, met een aantal aanpassingen daarin. De basisopzet van het testsysteem wordt in dit hoofdstuk beschreven, terwijl de details worden gegeven in Bijlagen B en C. Verscheidene softwarepakketten, geschikt voor transiënte dynamische simulatie van DG in een groot transmissienet, worden behandeld. De representatie van de verscheidene DG technologieën in de softwarepakketten wordt besproken, waarbij de nadruk ligt op de weergave van DG eenheden met *vermogenelektronische interfaces (converters)*.

Het onderzoek van de invloed van een hoog (penetratie) niveau van DG op de transiënte stabiliteit van het transmissienet wordt in Hoofdstuk 4 uiteengezet. De invloed van de toename van het DG niveau, de sterkte van de DG netkoppeling, verschillende DG technologieën, en DG beveiligingsschema's van via *vermogenselektronica gekoppelde* DG, zijn gesimuleerd en bediscussieerd. Er wordt aangetoond dat DG de transiënte stabiliteit van het transmissienet verschillend beïnvloedt afhankelijk van boven vermelde factoren. Echter, er is geen significant stabiliteitsprobleem gevonden tot de DG een 30% niveau bereikt, onafhankelijk van de DG technologie. Deze resultaten zijn logisch vanwege de nog steeds aanwezige centrale generatoren in het net, met de bijbehorende regeling van actief vermogen en blindvermogen en de inertie van de roterende massa, bij dit niveau van DG. Daarnaast is toepassing van DG een natuurlijke manier om de vermogenstransporten in de transmissielijnen te beperken. Dit verbetert de transiënte stabiliteit van het transmissienet, omdat grote vermogenstransporten een nadelige invloed hebben op de demping van de rotorslingeringen: hoe zwaarder de lijnen zijn belast des te zwakker de koppeling tussen de generatoren en de belastingen wordt en des te groter de slingeringen van de centrale generatoren kunnen worden, vooral bij lange lijnen.

In Hoofdstuk 5, ligt de nadruk van het onderzoek op de invloed van het toenemende DG niveau op de transiënte stabiliteit van het net als dit samen gaat met de vermindering van in bedrijf zijnde centrale generatoren, leidend tot een 'vertikale naar horizontale' transformatie van het elektriciteitsvoorzieningsysteem. De nadruk ligt op het gebruik van de vermogenelektronisch gekoppelde DG als actief vermogen leverancier. Daardoor, anders dan Hoofdstuk 4, impliceert het toenemende DG niveau een vermindering van roterende massa (inertie) en regelmogelijkheden van blindvermorgen in het net. In sommige gevallen wordt instabiliteit van het transmissienet bij een hoog DG niveau (meer dan 50%) gevonden. Verschillende oplossingen voor dit probleem worden voorgesteld middels *verandering van de inzet van de centrale generatoren* en *optimalisering van de vermogenstransporten*. In sommige gevallen moet een minimaal aantal centrale generatoren in bedrijf gehouden worden om instabiliteit van het net te

vermijden.

De resultaten van de Hoofdstukken 4 en 5 zijn gebaseerd op een deterministische benadering, waarbij de parameters van het testsysteem ingesteld zijn op hun typische waarden. Behalve een deterministische benadering kan ook een stochastische analyse worden gebruikt om de transiënte stabiliteit te bestuderen, zoals beschreven in Hoofdstuk 6. De nadruk van de studie ligt op de invloed van het stochastische gedrag van DG. De resultaten tonen aan dat het meenemen van het stochastische gedrag van DG leidt tot een vollediger en gedetailleerder overzicht van het functioneren van het systeem.

Hoofdstuk 7 tot slot behandelt de situatie waarbij het transmissienet aan een extreem scenario onderwerpen wordt, waar DG de totale belasting van het net dekt (100% DG niveau). DG eenheden zijn via vermogenselektronische interfaces opgenomen in zogenaamde "*actieve distributie systemen*" (ADS) en aangenomen is dat deze ook met vermogenselektronische interfaces zijn gekoppeld met het transmissienet. Het systeem is verondersteld nog steeds verbonden te zijn met een bron met constante 50 Hz frequentie bedoeld als een frequentie referentie voor de generatoren, maar wekt geen vermogen op in de stationaire toestand. Daarom moet iedere onbalans in vermogen door opwekking in de ADS gecompenseerd worden. Echter, vanwege de vermogenselektronische interfaces is het uitgangsvermogen van de DG eenheden (en de ADS) ontkoppelt van de netfrequentie. Daarom wordt in dit hoofdstuk de spanning gebruikt om de vermogensbalans te detecteren en te handhaven. Voor dit doel zijn specifieke regelconcepten ontwikkeld. De simulatieresultaten tonen aan dat door toepassing van deze regeltechnieken, de handhaving van de vermogenbalans gerealiseerd kan worden via de ADS.

Het onderzoek beschreven in dit proefschrift toont aan dat vanuit oogpunt van stabiliteit van het transmissienet voldoende inertie en spanningsondersteuning aanwezig moet zijn als hogere DG penetratieniveaus aan de orde zijn. Verder moet men zich bewust zijn van het feit dat het systeem zich stochastisch gedraagt, zeker met DG. In zekere mate kan regionale balanshandhaving worden uitgevoerd met lokale spanningsregeling.

Contents

Chapter 1

Introduction

A classical power system is characterized by a relatively small number of large, so-called centralized power plants for meeting the electric energy demand. These power plants are built based on the demand estimate for a certain period of time. Some constraints, however, limit the expansion and use of such large power plants and may induce a shift towards a more extensive use of small, decentralized power generators.

It is well-known that the implementation of small, decentralized power generators brings both positive and negative consequences to the existing power system. The technical consequences must be considered carefully in order to maintain the present reliability level of the power system. Some of these negative consequences will be focused on in this work. Several remedies to eliminate them or limit their impact will be suggested and discussed.

1.1 'Vertical' Power Systems

A power system is designed to supply electrical power to the consumers. Until now, mainly large, centralized generators have been utilized for the power generation. Synchronous generators are typical electromechanical energy transducers for large power plants, often close to cooling water, energy resources or supply routes and connected to the transmission system. If hydropower is available it may be used as input too.

So, a *classical* power system consists of three technical stages, namely: generation, transmission, and distribution. The generation system converts mechanical power that results from the conversion of primary energy sources, such as nuclear, hydro power, coal, gas, etc., into electrical. The transmission system transports the electrical power over a long distance to the load centers. The distribution system distributes the electrical power to the consumers/loads. This classical power system can be best illustrated by considering the different voltage levels (Figure 1.1).

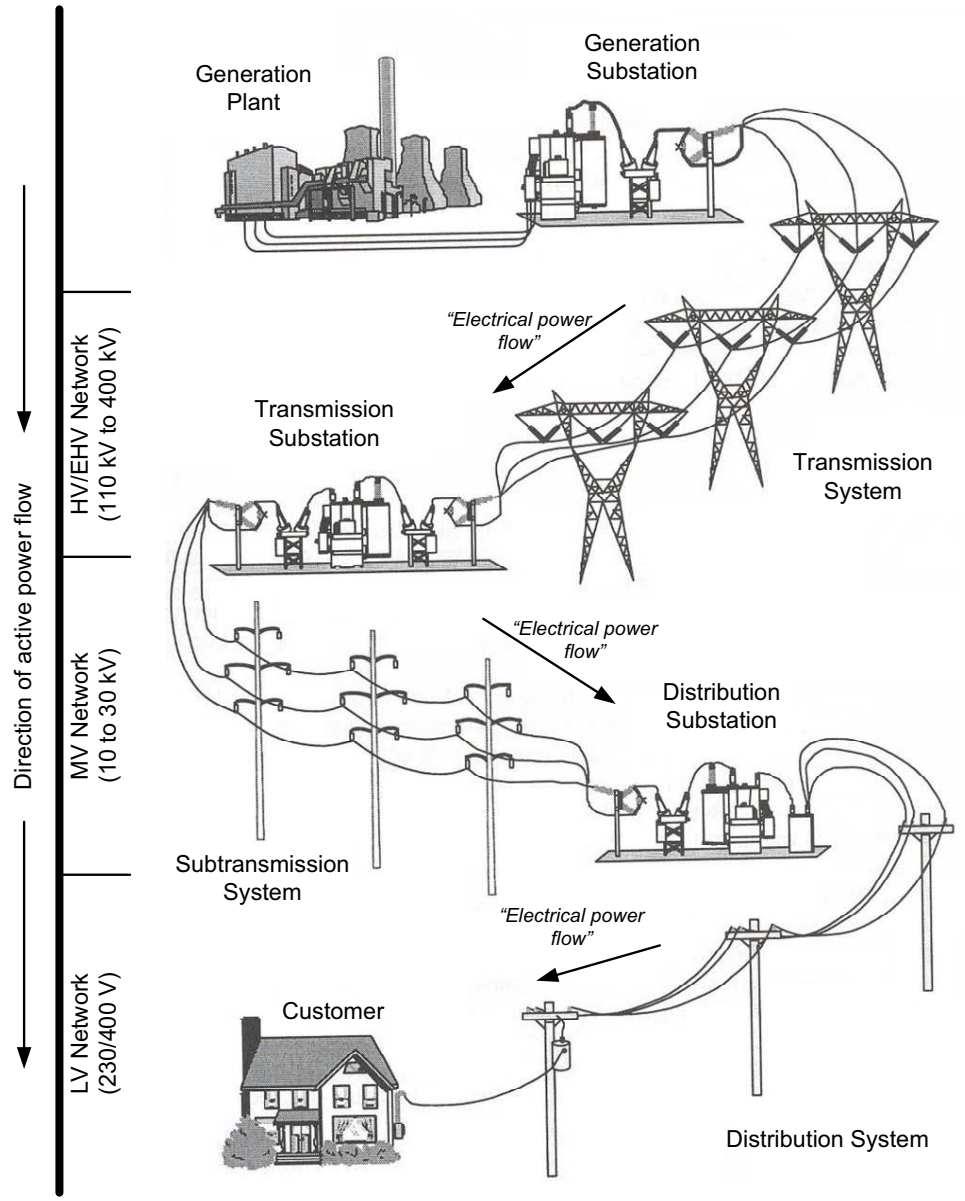

Figure 1.1: Vertically-Operated Power System (modified from [8])

After being generated at the power plant (typically at a voltage of 10 kV to 30 kV), the power is transformed to a higher voltage level in the generation substation. The High Voltage (HV) or Extra High Voltage (EHV) (110 kV to 400 kV) transmission systems transports the electrical power further to the (sub)transmission substations, where the power is transformed to Medium Voltage (MV) level (typically 10 to 30 kV), and where it enters the primary distribution systems. Finally, in the distribution substations, the power is transformed to Low Voltage (LV) level and is distributed to the consumers [78]. Therefore, electrical energy generally flows from the higher to the lower voltage levels in the network. Based on the different voltage levels, this type of power system can then be viewed as a 'vertically-operated' power system, which in this work will be referred to as a 'vertical' power system.

The expansion and the construction of large power plants are limited by both rational (e.g. economical, environmental and geographical) considerations and irrational constraints (e.g. social and political issues) [56].

1.2 Distributed Generation Concept

Nowadays, an increasing amount of electrical power is generated by decentralized power generators of relatively small scale (i.e. smaller than 50-100 MW). This way of electrical power generation is referred to as 'Distributed Generation' (DG) because it is spread out over the system. These small power generators are usually located in the vicinity of the electrical loads, and are mostly connected to distribution networks (i.e. at MV- or LV-networks) [12], [32].

In contrast to the conventional power plants, the development and the implementation of DG units are encouraged mostly by environmental forces. This has stimulated research, promotion, development and increased use of new, renewable, clean and environmentally friendly forms of energy [5], [27]. Renewable energy sources like wind, biomass, sun, tidal-, wave- and geothermal energy are used. Most of these renewable energy sources can be converted to electric power, in units in a range of hundreds kWs to some MWs, by (relatively) small generators that are connected to the distribution networks, close to the load centers.

Some types of distributed generation (DG) are based on conventional fossil energy sources, but are often because of their relatively low carbon emission classified as environmentally-friendly types of power generation. Within this class are the microturbine generator supplied by natural gas, and the Combined Heat and Power (CHP) generation, which is practically a parallel conversion of fuel into electrical and thermal energy (more carbon emission will be produced if the electrical and thermal energy are generated separately).

The rise of DG is supported by the advancements in supporting technologies like power electronic converters and controllers.

Currently there are many DG technologies available. An overview of these DG technologies is given in Chapter 2.

1.3 'Horizontal' Power Systems

Due to the possible large-scale implementation of DG units in the classical 'vertical' power system, a transition towards a more 'horizontal' power system may take place. In addition to the power injected in the EHV and HV system by the large power plants, DG units supply the system via the MV or LV networks. Therefore, the power can flow both 'vertically', i.e. from the higher to the lower voltage levels, as well as 'horizontally' from one MV or LV network to another or from a generator to a load within the same MV or LV network leading to a new term: the *horizontal* power system or *horizontally-operated* power system.

The implementation of DG turns the *passive* distribution network into an *active* one. In this active distribution network some costumers not only consume electricity, but they also generate and if generation surpasses their demand, supply the network. Figure 1.2 shows an example of both an active and a passive distribution network. In the active network the power flow is no longer in one direction (downwards), as is the case in the passive network, but may be bidirectional (down- and upwards).

In this way, it is possible that power is transferred from one distribution network to another. When we reflect further on this issue, we could even imagine that on certain moments in time the electrical power generated by the DG within the distribution networks may become sufficient to fulfill the total demand of the system. In this particular case, the remaining large (centralized) power plants may be shut down.

Figure 1.3 illustrates a 'Vertical-to-Horizontal' transformation of a power system. In the 'first' transformation step, a large amount of DG is implemented in the power system and all centralized generators remain but generate less (Figure 1.3: graph (a) changes to graph (b)). In the 'second' transformation step, the amount of DG in the system increases in such a way that a number of centralized generators (power plants) are shut down for efficiency reasons (Figure 1.3: graph (b) changes to graph (c)). Finally, in the 'third' transformation step, when power generated by DG within the active distribution networks is sufficient to match the total demand, all (remaining) centralized generators are out of service (Figure 1.3: graph (c) to graph (d)).

It is hard to imagine how a system under graph d could operate but theoretically these are the steps.

1.4 Dynamics of Power Systems

The power system is a dynamic system. Even under normal operation conditions, loads are connected and disconnected frequently and demand for both active and reactive power changes continuously. Besides, the power system is subject to disturbances caused by malfunctioning or failing equipment. The ability of a power system to remain in a state of operating equilibrium under normal operating conditions and to regain an acceptable state of equilibrium after being subjected to a disturbance is defined as the *power system stability* [34].

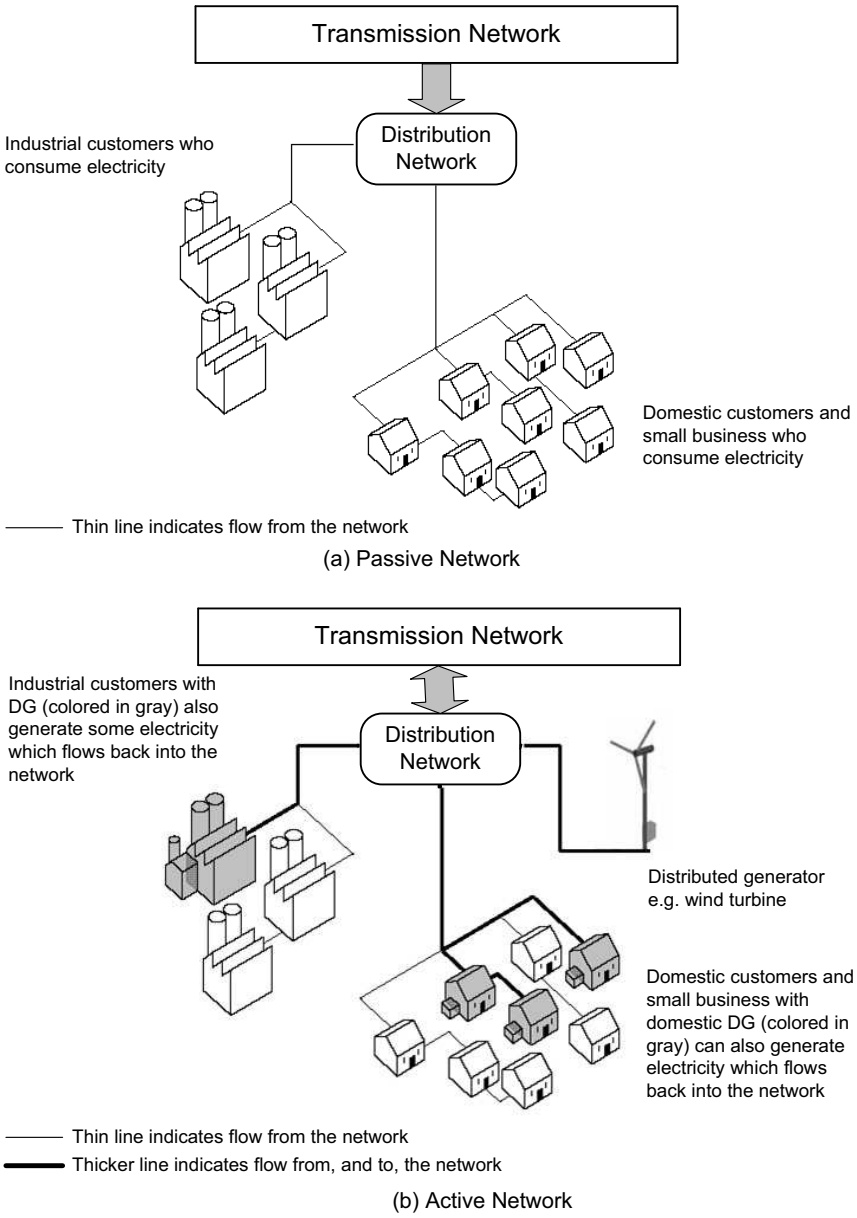

Figure 1.2: Conventional (passive) distribution network (top - a) and an active distribution networks with DG (bottom - b) (modified from [14])

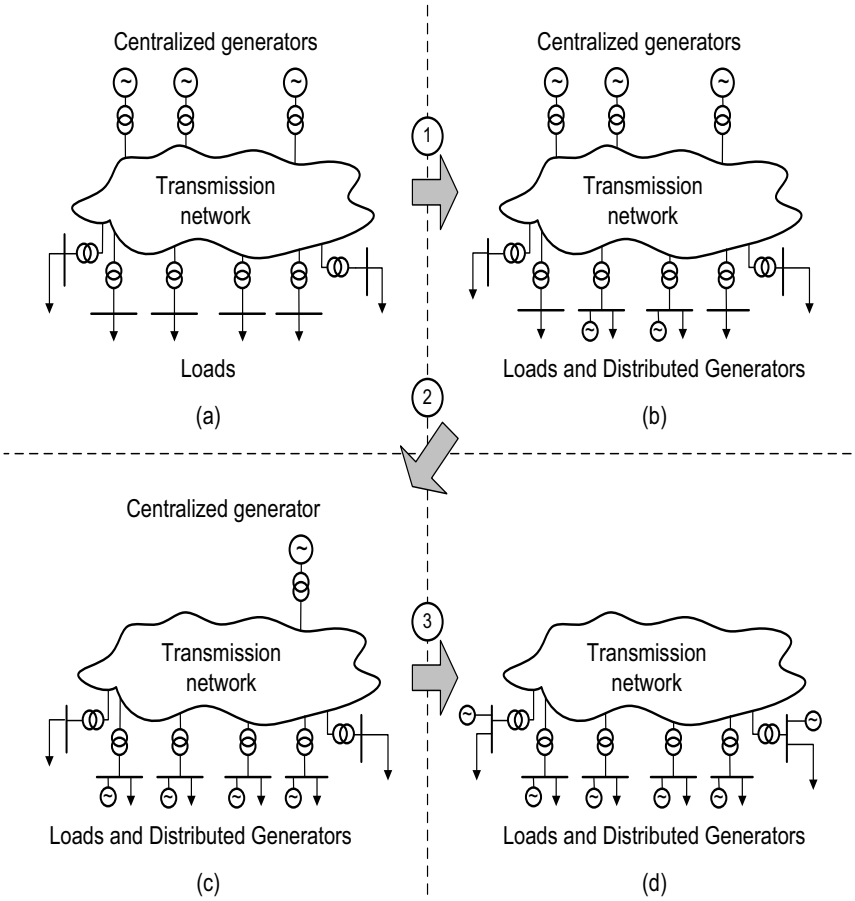

Figure 1.3: 'Vertical-to-Horizontal' transformation of the power system

More than 100 years of experience have lead to the present power system with many subsystems and dynamic elements, a lot of them equipped with control systems to stabilize the operation of the overall system. For instance, power plants are equipped with prime mover controllers to regulate the speed and thus the active power output, and excitation controllers to regulate the voltage and thus the reactive power output. When we consider the interconnected power system as a single system, a necessary condition for a stable operation is that more or less all the large synchronous generators remain in synchronism. Then it is up to the dynamics of the system whether stability can be maintained. Instability can also occur if a power system cannot maintain the voltage levels within a required range [34]. The implementation of DG influences both steady state and dynamic performance of a power system. In this work, however, the focus is on the dynamics.

1.5 Research Framework

The research presented in this work has been performed within the framework of the 'Intelligent Power Systems' project. The project is part of the IOP-EMVT program (Innovation Oriented research Program - Electro-Magnetic Power Technology), financially supported by SenterNovem, an agency of the Dutch Ministry of Economical Affairs. The 'Intelligent Power Systems' project is initiated by the Electrical Power Systems and Electrical Power Electronics Groups of the Delft University of Technology and the Electrical Power Systems and Control Systems Groups of the Eindhoven University of Technology. In total 10 Ph.D. students are involved and work closely together. The research focuses on the effects of the structural changes in generation and demand taking place, like for instance the large-scale introduction of distributed (renewable) generators [59]. The project consists of four parts (illustrated in Figure 1.4).

The first part (research part 1), *inherently stable transmission system*, investigates the influence of uncontrolled decentralized generation on stability and dynamic behavior of the transmission network. As a consequence of the transition in the generation, less centralized plants will be connected to the transmission network as more generation takes place in the distribution networks, whereas the remainder is possibly generated further away in neighboring systems. Solutions investigated include the control of centralized and decentralized power, the application of power electronic interfaces and monitoring of the system stability.

The second part (research part 2), *manageable distribution networks*, focuses on the distribution network, which becomes 'active'. Technologies and strategies have to be developed that can operate the distribution network in different modes and support the operation and robustness of the network. The project investigates how the power electronic interfaces of decentralized generators or between network parts can be used to support the grid. Also the stability of the distribution network and the effect of the stochastic behavior of decentralized generators on the voltage level are investigated.

In the third part (research part 3), *self-controlling autonomous networks*, autonomous networks are considered. When the amount of power generated in a part of the distribution network is sufficient to supply a local demand, the network can be operated autonomously but as a matter of fact remains connected to the rest of the grid for security reasons. The project investigates the control functions needed to operate the autonomous networks in an optimal and secure way.

The interaction between the grid and the connected appliances has a large influence on the power quality. The fourth part (research part 4), *optimal power quality*, of the project analyzes all aspects of power quality. The goal is to provide elements for the discussion between polluter and grid operator who has to take measures to comply with the standards and grid codes. Setting up a power quality test lab is an integral part of the project.

The research described in this thesis is within research part 1: inherently stable transmission systems.

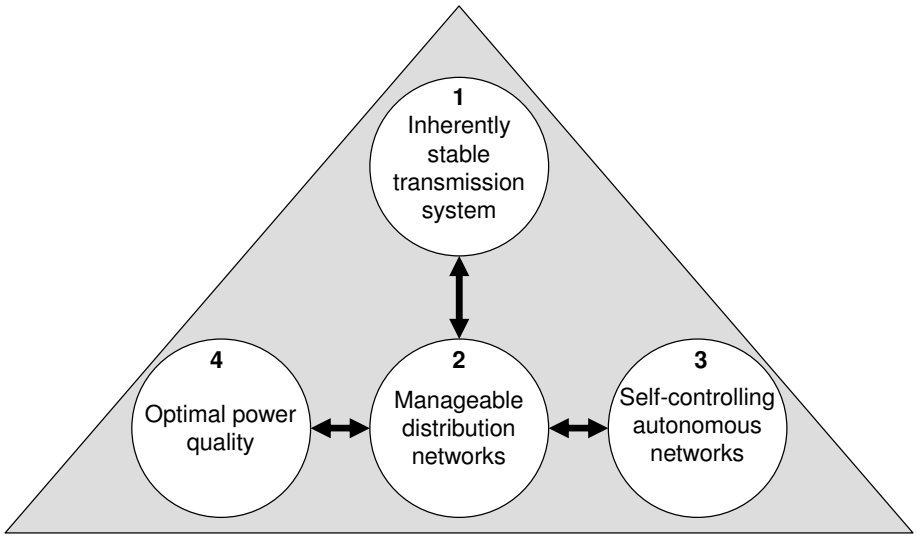

Figure 1.4: Research items within the 'Intelligent Power Systems' research project

1.6 Objectives and Limitations

In this work, the following two objectives are set:

- Investigate the impact of a high DG penetration level on the stability of a power system.
- Investigate the stability of a power system that undergoes a 'vertical-to-horizontal' transformation.

This research is unique as it combines the investigation of an increasing DG penetration level and a power system that transforms from a vertical into a horizontal one. The focus is only on the dynamic impacts, i.e. the transient stability. Steady state and economic impacts are beyond the scope of this work.

For this purpose, power system simulation software package PSS/E is used, where models of the power (test) system and DG are included. Simulation scenarios of power systems with DG are defined later. Based on the simulation results, special emphasis is on the behavior of the centralized generators in service.

1.7 Outline of the Thesis

The thesis is organized as follows:

- In Chapter 2, an overview of the current DG technologies is given. The emphasis is on the classification of the different DG technologies according to their potential impact on the power system stability.
- An overview of power system stability is presented in Chapter 3. In this chapter, the term "inherently stable transmission system" is defined. Furthermore the research approach and the simulation setup, used and presented throughout the work, are discussed, including test system, software, system stability indicators, basic associated controls of system elements and parameters used.
- In Chapter 4, the impact of DG implementation on the power system transient stability is discussed. Different scenarios of a power system with a high DG penetration level are developed. The impact of different DG technologies, fault durations and locations, DG penetration level, DG grid-connection-option, and protection schemes of power electronic interfaced DG units are investigated.
- In Chapter 5, the scenarios for the 'vertical-to-horizontal' transformation of power systems are further elaborated. The transient stability impact of this transformation is analyzed and solutions for reducing the negative effects are discussed.
- In Chapter 6, a stochastic approach to the transient stability of system with DG within the framework of "vertical-to-horizontal" transformation is studied.
- In Chapter 7, a power system reaching 100% DG implementation is studied. DG units are implemented within Active Distribution Systems. Control methods to maintain the power balance in such a power system with Active Distribution Systems are suggested.
- The conclusions and recommendations for future work are given in Chapter 8.

Chapter 2

Distributed Generation

The impact of distributed generation (DG) on the dynamic stability of power systems is studied. Therefore, it is important to examine characteristics of DG that influence this behavior. As mentioned in Chapter 1, DG units can be based on various (both conventional and alternative) primary energy sources. The type of primary energy source and the conversion process determine, to a large extent, the output power characteristics of DG and the type of grid connection applied.

Based on the output power characteristics, DG can be classified as dispatchable or non-dispatchable as is described in Section 2.2. The output power of non-dispatchable units, especially the ones driven by renewable energy sources, can show high output-power fluctuations. Energy storage systems, as described in Section 2.3, can be applied to smooth this intermittent effect.

In Section 2.4 the way DG is connected to the network (grid) is reviewed. There are two options, depending on both the type of primary energy source and prime mover: a direct and indirect grid connection. A direct grid connection is made by using the common/classical synchronous and induction generators, whereas an indirect grid connection is made by means of power-electronic converters. Section 2.5 elaborates on this issue. Concluding remarks are made in Section 2.6.

2.1 State-of-the-art DG Technology

Many definitions of distributed generation (DG) exist. CIGRE Working Group 37.23, for example, has defined distributed generation (DG) as electrical generation that is not centrally planned, not centrally dispatched*, and connected to the distribution network [12]. A DG unit usually produces electric power well below 100 MW [32], [33]. Other literature however advocates a boarder and

*not centrally dispatched: it cannot be controlled from a system control center; it does not implicate that the unit cannot be controlled locally

more straightforward definition of DG: a DG source is an electric power generation source connected directly to the distribution network or on the customer side of the meter [1], [52]. Thus, the way that a generator is implemented in a power system determines its classification as DG, and *not* the type of primary energy source used. However, many generator units that are driven by renewable sources of energy inherently possess the characteristics of DG.

2.1.1 Conventional Fossil-Fuel Based Generators

Within the category DG, the term 'Conventional Fossil-Fuel Based Generator' is used to describe small fossil-fueled power plants within a range of kWs up to 100 MW [7], [12], [33]. The reciprocating engines and gas turbines are the most common in this category.

Reciprocating engines are characterized by low capital cost, possible thermal and electrical cogeneration, and good modularity and flexibility. Furthermore they are reliable [7], [12]. Reciprocating engines, however, have drawbacks. The use of diesel or gasoline gives high emission levels [30]. The emission can be reduced to some extent by using natural gas as energy source. A large number of moving parts leads to high noise levels pollution and increases the maintenance cost [7].

Gas turbines are commonly used in industry [12]. In oil industry for example, the associated gas from the oilfield is frequently used to generate electricity. The use of natural gas results in lower emission when compared to reciprocating engines. As DG, gas turbines are mostly encouraged by the development of microturbines, highlighted in the next subsection.

2.1.2 Microturbines

A 'micro' gas turbine (microturbine) produces electric power in the range of 25-500 kW. An electrical generator is integrated within the microturbine, that operates at a high speed (50,000 to 120,000 RPM). The electric power is produced with a frequency (in the order) of thousands of Hz [2]. Therefore, a power-electronic converter is used to interface the generator and the grid. Within the power-electronic interface, the high-frequency electrical power is converted to DC before it is inverted back to the low-frequency AC of the grid.

Most microturbines use natural gas. As a consequence, microturbines are typically characterized by low emission levels. The use of renewable energy sources such as ethanol is also possible [15].

2.1.3 Combined Heat and Power (CHP) Plants

Combined Heat and Power (CHP), also known as cogeneration, is the simultaneous production of electrical power and useful heat [33]. Reciprocating engines, gas turbines, and microturbines can be used in CHP schemes. CHP generation on a large scale is usually based on fossil fuel. In general, CHP is heat driven

and electricity is the by-product. With this simultaneous process, the overall efficiency of a CHP plant can be around 85% [12], [33].

2.1.4 Small Hydro-Power Plants

A hydro-power plant generates electricity from the motion of a mass of water, where a power house is installed. This water movement can be obtained, for example, from a run-of river or a river with a small impoundment [66]. A small hydro-power plant produces electric power up to 10 MW. Hydro power plant technology has reached maturity. A small hydro-power plant has less impact on the environment and ecosystem, when compared to a large hydro-power plant, and is easy to build within a short construction schedule [66]. Once built, its maintenance cost is minimal [62].

2.1.5 Wind Turbines

A wind turbine generates electricity by extracting kinetic energy from the wind passing through its blades. Wind energy is one of the most promising energy sources to be used for renewable electricity generation [51]. Apart from using a small wind turbine as DG for generating emission-free power, however, the increasing interest for implementing wind turbines is mostly driven by the availability of wind energy for generating power at large scale of MWs or even GWs [77].

2.1.6 Photovoltaics

Photovoltaic (PV) power generation systems convert sunlight directly into electricity [51]. A PV cell consists of two or more semiconductor layers of specific physical properties. These layers are arranged in such a way that when the PV cell is exposed to sunlight, the photons cause the electrons to move in one direction (crossing the junctions of the layers) and a direct current (DC) is generated.

Currently, PV energy cost is still high. However, the capital cost of PV modules has declined in the past decades. PV implementation is encouraged by the infinite availability of sun energy, long life cycle and simple maintenance (since there are no moving parts), high modularity and mobility, and short design, installation and start-up time of a new plant [51].

2.1.7 Fuel Cells

DC power can also be generated by an electrochemical process. An example is the so-called fuel cell. It consists of a positive electrode (anode) and a negative electrode (cathode). To generate electricity, fuel (usually hydrogen) and an oxidant must be supplied to the anode and the cathode, respectively. Electrochemical reactions create ion flows, that generate electricity. One fuel cell

only produces a small amount of electricity, and larger amounts can be obtained from a stack of fuel cells [7], [13].

Fuel cells are modular, portable and produce low noise pollution, because there are no moving parts [39]. These characteristics make fuel cells suitable as DG in, for examples, remote areas. In the future, electrical networks (both AC and DC) can be combined with a gas and hydrogen infrastructure. This new structure may further increase the implementation of fuel cells as DG [19].

2.1.8 Geothermal Power Plants

Geothermal power plants convert the energy contained in hot rock into electricity by using water to absorb the heat from the rock and transport it to the surface of the earth. The heat from geothermal reservoirs provides the force that rotates the turbine generators and produces the electricity. The used geothermal water is then returned (injected back) into the reservoir to be reheated. This cycle will maintain the pressure of the reservoir and sustain the reservoir [57].

A geothermal power plant is relatively sustainable.A field may remain productive over a period of tens of years. It produces no pollutant and no unwanted product, if any, can be disposed underground [68], [80].

2.1.9 Biomass Power Plants

The term “biomass” describes all organic matter that is produced by photosynthesis. It includes all water- and land-based vegetation and trees, municipal biosolids (sewage), animal wastes (manures), forestry and agricultural residues, and certain types of industrial wastes [26], [72]. Biomass is considered a substitute for fossil fuels. Practically, biomass is converted to thermal energy, liquid, solid or gaseous fuels and other chemical products through a variety of conversion processes [72]. The latter forms are then converted into electricity. The biomass products, for example, can be used as fuel to generate electricity. The gaseous fuels can be applied in fuel cell systems.

In general, biomass is abundantly available and can be considered as a renewable.

2.1.10 Tidal Power Plants

Tidal energy is derived from the gravitational forces of attraction that operate between the earth and the moon, and the earth and the sun. Energy is extracted either directly by harnessing the kinetic energy of currents due the tides or by using a basin to capture potential energy from the difference in height of a rising and falling mass of water. To generate electricity, tidal flow is extracted by means of propellers with large diameters. In the latter technique, a huge dam, called a 'barrage' is built across a river estuary. When the tide goes in and out, the water flows through tunnels in the dam. The ebb and flow of the tides can be used to turn a turbine. When the tides comes into the shore, they

can be trapped in reservoirs behind dams. Later, when the tide drops, the water dam can be used like in a regular operation of a hydroelectric power plant [16].

Tidal power is a renewable energy source. Tidal power plants produce no pollutant. They also cause no fundamental change of the natural rhythm of the tidal cycle and no inundation of the adjacent area. These factors encourage the implementation of tidal power plants [6].

However, building a tidal power plant has to be planned carefully considering the potential ecological impacts, especially during the construction [22].

2.1.11 Wave Power Plants

Waves are generated at the surface of oceans by wind effects which in turn result from the differential heating of the earth's surface. Wave energy is complementary to tidal power, it uses the essentially up-and-down motion of the sea surface (wave power), instead of using the energy of the sea rushing backwards and forwards (tidal power). A wave power plant extracts wave energy and converts it into electricity [79].

The wave power plant is promoted as electricity generation available in abundance throughout the world; it is clean and non-polluting, renewable, and suited to electrify remote communities, especially as DG [17]. However, just like a tidal plant, the erection of a wave power plant should be planned carefully, so that the ecological impacts are minimized.

2.2 Output Power Characteristics

One of the main characteristics of a power system is that the supply and the demand must be kept in balance at any time. In a steady-state operation of a traditional power system, the use of synchronous generators (within the power plants) enables the power output of each plant (and each generating unit within the plant) to be dispatched for any specified load condition [25]. Dispatching a power plant (and a generator unit) is a function of the availability of the primary energy sources that drives the prime mover and the flexibility of the conversion process (ramping up and down). By definition DG units are not *centrally dispatched*[†], but several DG technologies enable the DG unit to be *controlled* locally. The DG operator can determine an exact power output of the DG units by controlling the primary energy sources (or fuels) that are supplied to the DG units. Other DG technologies are based on renewable energy sources where the operator cannot dispatch the DG units because the behavior of the primary energy sources cannot be controlled. In case of wind turbines and photovoltaic panels, for example, no extra primary energy can be supplied to the generator units in order to produce more electricity. Normally, most of the renewable energy based electrical generation is operated in such a way that the electricity production is maximized.

[†] the non-dispatchable characteristics of DG units are important when a stochastic approach is considered. Such approach is applied in this thesis in Chapter 6

Table 2.1: Controllable and Non-controllable Classification of DG

DG technology	Controllable	Non-controllable
Conventional Fossil-Fuel Based Generators	√	
Microturbines	√	
Combined Heat and Power (CHP) Plants		√
Small hydro-power plants		√
Wind turbines		√
Photovoltaics		√
Fuel cells	√	
Geothermal power plants	√	
Biomass power plants	√	
Tidal power plants		√
Wave power plants		√

In short, DG technologies can be classified into two categories:

- Controllable DG.
- Non-Controllable DG.

As a summary, Table 2.1 lists the various DG technologies and their classification as controllable and/or non-controllable generation.

2.2.1 Controllable DG

Controllable DG is characterized by its ability to control the fuel supply to the generator. As a result, the output power can be determined, and dispatched.

Among the DG technologies that can be classified as controllable DG are conventional fossil-fuel based generators, microturbines, fuel cells, geothermal power plants, and power plants driven by biomass. Except for the fuel cells, these technologies utilize conventional rotating electrical machines for power conversion (synchronous or induction generators), driven by prime movers based on reciprocating or combustion turbine technologies. By controlling the fuel that is supplied to the prime mover, the torque of the prime mover can be adjusted.

A note should be made with regard to geothermal power plants. The geothermal primary energy source is not as flexible as fossil fuels for dispatching the generator units [68].

2.2.2 Non-controllable DG

Non-controllable DG represents DG technologies where the DG operator cannot determine the power output of the DG units. Among the DG technologies that can be classified as non-controllable DG are small hydro power plants, wind turbines, photovoltaics, tidal- and wave power plants and CHP plants.

Small hydro-power plants

Because of the non-availability of large power impounding (dam), the power output of a hydro turbine (the prime mover in the small hydro-power plant) is practically driven by a direct-captured water flow. A simple expression of the power output for a small hydro-plant is [33]

$$P = QH\eta\rho g, \tag{2.1}$$

with P the output power [W], Q the flow rate [$\mathrm{m^3 s^{-1}}$], H the effective head [m], η the overall efficiency, ρ the density of water [$\mathrm{kgm^{-3}}$], and g the gravitional constant [$\mathrm{ms^{-2}}$].

For small hydro-power plants, H, η, ρ, and g in (2.1) are deterministic and constant. Without significant storage capacity, a small hydro-power plant may experience a very large variation in available water flow (Q), and output power (P) [33]. Thus, a small hydro-power unit is non-dispatchable.

Wind turbines

The power generated by a wind turbine (provided that the upstream wind velocity, v, is between minimal and maximal values, e.g. $4 < v < 25$ [$\mathrm{ms^{-1}}$]) can be expressed as [33], [51]

$$P = \frac{1}{2} C_p \rho v^3 A, \text{ with } C_p = \frac{(1 + \frac{v_o}{v})[1 - (\frac{v_o}{v})^2]}{2}. \tag{2.2}$$

In (2.2), P denotes the output power [W], C_p the power coefficient, v_o the downstream wind velocity at the exit of the rotor blades [$\mathrm{ms^{-1}}$], ρ the air density [$\mathrm{kgm^{-3}}$], and A the swept area of the rotor blades [$\mathrm{m^2}$].

In practice, ρ, A, and to some extent C_p, are deterministic and constant values. Thus, the power produced by a wind turbine is mainly characterized by the wind velocity. The wind velocity itself has a stochastic nature; any wind speed can occur at any time [61]. Moreover, when the upstream wind velocity (v) is either below minimal or above maximal operating values of the wind plant, e.g. $v < 4$ or $v > 25$ [$\mathrm{ms^{-1}}$], the output power equals zero. As a result, a stochastic output power results, especially when a single wind turbine or plant is regarded [50].

Photovoltaics

The power generated by a PV module is given in (2.3) [51] as

$$P = \eta \times (E_{ed} \times A_{PVtotal} + E_{es} \times Area_{PVwithsun}), \tag{2.3}$$

where

$$A_{PVwithsun} = (\overrightarrow{S} \times \overrightarrow{P}) \times A_{PVtotal} \tag{2.4}$$

and

$$\overrightarrow{S} = [S_x S_y S_z], |\overrightarrow{S}| = 1, \quad (2.5)$$
$$\overrightarrow{P} = [P_x P_y P_z], |\overrightarrow{P}| = 1, \quad (2.6)$$
$$\overrightarrow{S_x} = \cos(\theta) \times \cos(\alpha_{sun}), \quad (2.7)$$
$$\overrightarrow{S_y} = \cos(\theta) \times \sin(\alpha_{sun}), \quad (2.8)$$
$$\overrightarrow{S_z} = \sin(\theta), \quad (2.9)$$
$$\overrightarrow{P_x} = \cos(\beta) \times \cos(\alpha_{panel}), \quad (2.10)$$
$$\overrightarrow{P_y} = \cos(\beta) \times \sin(\alpha_{panel}), \quad (2.11)$$
$$\overrightarrow{P_z} = \sin(\beta). \quad (2.12)$$

In (2.3) to (2.12) P denotes the power extracted from the sunlight [W], η the efficiency of the solar panel, E_{ed} and E_{es} the diffuse- and the direct-horizontal irradiance [Wm^{-2}], $\overrightarrow{S}$ and $\overrightarrow{P}$ the solar- and panel orientation, θ and α_{sun} the altitude- and azimuth angle of the sun [rad], and β and α_{panel} the altitude- and the azimuth angle of the panel [rad].

In practice, $A_{PVtotal}$, η, β and α_{panel} are deterministic and constant. Therefore, the generated electricity is characterized by E_{ed}, E_{es}, θ and α_{sun}. The altitude- and the azimuth angle of the sun (θ and α_{sun}) have daily and seasonal patterns, whereas the characteristics of E_{ed} and E_{es} are intermittent. Weather changes and cloud movement, for example, strongly influence the values of E_{ed} and E_{es}, and the generated electricity. The power generation of PV is non-controllable [81].

Tidal power plants

The power output of a turbine operating in flowing water is [74]

$$P = \frac{1}{2}\rho A C_p v^3. \quad (2.13)$$

In (2.13), P denotes the output power [W], ρ the density of the fluid [kgm^{-3}], A the area of the flow covered by the device [m^2], C_p the power coefficient of the device (the percentage of power that the turbine can extract from the water flowing through the turbine), and v the velocity of the water [ms^{-1}].

For a tidal power plant, ρ, A, and C_p in (2.13) are deterministic and constant. Therefore, the output power P depends on the velocity of the water v. Thus, the tide, which is predicable but variable in nature [9], is the only factor that affects the generating activity of a tidal power plant. This makes the tidal power generation non-controllable.

Wave power plants

The power production of a wave power plant can be assessed using [45], namely

$$P_{abs} = \alpha A_w H_s^{1.5}. \quad (2.14)$$

In (2.14) P_{abs} denotes the average absorbed power, A_w the float water plain area [m^2], and H_s the significant wave height [m].α is a coefficient that equals 0.166 [$kgm^{-1.5}s^{-3}$] under ideal conditions [45].

For a wave power plant, α and A_w are deterministic. The output power depends practically on the wave height (H_s), neither constant nor controllable. Hence, a wave power plant is non-controllable.

2.3 Energy Storage Systems

A large-scale implementation of renewable energy sources for power generation could be expected in future. With the non-controllable nature of these generators, especially when renewable energy sources such as wind, wave and sun are exploited, the output power is difficult to predict. Moreover, high power fluctuations from these generators can be expected. In this case, energy storage systems/devices may be needed to cover the resulting imbalances between the power generation and the consumptions [64], [67]. In the following sections, energy storage systems, and their technical characteristics from a power system point of view, are highlighted.

2.3.1 Batteries

Batteries store energy in electrochemical form. There are two basic types of batteries. The so-called *primary battery* converts chemical energy into electrical energy in a non-reversible process and is discarded after discharge. The *secondary battery* works in a reversible reaction. It converts chemical energy into electrical in discharge, and vice versa in charge mode [51].

Batteries are the most widely-used devices for electrical energy storage in a variety of applications. Batteries can store rather large amounts of energy in a relatively small volume. They are modular, so that output power in the order of MWs is accessible. They are also quiet during operation, which makes them suited for implementation near load centers where also DG can be implemented [36], [64].

2.3.2 Hydrogen Fuel Cells

Hydrogen fuel cells store energy in electrochemical form. Hydrogen is produced by electrolysis of water using the off-peak electricity such as coming from wind turbines, photovoltaics, hydro or even nuclear power plants. This hydrogen can be used to operate fuel cells when there is a high demand for electricity. In this way, the hydrogen fuel cell energy storage can be 'charged' and 'discharged' reversibly.

Hydrogen fuel cells are environmentally friendly, if the hydrogen is produced by electrolysis of water, and no fossil-based fuel is used [64].

2.3.3 Redox Flow Batteries

Redox flow batteries store energy in electrochemical form. They are classified in between secondary batteries and hydrogen fuel cells and they have the characteristic of secondary batteries as they can be charged and discharged [54].

Flow batteries have a number of advantages. For example, the power output can easily be varied by increasing the size of the membranes, and the storage capacity can be raised by increasing the size of the tanks of the electrolytes [54].

2.3.4 Flywheel Systems

Flywheels store energy mechanically as kinetic energy [64]. A flywheel system consists of a flywheel, a motor/generator, and power-electronic converter. The flywheel speeds up as it accumulates energy and slows down as energy is released [29]. A flywheel system has a high energy-storage density. It also has an unlimited number of charging and discharging cycles.

2.3.5 Ultracapacitors

Ultracapacitors store energy in the form of electrostatic energy (static charge). Similar to a regular capacitor, the electric energy is stored by means of charge separation [10]. However, compared to ordinary electrolyte capacitors, ultracapacitor's capacitance can be more than tens times higher. Its equivalent internal resistance is more than tens times lower than that of a battery, allowing more than tens times higher discharging/charging currents [23]. This makes the ultracapacitor suited for short-term, high-power applications. An ultracapacitor has an unlimited number of charge and discharge cycles at high rates [10], [23].

2.3.6 Superconducting Magnetic Energy Storage (SMES) Systems

Superconducting Magnetic Energy Storage (SMES) systems store energy in the magnetic field created by the flow of direct current in a superconducting coil. The stored energy can be released by discharging the coil.

The use of SMES is encouraged by several factors [40]. Firstly, its efficiency is very high (up to 95%) as no conversion of energy to other forms is involved. Secondly, it can very rapidly dump or absorb power from the grid as the only limitations are the control loop and the switching time of the solid-state components connecting the coil to the grid.

2.3.7 Pumped-Hydroelectric Plants

Pumped-hydroelectric plants store energy in the form of potential energy. They use off-peak power to pump water uphill to an elevated reservoir. When electricity is needed, the water is released to flow to a lower reservoir, and its potential energy is used to drive turbines [64].

A pumped-hydroelectric energy system enables large-scale energy storage with a high capacity and power rating. It has an unlimited charging and discharging cycle and long life duration. The implementation of such an energy storage system is limited by the requirement of a significant land area with suitable topography for the upper and lower plants.

2.3.8 Compressed-Air Systems

Compressed-air energy storage systems store energy in the form of potential energy by compressing air within an air reservoir, using a compressor powered by off-peak electric energy. When electricity is needed, the air is withdrawn, heated via combustion, and run through expansion turbines to drive an electric generator. During discharge, the plant's generator produces power using a conventional natural gas combustor and the compressed air. When charging, the generator operates in reverse - as a motor (powered by the off-peak electric energ) - to provide mechanical energy to the air compressors [64], [65]. Such a plant uses about one-third of the premium fuel of a conventional simple-cycle combustion turbine and produces one-third of the pollutants per kWh generated. This technology is considered as a hybrid storage and generation plant because it uses fuel and electricity in its storage cycle [64]. Among the positive aspects of a compressed-air energy storage system, are its availability for large-scale storage (high capacity and power rating), the unlimited charge and discharge cycles, and the long life duration [65], however it needs specific geography.

Figure 2.1 shows an indication of the working areas of these energy storage systems.

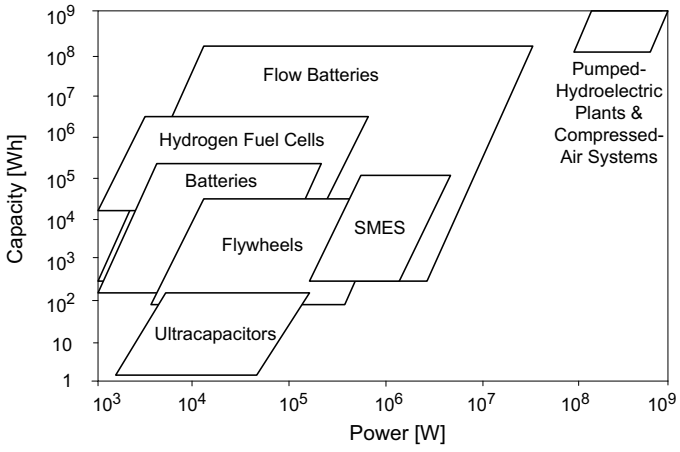

Figure 2.1: Indication of the working areas of different energy storage systems [4]

2.4 DG Grid-Connection Characteristics

Public electrical power systems operate as AC (Alternating Current) systems standardized at either 50 Hz or 60 Hz. Power is mostly generated by means of synchronous generators. The synchronous generators driven by their turbines are responsible for maintaining the frequency in the system. The frequency of the system voltage is directly proportional to the speed of the synchronous generators, i.e.,

$$f = \frac{p}{60} n_{syn}, \tag{2.15}$$

where n_{syn} denotes the synchronous speed of the generator in revolutions per minute [rpm], p the number of pole pairs of the magnetic field circuit, and f the frequency of the generated voltage [Hz].

Due to the variety of primary energy sources/prime movers, DG can generate electricity by means of either *rotating electrical machines* or *static electrical generators*. When the primary energy is converted into mechanical energy that is used to drive electric rotating machines (synchronous or induction machines), AC power is generated. If this AC power is generated at the system frequency or close to it, the generator can be *directly* coupled to the grid. However, if the frequency deviates from the system frequency, power electronic interface must be used. This may occur if the primary energy sources are intermittent in nature (e.g. wind, tidal, wave) and if it is economically better to adapt the speed of the generator accordingly. DG may also generate AC power by means of a fast-rotating prime mover (e.g. a microturbine). In this way, AC power is generated at a constant, but higher frequency than that of the grid. Also in this case, an interface is required. When DC power is generated (i.e. $f = 0$), as with solar panels and fuel cells, an interface that converts DC to AC (at the system frequency) is a must.

In this way, the DG connection to the power grid can be classified into two categories:

- Direct grid-connected DG.
- Indirect grid-connected DG.

2.4.1 Direct Grid-Connected DG

Figure 2.2 shows a schematic diagram of a DG unit connected directly to the AC grid. The prime mover operates at a constant speed, and drives the generator. In general, this generation (or conversion) can be done by means of either a synchronous or an induction generator.

DG units equipped with a synchronous generator

For a synchronous generator, (2.15) is applicable. By controlling the prime mover, so that it operates at a constant speed, the generator can produce power at the grid frequency. This is the case in steam plants, gas turbines, combined cycle plants and co-generation plants. The difference is in the energy source that drives the prime mover.

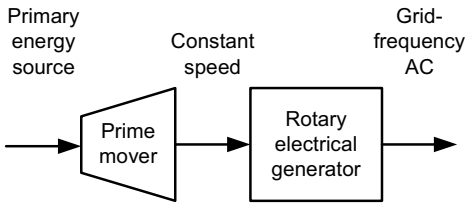

Figure 2.2: Schematic diagram of direct grid-connected DG

DG units equipped with an induction generator

When the prime mover does not operate at a constant speed, an induction generator may be used. In this case, n is no longer constant and

$$n = (1 - s)n_{syn}, \tag{2.16}$$

where s represents the slip.

Induction generators are usually applied in small hydro-power plants and older design or small wind turbines. In this case the speed of the induction generator may vary with the turning force (moment, or torque) applied to it. In practice however, the difference between the rotational speed at peak power and at idle is very small, about 1 per cent [69]. Usually, a gearbox is used (Figure 2.3) to connect the low-speed driving shaft to the high-speed generator shaft (1200 to 1500 rpm).

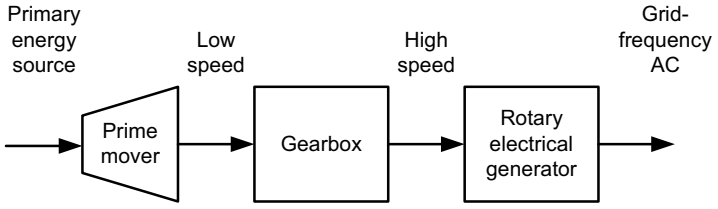

Figure 2.3: Schematic diagram of grid connected DG via gearbox

2.4.2 Indirect Grid-Connected DG

A power system operates at a constant system/grid frequency. Several DG types generate electricity as DC (e.g. solar panels and fuel cells), high-frequency AC (e.g. microturbines) or AC with variable frequency (e.g. certain types of wind turbines). Therefore, an interface is necessary to connect these devices to the grid. As such, a DG unit is connected to the grid in an *indirect* way.

For indirect grid-connected DG, we basically distinguish two situations:

- DG generating DC.
- DG generating either high-frequency AC or AC with a variable frequency.
- Induction generator with power electronic converter in the rotor.

DG generating DC

A DG unit with DC output is primarily characterized by static electric generation, i.e. no rotating parts are involved. Examples of these kind of DG units are fuel cells and solar panels. Figure 2.4 shows a simplified lay-out of such a plant. The primary energy sources are converted into electricity without of a rotating electrical machine. The DC output may be fluctuating and is smoothed by a capacitor before converted to AC at the grid frequency. In addition, a filter can be implemented at the output-stage of the inverter to clean the AC voltage.

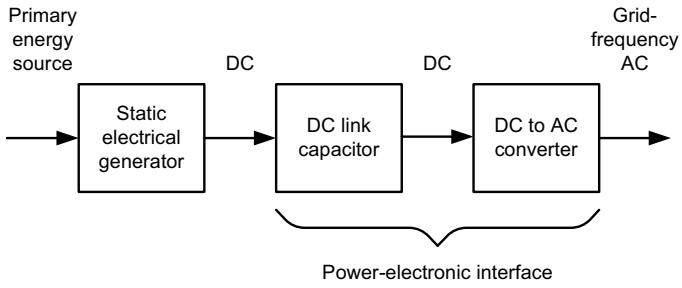

Figure 2.4: Interface-connected DG with DC output

DG generating high/variable-frequency AC

Some DG units, such as microturbines, wind turbines and tidal power generators, use rotating electrical machines for electricity generation but are connected to the grid via power-electronic interfaces. There are two situations in which power-electronic converters are needed to interface the rotating electrical machine to the grid:

- When the rotating electrical machine generates a high-frequency AC (far beyond the grid frequency).
- When the primary energy sources cause the prime mover to drive the rotating electrical generator at a variable speed, leading to a variable-frequency AC.

This is illustrated in Figure 2.5. The high-frequency AC, or AC with variable frequency, is rectified into DC. A capacitor is used to smooth the DC, before it is converted into grid-frequency AC. A filter can be implemented to clean the resulting AC voltage.

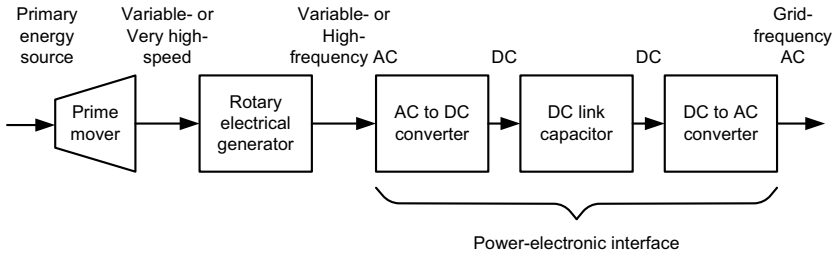

Figure 2.5: Interface-connected DG with AC output

Induction generator with power electronic converter in the rotor

The stator windings of a variable speed induction generator can be connected directly to the grid with the rotor windings connected to (bi-directional) power electronic interface (Figure 2.6). The mechanical and electrical rotor frequencies are controllable over a certain range and the electrical stator and rotor frequency can be matched, independently of the mechanical rotor speed [28], [75].

Table 2.2 summarizes the grid connection classifications of DG.

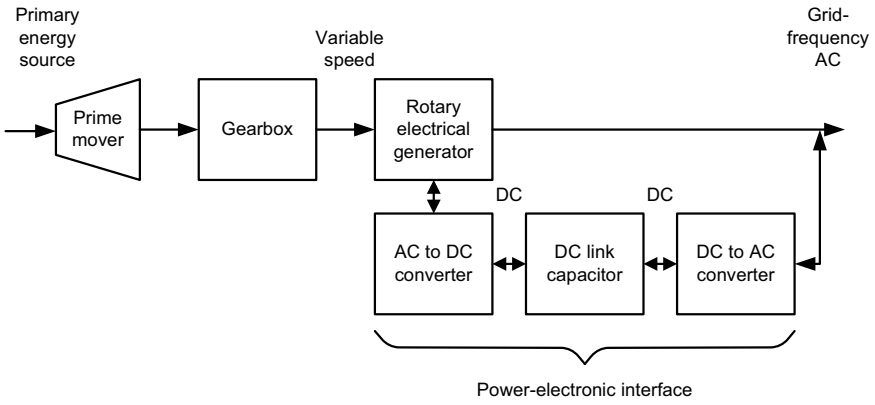

Figure 2.6: Induction generator with power electronic converter in the rotor

Table 2.2: Direct and Indirect grid-connected DG

DG Technology	Rotating Electrical Generator (AC output)	Static Generator (DC output)	Direct Grid-Connected	Indirect Grid-Connected
Conventional Generators	√		√	
Microturbines	√			√
CHP Plants	√		√	
Small Hydro-Power Plants	√		√	
Wind turbines	√		√	√
Photovoltaics		√		√
Fuel cells		√		√
Geothermal Power Plants	√		√	
Biomass Power Plants	√	√	√	√
Tidal Power Plants	√		√	√
Wave Power Plants	√		√	√

2.4.3 Connecting Energy Storage to the Grid

Energy storage can be connected to the grid by means of power-electronic interfaces too. When the energy storage device is charged/discharged by DC (e.g. batteries, hydrogen fuel cells, flow batteries, ultracapacitors, and SMES systems), power-electronic inverters are necessary to convert the stored energy to grid-frequency AC (and vice versa). When a high-speed flywheel is used, a power-electronic interface is necessary to convert the high-frequency AC to grid-frequency AC.

When the energy is stored by means of pumped-hydroelectric plants and compressed-air systems, rotating electrical generators are used to extract the stored energy and convert it into electricity (grid-frequency AC). In this scheme, the generator can be connected directly to the grid.

2.5 DG Prospects: Converter-Connected DG

A large-scale implementation of DG units may be foreseen, with emphasis on renewables. Therefore, a large amount of generation will be 'hidden' behind power-electronic interfaces. This will certainly exert a major influence on the power system and its operation. Power-electronic converters can be used to maximize the energy yield, for active and reactive power control, and for power-quality improvement [60]. The role of power-electronic interfaces will become even more important if hybrid networks that combine AC and DC, as well as flexible energy storages are implemented [19].

When power-electronic converters are used to interface DG with the grid, the impact of the protection scheme should be considered, as it may influence the power system dynamic behavior [58], [60]. There are two possible protection systems for DG units that are connected to the power system via a

power-electronic interface. The first type of protection systems *automatically* disconnects the DG from the power system when the voltage of the system drops below a certain level, and reconnects the DG as soon as the voltage recovers. The other keeps the DG connected to the power network during a fault (ride-through capability). In this thesis, power-electronic interfaced DG with a protection scheme of the first type is considered. However, as comparison, the impact of power-electronic interfaced DG with a protection scheme of the latter type is simulated in Sections 4.4 and 5.5.

Currently, most technical standards require a protection scheme of the first kind [3], [24]. This is mostly motivated by the following objectives:

- To preserve selective protection with simple overcurrent relays as usually applied in the radially-operated MV and LV networks.
- To prevent the DG units from remaining connected to the grid during the reclosure dead time; they could keep the network energized and negate the self-extinction of arcing faults and in case of permanent faults the presence of DG still connected to the grid can be dangerous for utility personnel during repairs.

2.6 Summary

Many definitions of DG exist. From the well-known CIGRE Working Group 37.23 [12], DG is basically defined as electrical generation which is not centrally planned and dispatched, and is mostly connected to the distribution network. A broader and more straightforward definition of DG is advocated by [1] and [52], which includes all electrical generation sources connected directly to the distribution network or on the customer side of the meter.

An overview of the state-of-the-art of DG technology is given. Although its classification as DG depends on the way a generator is incorporated into a power system, in many literature, however, DG is distinguished based on the primary energy sources [7], [52]. The reason is that many generator units driven by renewable sources of energy inherently possess DG characteristics. In this chapter, the existing DG technologies are briefly highlighted according to the primary energy sources.

Another way of examining DG is by looking at the interactions between the generator and the grid. In this way, there are two classifications: (1) based on the output power characteristic, and (2) based on the way DG is connected to the network. Although these two aspects are well-known, these classifications are seldom explicitly presented in literature. In this chapter, however, this distinction is made, as it gives basic ideas and illustrations for supporting modeling of DG used in the simulation in the later chapters. The classification of DG based on the output power characteristics gives basic ideas on stochastic approach done in Chapter 6. The classification of DG based on the way a DG is connected to the network provides a basic idea on modeling of DG for power system transient simulation used in Chapters 3-5.

Literature survey on DG characteristics reveals that the output power of non-controllable DG units, especially the ones driven by renewable energy sources, can show high output-power fluctuations. Energy storage systems can be applied to smooth these intermittent effects.

This chapter ends with an overview of power-electronic interfaced DG. The basic elements of protection schemes, taken from literature, of such DG units are highlighted.

Chapter 3

Stability of Systems with DG

A requirement of power system operation is to balance the electricity supply and the demand at any time, including grid losses. A properly designed and operated power system should be able to maintain this balance both under normal conditions (steady state) as well as after disturbances (dynamic).

A power system is always dynamic. Even under normal operating conditions, both active and reactive demands continuously change. As a system with interconnected machines and components may cover a wide geographical area, a power system is often subjected to disturbances. For a reliable service, it is key that the system remains in operation and is able to return to a stable state. The ability of a power system to return to a state of operating equilibrium under normal conditions and to regain a new equilibrium after being subjected to a disturbance is defined as *power system stability* [34].

The state-of-the-art DG technologies presented in Chapter 2 leads to the classification of DG based on the output power behavior and grid connection characteristics. This chapter emphasizes on the DG impact on the transmission system stability. An introduction on the phenomena of power system stability is the start of this chapter. The connection of this chapter with Chapter 2 is mainly found in Section 3.4, where the modeling of DG technologies and software used for large transmission system transient simulations are presented.

3.1 Classification of Power System Stability

All measured (or calculated) physical quantities, such as the magnitude and phase angle of the voltage at each bus and the active/reactive power flowing in each line, describe the operating condition of a power system. If they are constant in time, the system is in *steady state*. When this steady-state condition is subjected to a sudden change or a sequence of changes in the system quantities, the system undergoes a *disturbance* from its steady state [25].

Depending on their origin and magnitude, there exist *small* and *large disturbances*. For small disturbances, a change from a steady-state condition can be analyzed by using the linearized system's dynamic and algebraic equations. Small variations in load and generation are examples of such small disturbances. Disturbances like transmission system faults, large load changes, loss of generating units, and line switching are examples of large disturbances [25]. In these cases, the linearized dynamic and algebraic equations are no longer valid.

A system is said to be *steady-state stable*, if it is able to return to essentially the same steady-state condition of operation after being subjected to a small disturbance. In many cases, especially under large disturbances, a system reaches a new acceptable steady-state condition is different from the original steady-state condition. The system is called *transiently stable*.

One can distinguish three types of instability mechanisms depending on which parameters are most affected by the disturbance: rotor angle, voltage and frequency.

Furthermore, power system stability can be further classified based on the typical ranges of the time period of response actions as *short-term* (seconds), or *long-term stabilities* (minutes).

The various types of power system stability can be classified correspondingly as the diagram in Figure 3.1 [34].

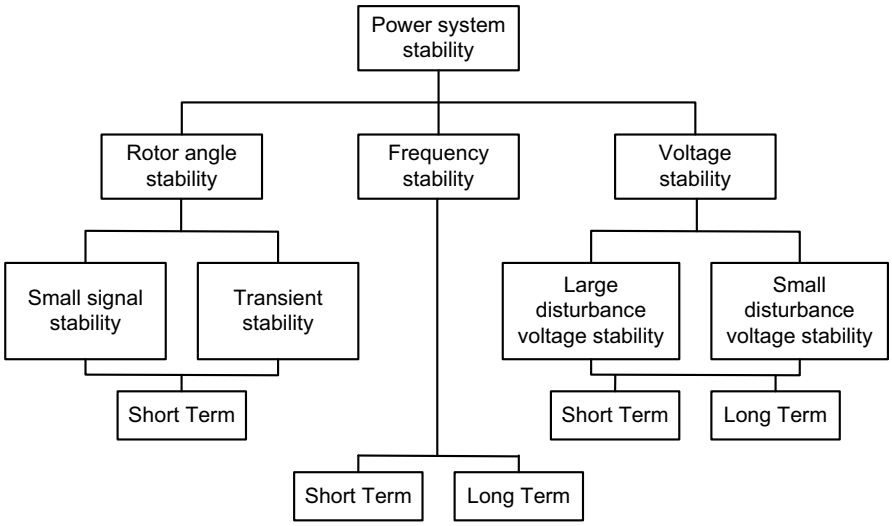

Figure 3.1: Classification of power system stability [34]

3.1.1 Rotor Angle Stability

Rotor angle stability concerns the ability of interconnected synchronous machines in a power system to remain in synchronism under normal operating

conditions and after being subjected to a disturbance. Instability that may result occurs in the form of increasing angular swings of some generators, which leads to the loss of synchronism [34].

When the disturbance is relatively small, stability (which is then called *small signal stability*) can be analyzed using a linearized set of system equations. In case of transient stability, however, the resulting system response involves large excursions of generator rotor angles, and is influenced by the non-linear power-angle relationship [11], [34]. The latter is mainly focused on in this work.

3.1.2 Voltage Stability

Voltage stability is defined as the ability of a power system to maintain steady acceptable voltages at all buses in the system under normal operating conditions and after being subjected to a disturbance. The instability that may result occurs in a progressive and uncontrollable drop in voltage [34]. Voltage stability can be classified into *small disturbance voltage stability* when it is concerned with a system's ability to control voltages following small perturbations such as small changes in loads, or *large disturbance voltage stability* when it is concerned with a system's ability to control voltages following large disturbances such as transmission system faults [11], [34]. Analyzing voltage stability is not in the scope of this thesis.

3.1.3 Frequency Stability

Frequency stability is the ability of a power system to maintain the frequency within an acceptable range, following a system upset resulting in a significant imbalance between generation and load [34]. The instability may result in switching off of generators, overloading of lines and most probable splitting up the system in subsystems. Frequency stability could concern any disturbance and therefore it is not classified into the *small* nor the *large disturbances*. Different from rotor angle stability, frequency stability is determined by the overall response of the system (or each island, in case of the system split into islands) as evidenced by the mean frequency, rather than the relative motion of generators. Frequency is only touched upon in Chapter 7, where keeping power balance in power system with Active Distribution Systems will be discussed.

3.2 Rotor Dynamics of Synchronous Machines

As long as a power system can rely on synchronous machines for generation of electrical power, a necessary condition for satisfactory system operation is that all synchronous machines remain in synchronism [34].

3.2.1 Swing Equation

The governing equation for rotor motion of a synchronous machine is based on the elementary principle in dynamics which states that the net accelerating

torque, T_a, is the product of the total moment of inertia of the rotor, J, and its angular acceleration [25]

$$J\frac{d^2\theta_m}{dt^2} = T_a = T_m - T_e, \tag{3.1}$$

with θ_m the angular displacement of the rotor with respect to a stationary axis. In (3.1), T_m and T_e are the driving torque of the prime mover and the net electromagnetic torque, respectively. The machine is said to be working in synchronous speed (or in synchronism) if $T_a = 0$, i.e. $T_m = T_e$.

For a given speed of *synchronously rotating reference axis*, ω_{sm}, the angular displacement can be rewritten as

$$\theta_m = \omega_{sm} \cdot t + \delta_m, \tag{3.2}$$

where δ_m as the angular displacement of the rotor from the synchronously rotating reference axis. By introducing the angular velocity of the rotor from the synchronously rotating reference axis $\omega_m = \frac{d\theta_m}{dt}$ for a convenient notation and twice differentiating (3.2) with respect to time, combining it with (3.1) and recalling that power (P) equals torque (T) times angular velocity (ω) one arrives at the equation

$$M\frac{d^2\delta_m}{dt^2} = P_a = P_m - P_e, \tag{3.3}$$

where $M = J\omega_m$ is the *inertia constant* of the machine, and P_a, P_e and P_m are the accelerating, the electrical and the mechanical power, respectively. The above equation (3.3) can be further normalized in terms of unit *inertia constant* H, defined as the kinetic energy at rated speed divided by the rated apparent power of the generator S_{mach} as [25]

$$H = \frac{1}{2}\frac{J\omega_{sm}^2}{S_{mach}} \tag{3.4}$$

or

$$H = \frac{1}{2}\frac{M\omega_{sm}}{S_{mach}}, \tag{3.5}$$

yielding

$$\frac{2H}{\omega_{sm}}\frac{d^2\delta_m}{dt^2} = P_a = P_m - P_e. \tag{3.6}$$

Moreover, by noting that both δ_m and ω_{sm} are expressed as mechanical speed, provided both ω_s (the synchronous speed of the rotor) and δ (the angular displacement of the rotor from the synchronously rotating reference axis) have consistent units, (3.6) can be written as [25]

$$\frac{2H}{\omega_s}\frac{d^2\delta}{dt^2} = P_a = P_m - P_e. \tag{3.7}$$

Equation (3.7) is called the *swing equation* of the machine. It is the fundamental equation in the stability study, governing the rotational dynamics of a

synchronous machine. The graph of its solution is known as the *swing curve*. The dynamic behavior of a synchronous machine can be described by means of this equation and its graph, given initial conditions for speed and angle. An inspection of the swing curves of all machines of the system can be used to show whether a particular machine remains in synchronism after being subjected to a disturbance [25].

3.2.2 Power-Angle Equation

When using the swing equation (3.7) H and ω_s are known parameters of the synchronous machine. Therefore, the behavior of the angular positions of the rotor of synchronous machines (δ) are dictated only by P_m and P_e for a given machine and rated system frequency. Due to the characteristic of the prime mover and the related controllers, P_m can be assumed constant during a transient disturbance. This assumption is based on the fact that, while the electrical network reacts almost instantaneously under disturbances, the turbine has some delay before its control mechanism causes it to react. Therefore, only P_e is essential for the solution of the swing equation. This is valid for time frames smaller than 10 seconds (short term stability).

The machine will always operate at steady-state synchronous speed if $P_e = P_m$. If $P_e \neq P_m$, e.g. in a response to a disturbance, the rotor deviates from synchronous speed.

The behavior of P_e is better explained using a generic *two-machine* system as shown in Figure 3.2. This system consists of a synchronous generator(1), connected to a large external system (2), modeled as a machine with very large inertia, a so called "infinite bus". In this system, a simple model consisting of a constant voltage behind a transient reactance is used to represent both machines.

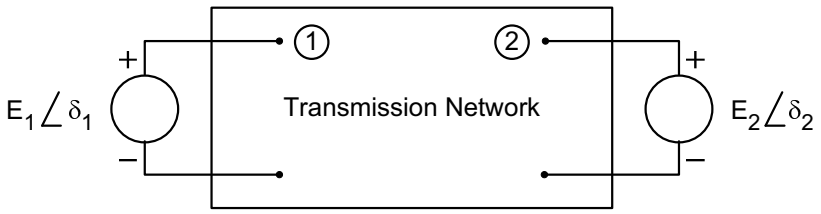

Figure 3.2: Schematic diagram of the two-machine system for stability studies. Transient reactances associated with the transient internal voltages of both machines E_1 and E_2 are included in the transmission network [25]

The admittance matrix

$$\mathbf{Y_{bus}} = \begin{bmatrix} |Y_{11}|\angle\theta_{11} & |Y_{12}|\angle\theta_{12} \\ |Y_{21}|\angle\theta_{21} & |Y_{22}|\angle\theta_{22} \end{bmatrix} \tag{3.8}$$

represents the transmission network between bus 1 and 2, including the transient reactances of the two equivalent machines. The electric power output of the feeding generator P_e is determined by

$$P_e = P_c + P_{max}\sin(\delta - \gamma), \tag{3.9}$$

where

$$P_c = {E_1}^2\mathrm{Re}(Y_{11}), \qquad P_{max} = E_1E_2|Y_{12}|, \tag{3.10}$$

and $\delta = \delta_1 - \delta_2$, with δ_1 and δ_2 the angular displacement of the rotor from the synchronously rotating reference axis associated with the transient internal voltages E_1 and E_2. Furthermore, $\gamma = \theta_{12} - \pi/2$, with $\theta_{12} = \arg(Y_{12})$. If the network resistance is neglected, such that all the elements of $\mathbf{Y_{bus}}$ are purely imaginary (susceptances), then $P_c = 0$ and $\gamma = 0$, and (3.9) reduces to

$$P_e = P_{max}\sin\delta, \tag{3.11}$$

where $P_{max} = E_1E_2/X_{12}$ with X_{12} the transfer reactance between E_1 and E_2, corresponding to $|Y_{12}|$.

3.2.3 Equal Area Criterion

Combining (3.7) and (3.11), yields

$$\frac{d^2\delta}{dt^2} = \frac{\omega_s P_m}{2H} - \frac{\omega_s P_{max}}{2H}\sin\delta, \tag{3.12}$$

or

$$\frac{d^2\delta}{dt^2} = \frac{\omega_s P_m}{2H} - \frac{\omega_s E_1' E_2'}{2HX_{12}}\sin\delta. \tag{3.13}$$

The non-linearity is clear even for this simple example.

Formal solutions of such an equation cannot be explicitly found. In this case, one could rely on numerical methods to obtain the solution [25]. For illustration purposes a two-machine system is commonly used in many text books. In this case, the examination of the system stability can be done with a direct approach without solving the swing equation. It is assumed that a temporary three-phase fault occurs at bus-1 (Figure 3.3). The fault is cleared after a certain period of time, without disconnecting any transmission equipment. The plotted power-angle curve of most critical stable situation is shown in Figure 3.4.

The original (steady-state) operation is characterized by the (pre-fault) rotor angle δ_0, located at the crossing of the horizontal line $P = P_m$ with a curve drawn and sketching the original P_{e0} curve. For simplification purposes, a three phase to ground fault through no intermediate fault impedance is assumed. The

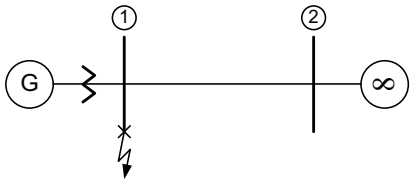

Figure 3.3: Example of two-machine system for stability studies. A fault is applied at bus-1

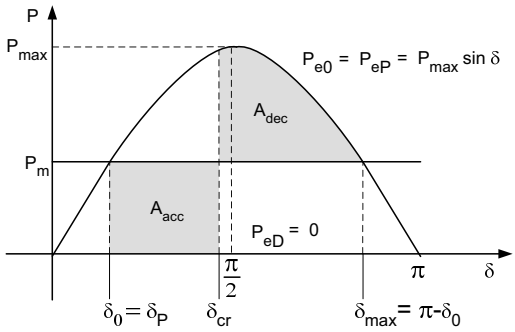

Figure 3.4: Plotted power angle curves showing the critical clearing angle δ_{cr}. P_{e0}, P_{eD} and P_{eP} represent the air-gap power as well as the terminal power before (pre-fault), during and after the fault (post-fault), respectively. The accelerating area A_{acc} and the decelerating area A_{dec} are equal

effective transmission system is unaltered except when the fault is present. The short circuit is effective at bus-1 so that the electrical power output from the generator, P_{eD}, is zero until the fault is cleared. So, the during-fault curve P_{eD} equals zero and the post-fault curve P_{eP} equals the original P_{e0} curve. The post-fault equilibrium point is determined by the intersection of P_m with P_{eP} (equals P_{e0}) and this provides δ_P. Respectively, the unstable equilibrium point (UEP) is equal $\delta_{max} = \pi - \delta_0$. If the angle δ reaches a value larger than UEP, there is insufficient decelerating energy. This leads to instability [82].

The *Equal Area Criterion (EAC)* simply recognizes the fact that the faulted system is still capable of recovering stability as long as the inequality $A_{acc} < A_{dec}$ is satisfied. The borderline case corresponds to

$$A_{dec} = A_{acc}. \tag{3.14}$$

Considering the applied fault and the power-angle curve (Figure 3.4), the accelerating A_{acc} and the decelerating area A_{dec} can be written as

$$A_{acc} = \int_{\delta_0}^{\delta_{cr}} P_m d\delta, \qquad A_{dec} = \int_{\delta_{cr}}^{\delta_{max}} (P_{max} \sin\delta - P_m) d\delta. \tag{3.15}$$

By solving (3.15) in combination with (3.14), the system reaches the *critical clearing angle* (CCA, denoted by δ_{cr}) at

$$\delta_{cr} = \cos^{-1}((\pi - 2\delta_0)\sin\delta_0 - \cos\delta_0). \tag{3.16}$$

Integrating (3.7) twice, provided that $P_a = P_m$ (P_e, i.e. P_{eD}, is zero during the disturbance), at the instant of the critical fault clearing, the increase in rotor speed and the angle separation between the generator and the infinite bus become

$$\delta(t)|_{t=t_{cr}} = \frac{\omega_s P_m}{4H} t_{cr}^2 + \delta_0. \tag{3.17}$$

The corresponding *critical clearing time* (CCT) is obtained as

$$t_{cr} = \sqrt{\frac{4H(\delta_{cr} - \delta_0)}{\omega_s P_m}}. \tag{3.18}$$

3.3 System Stability Indicators

To assess the performance of power systems indicators are needed. As it has been derived from the Equal Area Criterion concept, the Critical Clearing Angle (CCA) of (3.16) and the Critical Clearing Time (CCT) of (3.18) indicate a borderline situation where the faulted system is capable of recovering stability as long the angle of the synchronous machine is less than the CCA or the fault clearing time is shorter than the CCT. On the other hand, when both CCA and CCT are surpassed, the rotor of the machines speeds up, and the rotor angle increases without limit. Therefore, considering this clear analytical/explicit relationships between the CCA/CCT and power system stability, the CCA and CCT are often used as power system stability indicators. When a fault is applied in a power system, the difference between the actual clearing angle and actual clearing time and their respective critical counterparts (CCT and CCA) defines the "stability margin" of the system (assuming the system is stable and there is a positive margin).

However, when simulations are to be done on large power systems, as well as on a more general case than a simple power system (e.g. two-machine system or one machine infinite bus system) the CCA and CCT cannot be explicitly found without computer simulation [25]. One of the practical methods for determining CCT (and CCA) of a power system is the time-domain numerical integration method (the step-by-step time domain simulation) [82], where the determination of CCT (and CCA) requires several time domain simulation runs.

In this work more practical transient system indicators are used, as proposed firstly in [71], namely:

- Maximal rotor speed deviation.
- Oscillation duration.

3.3.1 Maximum Rotor Speed Deviation

The maximum rotor speed deviation is defined as the maximum rotor speed value attained during the transient phenomenon [71].

This indicator is proposed to assess the rotor-angle-stability performance of (centralized) synchronous generators that drive a transmission system with limited inertia. It suggests that the more/faster the rotor speed (of the synchronous generators) deviates from the rated value when a disturbance occurs, the more instable the system becomes. Thus when two cases are compared, as a fault is simulated, at a certain clearing time a higher maximum rotor speed deviation (the faster the rotor accelerates) suggests a lower stability margin.

A remark should be made here. In this work, a test system with limited inertia is used (Section 3.5.1). The system is considered stable if after a fault (disturbance) all (or a limited number of) centralized generator units in the test system remain in synchronism.

3.3.2 Oscillation Duration

The oscillation duration is defined as the time interval between the start of the fault and the instant after which the rotor speed stays within a bandwidth of 10^{-4} pu (on the basis of the rated rotor speed) during a time interval longer than 2.5 s [71].

In the absence of damping, the rotor would continue to oscillate around the rotor angle of the operating point (δ_0 in Figure 3.14). As long as this is the case, there is a risk of instability. In the analysis within this work, when scenarios are compared, an identical disturbance will be applied in each scenario. The oscillation of the rotor speed that deviates from the rated speed is recorded. The indicator of oscillation duration implies that the longer the rotor speed deviates from the rated value when a disturbance occurs, the more instable the system is. In other words, the shorter the rotor speed deviates from rated, when a disturbance occurs, the more stable the system is.

Above all, efficiency in computing time is obtained by using these indicators rather than CCT (and CCA).

Figure 3.5 shows both indicators of maximum rotor speed deviation and the oscillation duration [71]. To quantify the indicators, (3.19)-(3.21) are used:

$$\text{maximum rotor speed deviation} = |\omega_{r,max} - \omega_{r,nom}|, \tag{3.19}$$

with $\omega_{r,max}$ and $\omega_{r,nom}$ denoting the maximum and the rated rotor speed of a centralized generator [rpm],

$$\text{oscillation duration} = t_{osc} - t_f, \tag{3.20}$$

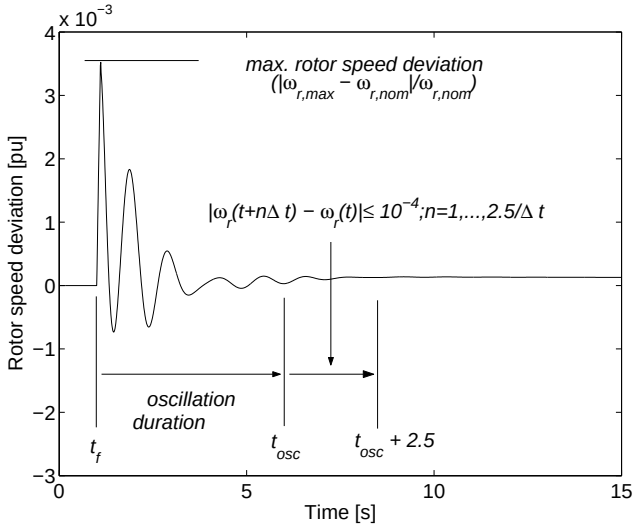

Figure 3.5: Transient stability indicators: maximum rotor speed deviation and oscillation duration [71]

with t_f the time [s] when the fault is applied, and

$$t_{osc} = min\{t : |\omega_r(t + n\Delta t) - \omega_r(t)| \leq 10^{-4}; n = 1, \cdots, \frac{2.5}{\Delta t}\}, \tag{3.21}$$

with $\omega_r(t)$ the rotor speed at a time t and Δt the simulation step (in this research $\Delta t = 10^{-3}$ s is used).

3.4 DG and Large System Dynamic Simulation

In the earliest stages, DG was implemented in power systems on a small scale. In this case, DG can be treated as negative load in power system dynamics studies. As DG implementation increases, the penetration level of DG may become important. In this case, the (original) conventional centralized power plants (e.g. thermal, nuclear or hydro) remain in operation and still cover a significant part of the load and the voltage and frequency control are still within the responsibility of the large/centralized synchronous generators. However, when DG penetration becomes very high, it begins to influence the overall power system behavior. Therefore, the dynamic behavior of the existing system due to this high degree of DG needs to be understood/studied, especially its interaction with the existing generating equipment, to which the power system stability problem is mostly related.

3.4.1 Modeling DG Technologies

As elaborated in Chapter 2, DG can be connected to the grid directly and/or indirectly via a power electronic converter.

There is a major difference in the response to voltage dips (that occur during a disturbance) of electrical machines at the one hand and power electronic converters at the other. The response of electrical machines is determined by the fundamental electro-mechanical laws and physical construction of the machine. Machines therefore have an inherent behavior during voltage disturbances. The power electronic converters response, not only depends on the physical construction (e.g. power electronic components cannot withstand large currents), but also for the largest part on the controller and its parameters. This makes it more difficult to provide a general model that can be used for simulation in power system studies [42].

Electrical Rotating Machines

The direct grid-connected DGs are based on directly coupled synchronous or induction generators. These technologies can be modeled using models of a conventional synchronous or induction generator, readily available in power system dynamics simulations software [53]. Therefore, the available models within the software can be used and they do not pose special problems in power system dynamics.

The challenge however lies on how to incorporate the DG in the distribution system commonly represented only by the load at the main connection between the transmission system and the distribution feeder in power system simulations. Section 3.5.3 deals further with this issue.

Converter Connected DG: Voltage Source Converter

When the indirect grid-connected DGs are considered, the output of these DG technologies are driven by the output of the power electronic interface basically representing a voltage source converter, the most used converter nowadays. The example of a circuit topology of such converter is taken from [42] as shown in Figure 3.6, where a first-order filter (L_f and R_f) between the converter and the grid is used to reduce the harmonics injected by the switching of the converters.

The operating principle of the grid connected voltage source converter can be summarized as follows [42], [70]:

- A setpoint for the active power to be supplied to the grid is determined by the electrical conversion either from a static electrical generator (Chapter 2) or prime mover and AC-DC-converter (Chapter 2).
- A setpoint for the reactive power is derived from the actual value of the terminal voltage (U_{grid}) if a terminal voltage controller is present.
- The actual values of terminal voltage and currents are measured and are inputs to the current controller.

- The current controller generates control signals for the semiconductor switches in such a way that the current that flows, injects the desired amounts of active and reactive power in the grid.

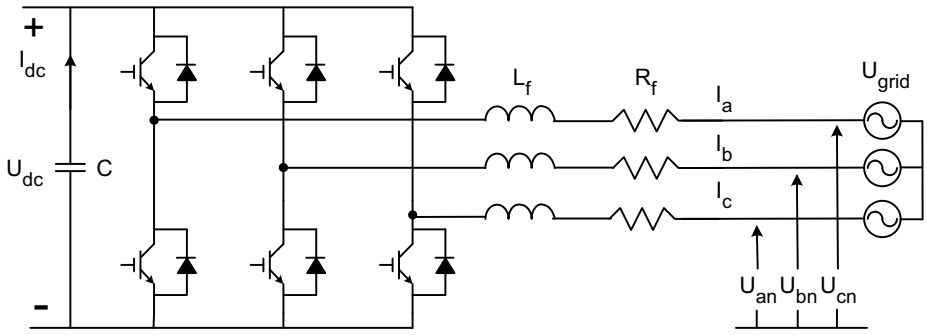

Figure 3.6: Three-phase full bridge Voltage Source Converter with 6 IGBT switches [42]

Converter Connected DG: Constant PQ-Sources

When transient studies are performed on large systems, it is usual to model the DGs as PQ-sources. Only the active power P and reactive power Q (or active and reactive current) supplied by the converter are of interest then. This is especially advantageous in power system dynamics simulations, because it facilitates the interaction with the load flow module, that uses active and reactive power as an input, as it is required by power system dynamics simulation packages. Moreover, the grid representation in the simulation packages and the typical time step used, do not allow detailed modeling of power electronics. The use of this PQ-source model for DG is justified in [70]. The steady state values and the time required to reach a new set point for this PQ-source model is similar to both the voltage source converter and the controlled current source converter with hardly any overshoot occurring [70]. Applying this model to power system dynamic simulation can done basically by following Algorithm 1:

Algorithm 1 Calculate I_{DG}

Require: P_{nom}; Q_{nom}

$P_{DG} \Leftarrow P_{nom}$

$Q_{DG} \Leftarrow Q_{nom}$

$\overrightarrow{I_{DG}} \Leftarrow \frac{(P_{DG}+jQ_{DG})^*}{\overrightarrow{U_{DG}}}$

P_{nom} and Q_{nom} denote the nominal/setpoint of the active and reactive power output of the converter connected DG unit. P_{DG} and Q_{DG} denote the 'real'

active and reactive power output of the converter connected DG unit. $\overrightarrow{I_{DG}}$ denotes the current generated by the DG unit and $\overrightarrow{U_{DG}}$ the terminal voltage where DG unit is connected (as complex phasors).

Due to the different protection schemes of converter connected DG, additional equations should be applied to Algorithm 1.

When the protection system automatically disconnects DG from the network when the voltage of the system drops below a certain level U_{min} (e.g. 0.85 pu) and reconnects the DG as soon as the voltage recovers, Algorithm 2 is applied.

Algorithm 2 Calculate I_{DG}

Require: P_{nom}; Q_{nom}; U_{min}
if $U_{DG} \geq U_{min}$ **then**
  $P_{DG} \Leftarrow P_{nom}$
  $Q_{DG} \Leftarrow Q_{nom}$
  $\overrightarrow{I_{DG}} \Leftarrow \frac{(P_{DG}+jQ_{DG})^*}{\overrightarrow{U_{DG}}}$
else
  $P_{DG} \Leftarrow 0$
  $Q_{DG} \Leftarrow 0$
  $\overrightarrow{I_{DG}} \Leftarrow 0$

When the protection system keeps the DG connected to the power network during a fault, Algorithm 3 is applied. Note that a current limiter is commonly applied in the latter case, due to the limitations ("by construction") of the converter. Two 'minimal' voltage levels are commonly applied here. When the voltage of the system drops below the first voltage level U_{min_1} (e.g. 0.85 pu), the output current of the DG is limited to the maximum value I_{max} (in practice, 100% up to 120% of the rated value). Further, when the voltage drops below the second voltage level U_{min_2} (e.g. 0.15 pu), the DG is disconnected from the network.

Most DG based on renewable energy generation is intended to maximize the active power output. Therefore it is common to set a PQ-source to represent the converter connected DG for these DG units as a source that delivers constant active power P and limited amount of reactive power Q [71]. On the other hand, the current limiter and the operating voltage applied in the DG gives a limitation in the total power $S_{nom} = \sqrt{P_{nom}^2 + Q_{nom}^2}$. Therefore, for a given operating active power P setting, the Q must be within a certain area, as constrained by the total apparent power.

3.4.2 Power System Dynamics Software Packages

For the investigation of DG impact on power system transient stability, the above DG models are integrated in the various simulation software packages, each with their own modeling assumptions and limitations, as discussed below.

Algorithm 3 Calculate I_{DG}

Require: P_{nom}; Q_{nom}; U_{min_1}; U_{min_2}; I_{max}
if $U_{DG} \geq U_{min_1}$ **then**
  $P_{DG} \Leftarrow P_{nom}$
  $Q_{DG} \Leftarrow Q_{nom}$
  $\overrightarrow{I_{DG}} \Leftarrow \frac{(P_{DG}+jQ_{DG})^*}{\overrightarrow{U_{DG}}}$
else if $U_{min_1} \geq U_{DG} \geq U_{min_2}$ **then**
  $I_{DG} \Leftarrow I_{max}$
  $P_{DG} \Leftarrow Re(\overrightarrow{U_{DG}}\overrightarrow{I_{DG}}*)$
  $Q_{DG} \Leftarrow Im(\overrightarrow{U_{DG}}\overrightarrow{I_{DG}}*)$
else $\{U_{DG} < U_{min_2}\}$
  $P_{DG} \Leftarrow 0$
  $Q_{DG} \Leftarrow 0$
  $\overrightarrow{I_{DG}} \Leftarrow 0$

There is a lot of power system dynamic simulation software available on the market today. Within this work, three power system software packages are utilized: PSS/E, MATLAB Power Systems Blockset and RTDS (which is not really software, but a "hardware digital simulator"). The capabilities of these three tools complement one another.

Basically, power system dynamics simulation software can be used when the phenomena of interest have a frequency of about 1 to 10 Hz. PSS/E falls within the software packages that offer dynamic simulation capability. In this type of software, only the fundamental harmonic component is simulated, whereas higher harmonics are neglected. This approach enables the representation of the network by a constant admittance matrix, as in load flow calculations. Further, it reduces the number of differential equations, as no differential equations are associated with the network and fewer with generating equipment and as it enables the use of a larger simulation time step [34]. As a result of this approach, power system dynamics simulation software alternately executes a load flow and a time-domain calculation, via integration of the differential equations that model dynamic system devices. From the load flow calculation, node voltages and branch flows result. During the time-domain calculation, the response of the dynamic device models to changes in their terminal voltage, current and/or frequency are determined. Therefore the use of this software is preferred when many simulation scenarios of DG implementation need to be run in a large power system like the simulations in this work in Chapters 4 and 5. Here, the converter connected DG is modeled as a constant PQ-Source.

When the frequencies of interest are higher, the packages that contain more detailed and higher order equipment models should be used. MATLAB Power Systems Blockset and the Real Time Digital Simulation (RTDS) fall within this category. In these packages for examples, the transmission network is represented in three-phase time-domain and a time step down to 1 μs is possible. Therefore the modeling of DG units in details as Voltage Source Converter or

Current Source Converter is only possible when such software is used. However this small step will have an impact on the execution speed, especially when simulation is done on large power systems. In the (rotor angle) transient stability studies performed in Chapters 4-6, the phenomena of interest have a frequency of between 1 to 10 Hz. Therefore, this level of detail is not needed, and power system dynamics software package PSS/E is used.

Particularly in Chapter 7 RTDS is used. The RTDS models of the voltage and current source converters that represent DG in that chapter are derived from the model earlier developed in MATLAB Power Systems Blockset [42].

3.5 Simulation Setup

This work deals with issues of DG affecting the bulk transmission system when a high DG penetration level is seen.

For this purpose, a model of the transmission system is needed. This model should be detailed enough to assess transient stability. At this level there are two possible data sets to use. The first possibility is using a real national transmission system, for example, the high voltage 380-kV Dutch network. The second possibility is using an existing test system normally used for dynamic stability. Here the second option is taken.

3.5.1 The IEEE 39-bus New England Test System

The IEEE 39-bus New England is a widely known test system used for dynamic simulations (Figure 3.7 and Table 3.1). As such, this system has a benefit when compared to other systems, such as the 380-kV Dutch High Voltage Grid, as it has been used extensively and described in literature, and the results from the simulations presented throughout this work can (to some extent) be compared with other work. The system is relatively small (39 bus, 10 centralized generators (CG), 46 transmission lines), but comparable to the 380-kV Dutch Network (28 bus, 19 CG ($\geq$ 250 MW), 27 transmission lines (380 kV and 220 kV)) [73].

Table 3.1: Characteristics of the New England Test System

System Characteristic	Value
# of buses	39
# of generators	10
# of loads	19
# of transmission lines	46
Total generation	6140.7 MW / 1264.3 Mvar
Total generation	6097.1 MW / 1408.7 Mvar

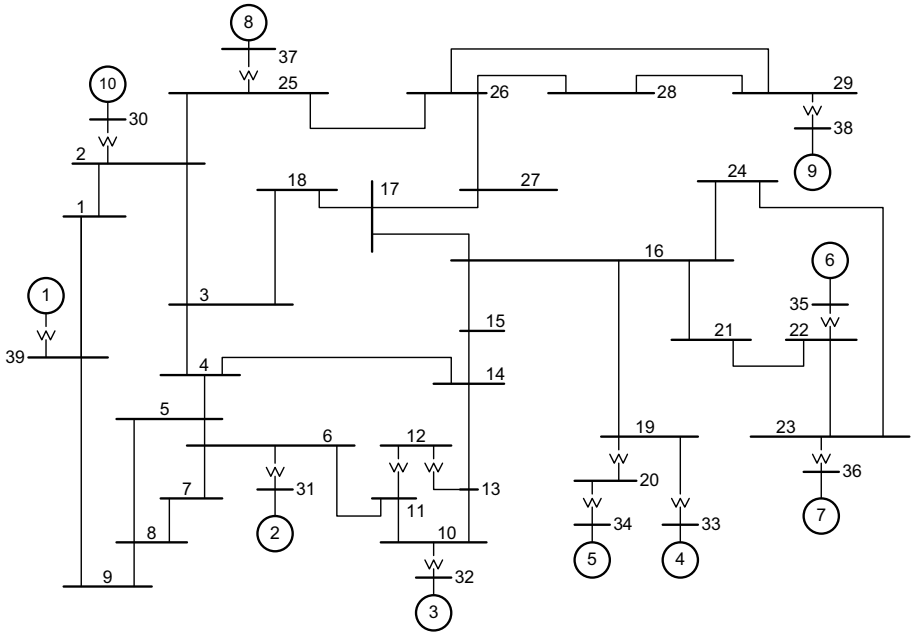

Figure 3.7: Single-line diagram of the 39-bus New England test system [49]

In this research, the basic parameters of the IEEE 39-bus New England dynamic test system are taken from [49], and listed in Appendix B. Note that some minor adjustments have been made. To represent a system with limited inertia, no bus is modeled as an infinite bus (every generator in this test system is set to have its inertia). Each CG is modeled as a two-axis (dq) model of synchronous machine [53] and is equipped with a simplified excitation system model and a steam turbine governor model. The details of these models and the representative values for the parameters are taken from [53] and [34], and attached in Appendix B. Each load is equally divided in constant impedance, constant power and constant current.

3.5.2 DG Technology

Two basic technologies can be used for connecting DG to the grid (Section 3.4.1): (i) electrical rotating machine connected directly to power grid, or (ii) converter connected generator indirectly connected to the grid. In this work, some options elaborated from both basic models are used to investigate the general impact of the DG on the system stability, namely:

- Squirrel cage induction generator (ASM), simulated by means of a third order induction generator model [53].

- Synchronous generator without grid voltage and frequency control (SM), as discussed in [71].
- Synchronous generator with grid voltage and frequency control (SMC) [71].
- Power electronic converter (PE), modeled as a constant PQ-source [71].
- Power electronic converter (modeled as a constant PQ-source), with grid voltage and frequency control (PEC) [71].

In case of ASM and SM , the electrical rotating machine is modeled based on the existing models available in the power system dynamic simulation software (Appendix C). Furthermore, PE is modeled by a source of constant active power and reactive power (PQ-Source). Since a standard model is not available for representing power electronics in the version of PSS/E version used [53], a so-called user-written model of a power electronic converter has been developed. This model is based on the algorithms 2 and 3 in Section 3.4.1. Controllers are applied when DG with grid voltage and frequency control is simulated (SMC and PEC). When SMC is considered, each DG is equipped with the simplified excitation system and a steam turbine governor model, as listed in Appendix C. When PEC is simulated, the active and reactive power controllers as depicted in Figure 3.8 are incorporated in the model. The challenge lies in the possibilities that many types and sizes of DG are incorporated in the system so that the generators as well and the controller parameters can be optimized. In this case, it is very complex to optimize the controllers parameters for the DG unit. Therefore simplifications are done as only one generic model is used to simulate one DG technology. Furthermore, once the types and the parameters of the controllers are set, they will neither be changed nor optimized throughout the simulations. This issue is also discussed in next section.

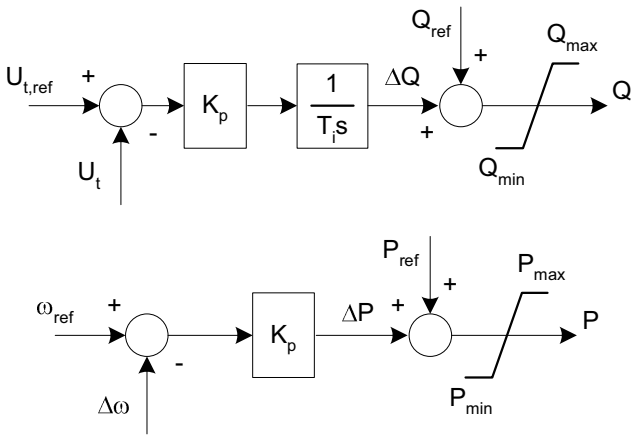

Figure 3.8: Reactive (above) and active (below) power controllers of a power electronic converter with grid voltage and frequency control in the test system

3.5.3 Incorporation of DG in Distribution Networks

In test systems used for transient stability studies, the high-voltage transmission system is normally modeled in detail, while the distribution system is represented only by the load at the main connections between the transmission system and the distribution systems. As described in Section 1.3, the structure of distribution systems is likely to change due to the implementation of DG. This is because, in an active distribution network, some generation and energy storage systems are located within the distribution system. Therefore, the most thorough approach to study the impact of such DG implementation on the transient stability is to model the distribution networks in detail along with all load types, distributed generators and energy storage. In many situations, however, it is not practical to obtain and to apply these details in the lower level distribution networks on a test system originally used to study the transmission level. Therefore, a simplification must be made using a distribution network model representing the aggregated load and generation in the system.

In this work a simple approach is used by representing the incorporation of DG in a distribution network as an equivalent load and generator earlier proposed in [18] and [71]. Only one DG technology (and not a mixture of several DG technologies) is assumed to be implemented at one load bus for one simulation case. After that, comparison of the impacts of one DG technology on the transmission system transient stability to another are investigated. In this way, the general model of connecting DG at a particular load bus as shown in Figure 3.9 can be used [18], [71].

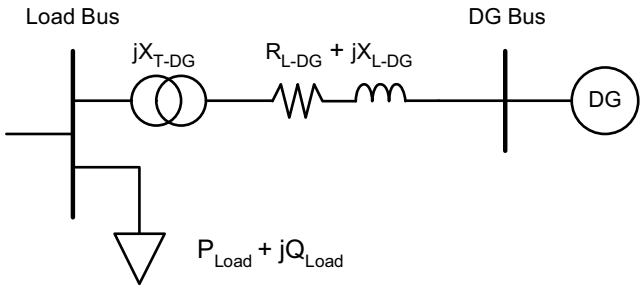

Figure 3.9: Model of connecting DG at a particular load bus

In this model the impact of different DG topology can be approached by changing the parameters of the impedance connecting DG ($X_{T,DG}$, $R_{L,DG}$, $X_{L,DG}$) to the transmission system. $X_{T,DG}$ and $X_{L,DG}$ represent the reactance of the transformer and the line between the DG and the transmission network respectively, and $R_{L,DG}$ represents the resistance of the line. For example, to compare the impacts of DG implemented far away from or close to the connection feeder, the impedance parameters can be set by increasing the parameters in the first case and reducing them for the latter. Also, when a distribution

network with a single-point concentrated DG is compared to a distribution network with scattered DG (that suggests a parallel connection), the impedance can be set differently (e.g. the line parameters $R_{L,DG}$, $X_{L,DG}$). These issues are treated in Section 4.2.

3.5.4 Behavior of Centralized Power Plants

Synchronous generators within centralized power plants that deliver the electrical energy within a power system are equipped with controllers (governing systems - governors, excitation systems - exciters) and protection schemes.

The governing systems for example provide a means of controlling power and frequency, a function commonly referred to as load-frequency control or automatic generation control. The excitation systems provide direct current to the synchronous machine field winding, in order to control the field current. The protective function ensures that the physical (mechanical and electrical) capability limit of the synchronous machine, excitation system and other equipment are not exceeded [34].

The characteristics of these control systems of course have an impact on the overall performance of the power system. Basically the effectiveness of the control systems in enhancing power system stability can be estimated and further optimized. For example, by adjusting the parameters of these controllers the behavior of the power system transient stability can be influenced [34].

When DG is implemented on a large scale it can be expected that the transient performance of the power system changes. It can be expected too that changing, for instance, the parameters of the controllers could counteract the influence on the performance of the system due to this DG implementation. This suggests that these parameters can be optimized for having the most optimal system transient stability performance. However, as the focus of this work is to investigate stability of the power system due to DG implementation ('vertical to horizontal' transformation of power system), we do not include the optimization of these controllers.

3.6 Summary

This chapter gives an overview of the power system stability phenomena. This chapter begins with classification of power system stability, which is taken from existing literature [35]. Then, review of existing knowledge is presented to provide insights into the mechanism, which leads to transient instability in power systems. Highlights are put on the rotor angle stability (of synchronous machines), which is the main focus of this research, by means of the swing equation, power-angle equation and equal area criterion. Attention is drawn on some of the existing system stability indicators (Critical Clearing Time (CCT) and Critical Clearing Angle (CCA)), and on more practical transient system indicators such as maximal rotor speed deviation and oscillation duration proposed

by [71]. The latter is used to assess power system stability performance on large power systems in this work.

Models and assumptions of DG implementation on (large) power system transient simulation are discussed, leading to the use of existing models of DG as electrical rotating machines and constant PQ-source for converter connected DG. The basic algorithm for simulation of converter connected DG as constant PQ-source is first introduced in [71]. In this thesis, different protection schemes of converter connected DG are added to the basic algorithm. Some power system dynamics software packages are highlighted, and the motivations that lead to the use of power system dynamics software package PSS/E in this research are presented.

This chapter also covers the development of the simulation setup used in this work: IEEE 39-bus New England test system [49]. Five DG connection technology options are taken into account based on the two basic alternatives: DG directly or indirectly connected to the grid. The options are: (1) squirrel cage induction generator, simulated by means of a third order induction generator model, (2) synchronous generator without or (3) with grid voltage and frequency control models derived from electrical-rotating-machine-based DG technology (an existing library in PSS/E [53]) and (4) power electronic converter [71] modeled as a constant PQ-source without or (5) with grid voltage and frequency control, for which, user-written model with different protection schemes are developed.

The representation and aggregation of DG in the distribution network [18] is discussed in this chapter. Finally, the chapter ends with highlights on the behavior and assumptions of the centralized power plants that are potentially impacted due the DG implementation.

Chapter 4

Impact of DG on Power System Transient Stability

This chapter investigates the impact of DG implementation on power system transient stability. Different scenarios of a power system with a high DG penetration level are developed. The impact of different DG penetration levels, fault durations and locations, DG grid-connection-strengths, DG technologies and protection schemes of power-electronic interfaced DG units are investigated and discussed.

The 39-bus New England Test System forms the starting point of the investigations. Throughout the chapter, DG technologies and DG topology are based on the simulation setup defined in Section 3.5.

4.1 DG Impacts

4.1.1 Simulation Scenarios

In this section, the impact of the DG penetration level on the power system stability is investigated. For this purpose, two simulation scenarios are defined. In the first scenario, *Scenario I*, the DG is implemented to cover the increment of the load, so that the DG penetration level rises along with the increasing load. In the second, *Scenario II*, DG supplies (part of) the existing (constant) load. As a result, the total power output from the centralized generators is reduced.

The DG penetration level is defined as [18]

$$\%DG_{penetrationlevel} = \frac{P_{DG}}{P_{DG} + P_{CG}} \times 100, \tag{4.1}$$

with P_{DG} and P_{CG} the total active power generated by DG and CG respectively.

The details of the scenarios are as follows:
Scenario I:

- The DG penetration level is raised to keep track with the increasing real and reactive power consumption of all loads. The increment of the real power consumption is covered by an equal amount of power produced by DG connected to each load bus via a j0.05 pu impedance (representing $X_T + X_L$ in Figure 3.9 with R_L neglected) on the 100 MVA system base. The DG penetration level increases in steps of 3.33 % up to 33.33%, corresponding to a 50% increment of the load i.e. the load increase within 25 years at a load growth of about 1.8%. Thus eleven sub-scenarios are obtained with DG penetration levels of 0.0, 3.33, 6.67, 10.0, 13.33, 16.67, 20.0, 23.33, 26.67, 30.0, and 33.33%.
- The active power generated by the CG is kept constant, except for the active power generated by the generator that acts as the swing bus (generator nr. 2, see Figure 3.7) for covering the losses. The increasing reactive power consumption is provided by centralized generators.

Scenario II:

- The DG (penetration) level is raised by decreasing the CG active power output in steps of 3.33 % down to a reduction of 33.33%, and the implementation of DG at every load bus to cover this decrement of active power. In this way, again eleven scenarios are obtained.
- The load remains constant in this scenario.

To assess the results of Scenarios I and II, *Base Case I* and *Base Case II* are additionally defined as:
Base case I:

- The load is increased in steps similar to that in Scenario I. However, the increasing load is supplied by raising the active power output of the CG. Thus in this case the centralized generators cover both active and reactive power increment.

Base case II:

- No increase in load similar to Scenario II and no DG penetration.

4.1.2 Transient Stability Simulation

The transient stability of the test system is investigated by applying a permanent three-phase fault to all possible branches cleared by tripping the faulty line after 150 ms. Every line, that can be missed according the $(N-1)$ adequacy standard, is subjected to a fault. In this way, 35 possible locations for faulty branches are simulated. Details are shown in Table 4.1.

To assess the transmission system stability, two transient stability indicators are examined:

- Maximum rotor speed deviation of large centralized generators.
- Oscillation duration.

Details of the indicators can be found in Section 3.3.

Table 4.1: Branch Number and Corresponding Buses

Faulty branch (nr.)	Corresponding buses	Faulty branch (nr.)	Corresponding buses	Faulty branch (nr.)	Corresponding buses
1	1-2	13	8-9	25	17-27
2	2-3	14	10-11	26	21-22
3	2-25	15	10-13	27	22-23
4	3-4	16	11-12	28	23-24
5	3-18	17	12-13	29	25-26
6	4-5	18	13-14	30	26-27
7	4-14	19	14-15	31	26-28
8	5-6	20	15-16	32	26-29
9	5-8	21	16-17	33	28-29
10	6-7	22	16-21	34	1-39
11	6-11	23	16-24	35	9-39
12	7-8	24	17-18		

4.1.3 Simulation Results

Scenario I

Figure 4.1 and Figure 4.2 show the simulation results displaying the transient stability indicators when the DG penetration level is increased according to Scenario I; the results of Base case I serve as a reference. The x-axis of each graph represents the number of the faulty branch (Table 4.1). The y-axis represents the DG penetration level [%] and the corresponding load increase [%]. Note that in Base case I the y-axis represents the load increase [%] only since there is no DG implemented ($DG_{level} = 0\%$). The z-axis represents the value of the stability indicator used (the maximum rotor speed deviation in Figure 4.1, and the oscillation duration in Figure 4.2). The bottom graphs of Figure 4.1 and 4.2, labeled CG, indicate the simulation results of Base case I. The titles ASM (squirrel-cage induction generator), SM (synchronous generator without grid voltage and frequency control), or PE (power-electronic converter without grid voltage and frequency control) above the graphs indicate the type of DG technology simulated (Section 3.5.2).

When the increasing load within the test system is covered only by increasing the CG active power output (Base case I), the stability indicators are generally increasing (i.e. a reduced stability in the system). When DG is implemented to cover the increased load within the system (Scenario I), in general the indicators do not increase (see graphs 'ASM', 'SM'). Some exceptions can be observed when power-electronic interfaced DG (without grid voltage and frequency control) is implemented (see graph 'PE'), but those can be prevented when the DG is equipped with grid voltage and frequency control. In general, the indicators show an improved stability (i.e. decreasing indicators) when the DG is equipped with grid voltage and frequency control. These results are not visualized here.

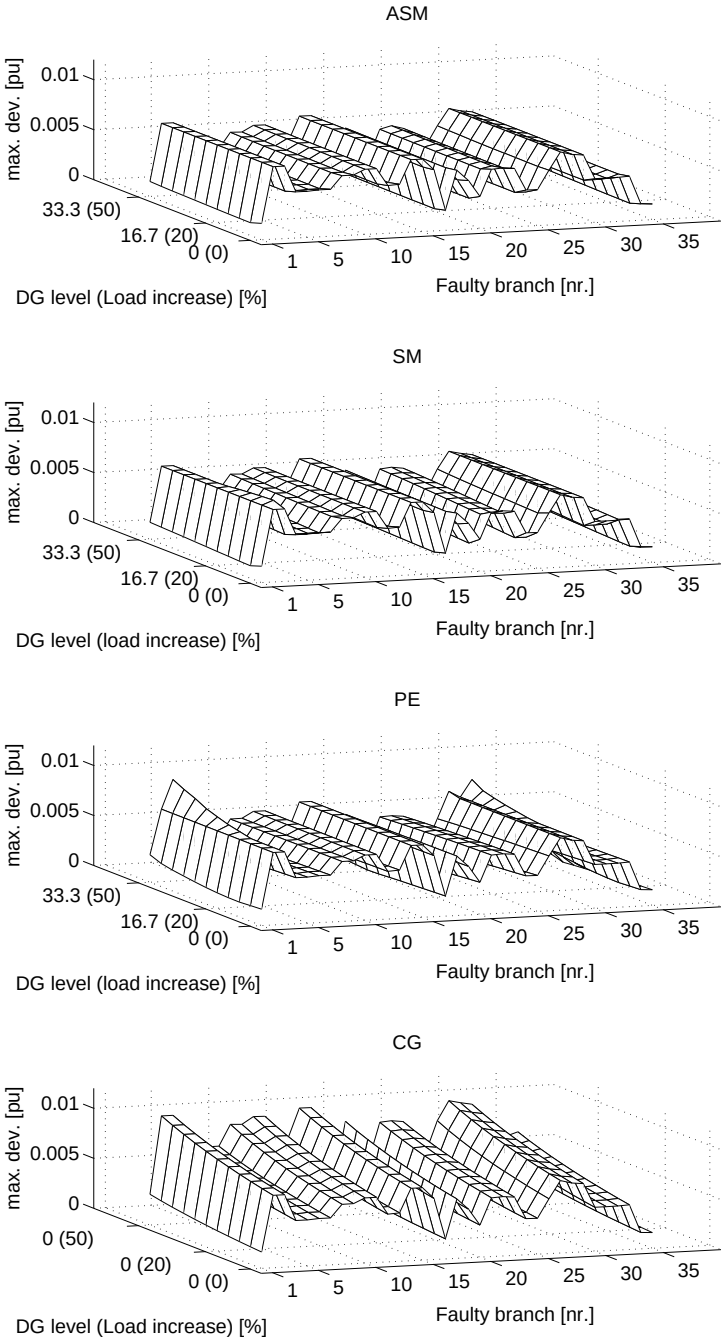

Figure 4.1: Maximum rotor speed deviation when the DG penetration level is simulated according to Scenario I (graphs 'ASM', 'SM' and 'PE') and the Base case I (graph 'CG'), and a fault is simulated in all defined branches (Table 4.1)

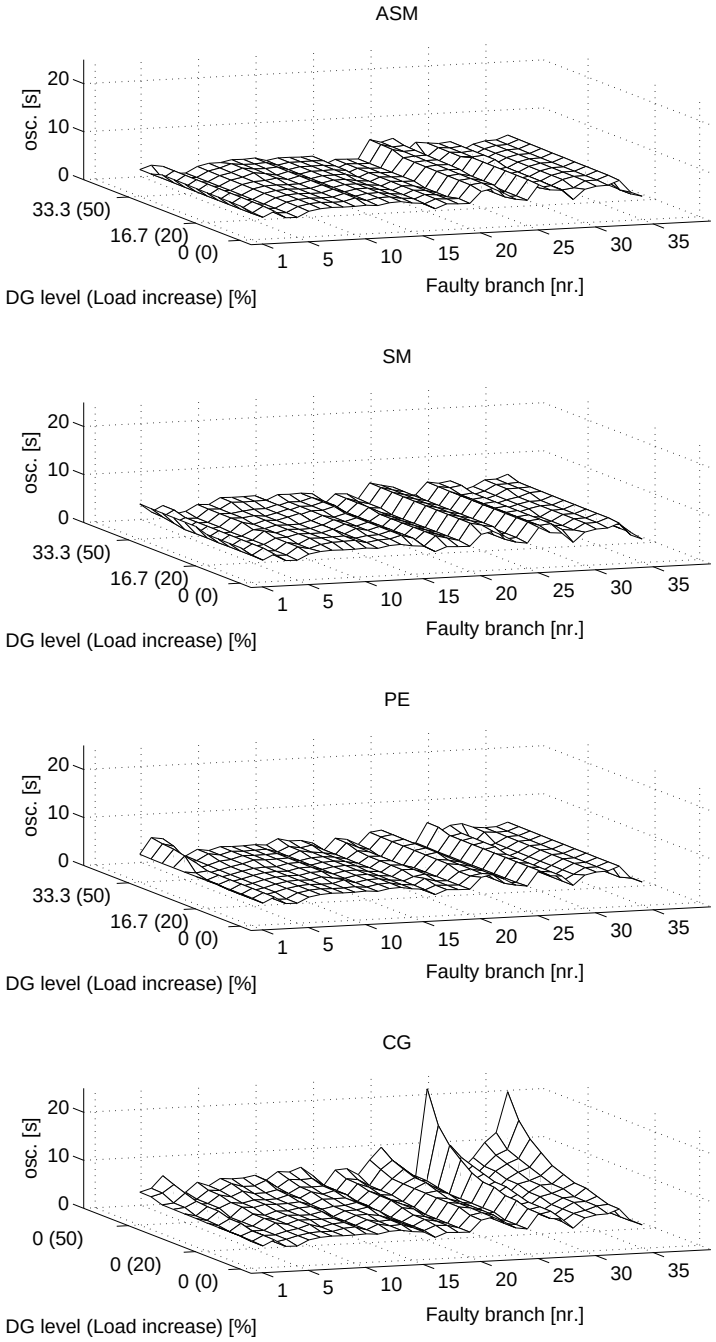

Figure 4.2: Oscillation duration when the DG penetration level is simulated according to Scenario I (graphs 'ASM', 'SM' and 'PE') and the Base case I (graph 'CG'), and a fault is simulated in all defined branches (Table 4.1)

Scenario II

Figure 4.3 displays the maximum rotor speed deviation when the DG penetration level is increased according to Scenario II. The x-axis of each graph represents the number of the faulty branch. The y-axis represents the DG penetration level [%] and the corresponding load increase [%]. The z-axis represents the value of the maximum rotor speed deviation in per unit. The bottom graph of Figure 4.3 (labeled 'CG') indicates the Base case II. In general the maximum rotor speed deviation decreases. The oscillation duration decreases along with the increasing DG level too (not visualized here). Both indicators show even better results when the DG is equipped with grid voltage and frequency control.

4.1.4 Remarks

In the simulation Scenarios I and II, no significant (transient) stability problems were found when the DG penetration level is increased up to 33.33% regardless of the DG technology used. Note that in these scenarios all centralized generators (the 10 CGs in the test system) remain in the system when the DG penetration level is increased.

The results can be explained as follows. In Scenarios I and II, all centralized generators remain in the system. Therefore, all active and reactive power controls as well as the inertia of the centralized generators are unchanged. However, the active power flows in the transmission lines are lower when DG is implemented as the active power generated by the DG is consumed directly by the load at the same feeder. Thus, the active power flows on the transmission lines are more or less constant when the DG covers the increasing load (Scenario I). The active power flows in the transmission lines even decrease when the DG covers (part of) the existing load (Scenario II). It is known that large power flows have a detrimental effect on the damping of oscillations [31]: the heavier the lines are loaded, the weaker the connections between the generators and the loads and the larger the oscillations of the centralized generators. Thus, when all CG units remain in the system, and the DG is implemented close to the loads, the DG implementation is a kind of 'load-reduction' that reduces the power flows in the transmission network and improves its transient stability.

We can compare the active power flows in each of the simulated branches according to simulation Scenarios I, II and also the Base cases I and II, with the system indicators. It can be observed that the 'surface' of the branch power flows are comparable with that of the system indicators of the scenarios.

Figures 4.4-4.6 show some examples of these comparisons.

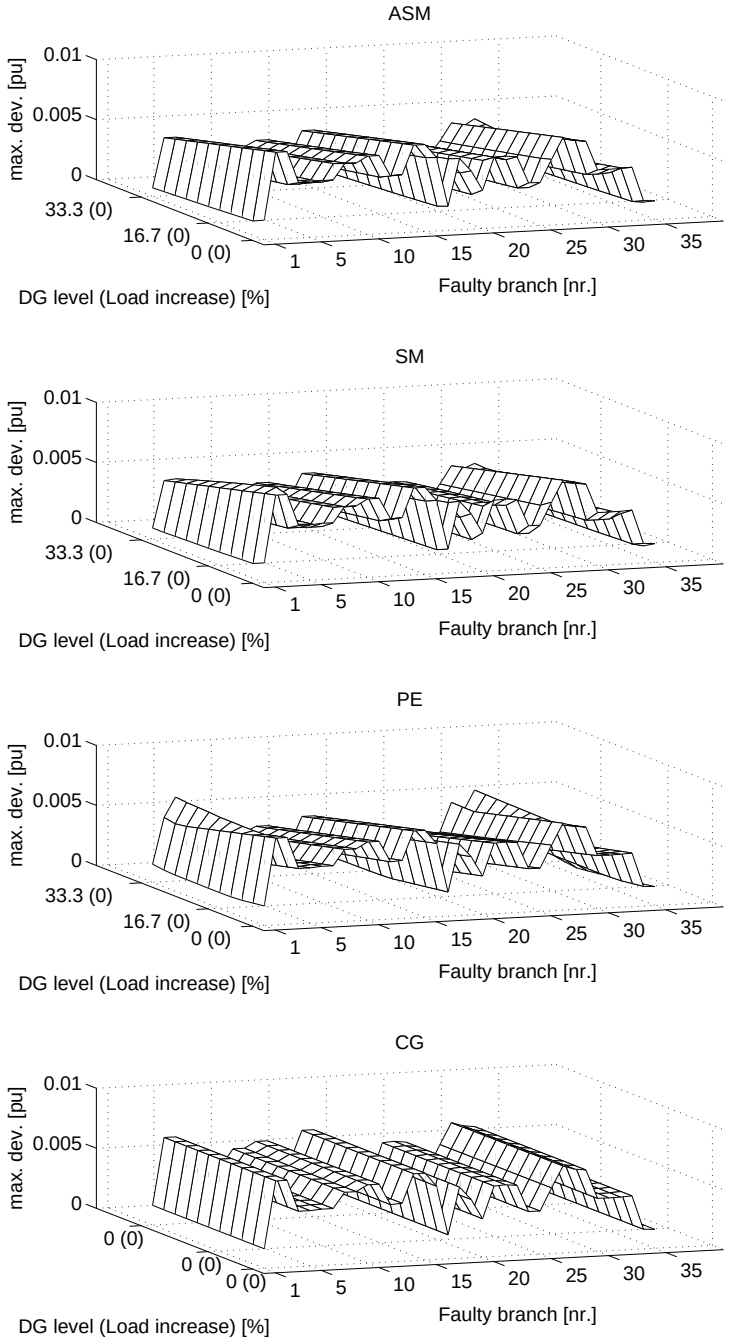

Figure 4.3: Maximum rotor speed deviation when the DG penetration level is simulated according to Scenario II and the Base case II (graph 'CG'), and a fault is simulated in all defined branches (Table 4.1)

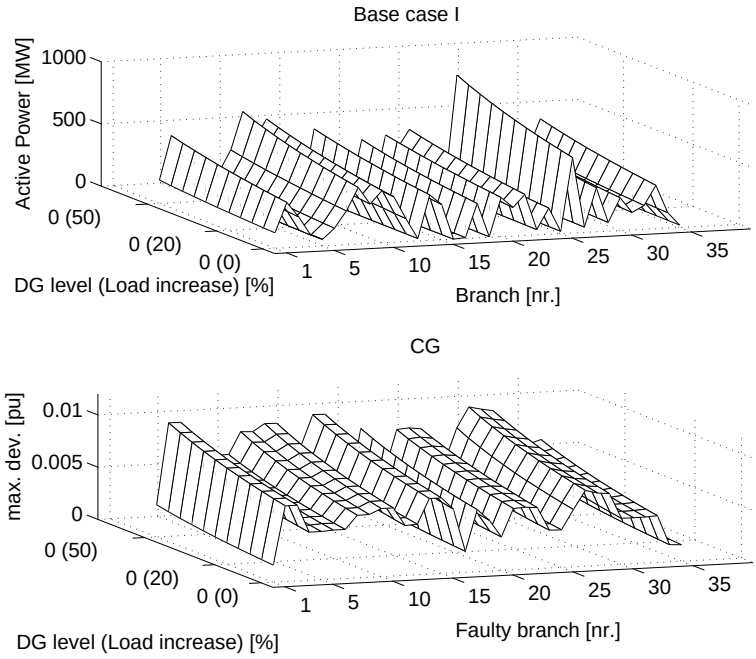

Figure 4.4: Active power flows in the simulated branches in the test system (top) and maximum rotor speed deviation (bottom) in Base case I

4.2 DG Grid-Connection Strength Impacts

In this section, the DG grid-connection strength is varied by changing the parameters of the impedance connecting the DG units to the system, as suggested in Section 3.5.3.

4.2.1 Distribution Network and DG Layout

The distribution system carries the power to the individual customers, in a certain geographical area. Both the geographical situation and the distribution of customers can vary from one area to another [21]. Moreover, there are many ways to connect DG to the distribution network. From the transmission system point of view, both elements may result in a DG implementation that can have a weaker or a stronger grid connection even when in both situations the DG penetration levels are equal. For example, DG may be implemented in a distribution network with a relatively low impedance, e.g. distribution networks in towns or city centers, or a distribution network with a relatively high impedance, e.g. the distribution network in a rural area with long laterals. DG units may also be spread throughout a distribution network, such as solar panels mounted on the

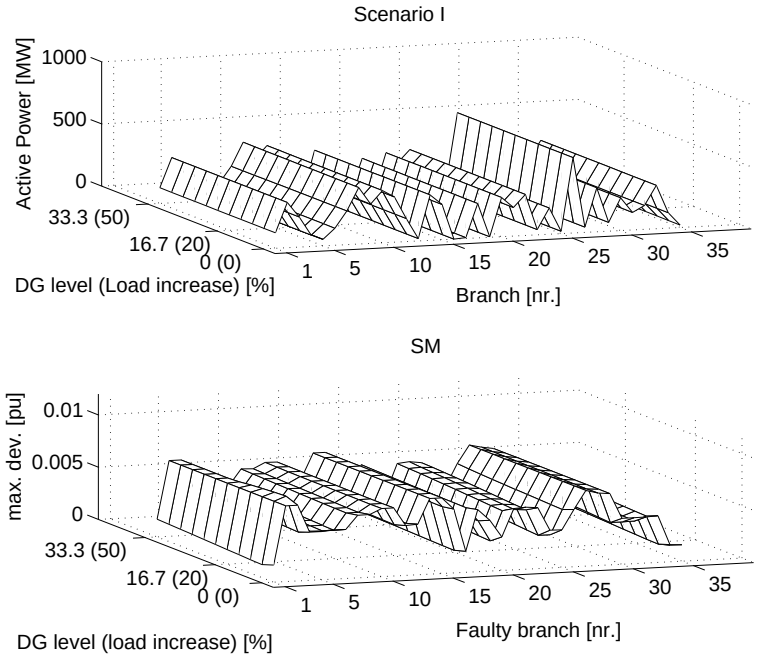

Figure 4.5: Active power flows in the simulated branches in the test system (top) and maximum rotor speed deviation (bottom) in simulation Scenario I ('SM' refers to the DG technology implemented)

roofs of houses, or concentrated in a few locations, e.g. a wind park connected to a distribution network at one substation only. The latter case may result in a higher impedance between DG and the transmission network.

4.2.2 Simulation Scenarios

The incorporation of DG in a distribution network is represented as an equivalent load and generator (Figure 3.9). The impedance between the aggregated DG (implemented at a particular load bus) and the transmission network is set according to

$$Z_{DG_i} = jX_{T,DG_i} + R_{L,DG_i} + jX_{L,DG_i}, \tag{4.2}$$

where Z_{DG_i} is the impedance between DG_i (the aggregate DG connected to load bus-i) and the transmission network.

The parameters in (4.2) are varied considering the following points:

- When DG is implemented in laterals of different length the value of $jX_{L,DGi}$ is varied.

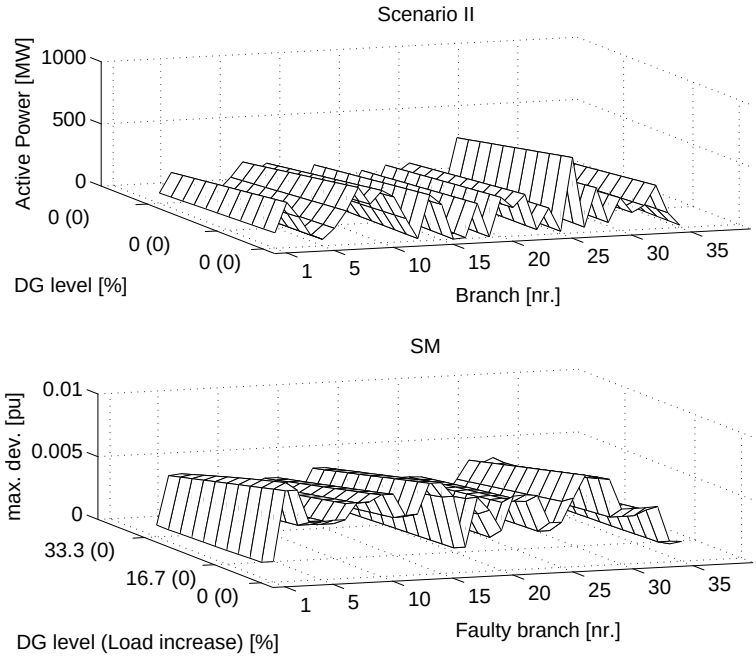

Figure 4.6: Active power flows in the simulated branches in the test system (top) and the maximum rotor speed deviation (bottom) in simulation Scenario II ('SM' refers to the DG technology implemented)

- When DG is spread out over many substations instead of concentrated in one, the value of $jX_{L,DGi}$ is varied related to the "size of DG" implemented in a particular distribution network:

$$jX_{L,DG_i} = \frac{j0.05pu}{par(P_{DG_i})}, \tag{4.3}$$

  where $par(P_{DG_i})$ is an integer whose value is proportional to the "size of DG_i" (the active power generated by the aggregate DG at a particular load bus-i).
- When DG is implemented in a distribution network with a high resistance, the value of $R_{L,DGi}$ is taken into account too.

To investigate the transmission system stability in relation to the DG grid connection strength, various Scenarios (*III-A*, *III-B*, *IV-A*, and *IV-B*) are defined (Table 4.2).

Table 4.2: Simulation Scenarios

Scenario	Keywords	|Impedance| (pu) ($\|Z_{DG_i}\|$)	Resistance (pu) (R_{L,DG_i})	Reactance (pu) (jX_{T,DG_i} $+jX_{L,DG_i}$)	DG penetration level (%)
III-A	Laterals different length, resistance neglected	$\{0.035 \cdots 0.08\}$	0	$j0.01$ $+\{j0.025 \cdots j0.07\}$	20
III-B	Laterals different length, resistance included	$\{0.035 \cdots 0.08\}$	$\frac{1}{3}\|j0.01$ $+X_{L,DG_i}\|$	$j0.01 + jX_{L,DG_i}$	20
IV-A	Constant length, concentrated	0.06	0	$j0.01 + j0.05$	$\{3.33 \cdots 33.3\}$
IV-B	Constant length, spread out over laterals	Agrees to equation (4.2)	0	$j0.01 + \frac{j0.05}{par(P_{DG_i})}$; $par(P_{DG_i}) =$ the integer of $\frac{P_{DG_i}}{100.0}$	$\{3.33 \cdots 33.3\}$

Note that X_{L,DG_i} in Scenario III-B is obtained by substituting the values of Z_{DG_i}, R_{L,DG_i} and X_{T,DG_i} in this table that correspond to Scenario III-B into equation (4.2). In this way, the values of X_{L,DG_i} and R_{L,DG_i} increase along with the increasing value of Z_{DG_i}

Scenario III-A and Scenario III-B are defined to investigate the impact of the DG grid-connection strength on the transmission system stability, when DG is implemented in laterals of different length. In Scenario III-A the value of R_{L,DG_i} is neglected, while in Scenario III-B it is taken into account. In these scenarios, a 20% DG penetration level is assumed (4.1).

Furthermore, ten sub-scenarios are derived from Scenario III-A by adjusting the value of jX_{L,DG_i} (jX_{T,DG_i} is kept constant at $j0.01$ pu) in such a way that the value of $|Z_{TN,DG_i}|$ in (4.2) raises from 0.035 pu to 0.08 pu, in steps of 0.005 pu. Accordingly, ten sub-scenarios are derived from Scenario III-B by adjusting the values of jX_{L,DG_i} and R_{L,DG_i} (jX_{T,DG_i} is kept constant at $j0.01$ pu) in such a way that the value $|Z_{TN,DG_i}|$ (in (4.2)) increases from 0.035 pu to 0.08 pu, in steps of 0.005 pu while the value of R_{L,DG_i} equals $\frac{1}{3}$ of $(X_{L,DG_i}+X_{T,DG_i})$.

Scenario IV-A and Scenario IV-B are defined to investigate the impact of the DG grid connection strength on the system stability, when DG is implemented either concentrated in one substation (*Scenario IV-A*) or spread out over many substations (*Scenario IV-B*). In Scenario IV-A it is assumed that when DG is implemented at load bus-i (DG_i), it is implemented in one particular point in the distribution network regardless the "size of DG", so that the parameters of (4.2) are constant: $jX_{T,DG_i} = j0.01$ pu and $jX_{L,DG_i} = j0.05$ pu (R_{L,DG_i} is neglected). In Scenario IV-B, it is assumed that DG is implemented in a distribution network with radial laterals; every 100 MW of aggregate DG is implemented in a different lateral. The parameters in (4.2) are $jX_{T,DG_i} = j0.01$ pu, R_{L,DG_i} is neglected and jX_{L,DG_i} is set according to (4.3) with $par(P_{DG_i}) = \frac{P_{DG_i}}{100.0}\frac{(\text{MW})}{(\text{MW})}$ rounded to the next larger integer. Thus, it is assumed that the larger the size of the aggregate DG is, the more spread out the locations of the DG units are, and the lower the impedance between DG and the transmission network becomes. Ten sub-scenarios are derived from both Scenario IV-A and Scenario IV-B by varying the DG penetration level in the test system from 3.33% to 33.33% in steps of 3.33% (4.1).

4.2.3 Transient Stability Simulation

The transient stability of the test system is investigated by applying a permanent three-phase fault, cleared after 150 ms, to all possible branches taken into account in the $N-1$ adequacy standard (Table 4.1).

To assess the transmission system stability, the maximum rotor speed deviation and the oscillation duration are investigated according to Section 3.3.

4.2.4 Simulation Results

Scenario III

With the DG penetration level fixed at 20%, increasing the impedance of the connection of the DG to the transmission system generally results in a slightly less stable transmission system, regardless of the DG technology implemented.

Figure 4.7 shows an example of the slightly increasing value for the transient stability indicators along with the increasing impedance connecting DG according to Scenario III-A, when the DG is implemented as synchronous machines without grid voltage and frequency control (SM). In Figure 4.7, the x-axis represents the number of the branch where a fault is applied. The y-axis represents the ten sub-scenarios with the increasing impedance value of the DG connection as defined in Scenario III-A, and the z-axis represents the stability indicator. For a better overview, the z-axis represents 'relative' values of the indicators used: the difference between the resulting maximum rotor speed deviation and the base case value and the difference between the resulting oscillation duration and the base case value. The base case corresponds to sub-scenario nr. 1.

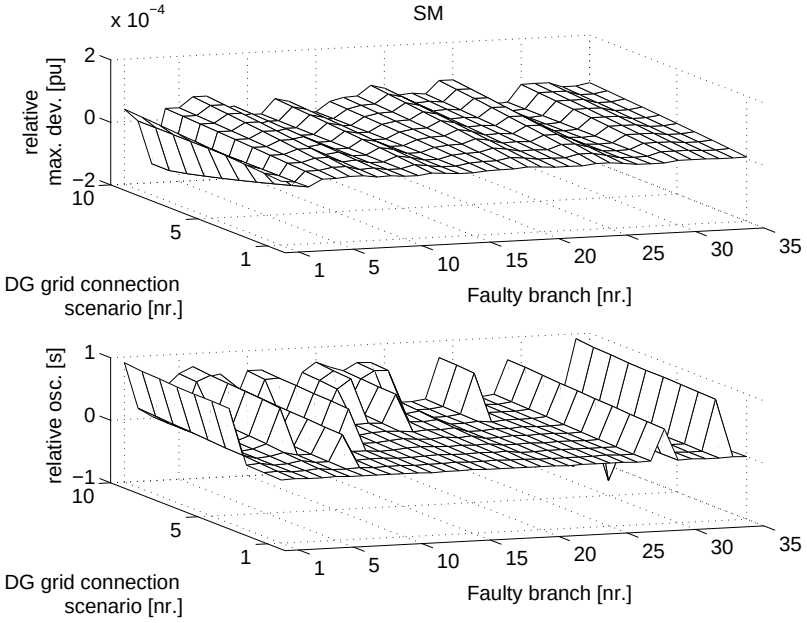

Figure 4.7: Relative value in system indicators (actual value minus base-case value (sub-scenario nr. 1)): maximum rotor speed deviations (upper graph); oscillation durations (lower graph) when Scenario III-A is applied and DG is implemented as synchronous machines without grid voltage and frequency control (SM)

When the resistive part of the impedance between DG and the transmission system is taken into account (Scenario III-B), similar results are obtained. Scenario III-B gives slightly higher values of the stability indicators (i.e. a reduced system stability) than Scenario III-A. This can be seen from the positive values that result from the substraction of values of Scenario III-A from those of Scenario III-B. Figure 4.8 shows an example of those differences, when DG is implemented as synchronous machines (SM).

Scenario IV

DG that is concentrated in one lateral (according to Scenario IV-A) results generally in higher system indicators than when the DG is spread out of several laterals (according to Scenario IV-B). By comparing the 'relative' values of the stability indicators (i.e. the difference between the maximum rotor speed deviations of Scenarios IV-A and IV-B and the difference between the oscillation durations of Scenarios IV-A and IV-B) generally positive values are obtained. Figure 4.9 shows an example of those differences, in case DG is implemented as synchronous machines (SM).

4.2.5 Remarks

In this section a general tendency is found that the values of the stability indicators slightly increase when the impedance in between the DG and the transmission system is raised. A higher impedance leads to a less stable system [63], [69].

Taking into account the resistance of the distribution system in which the DG is implemented, results in slightly higher stability indicators than when the resistance is neglected. This observation can be explained as follows. When we take the resistance into account, higher active power losses occur that must be supplied by the swing generator (one of the CGs) and gives somewhat larger power flows in the transmission lines.

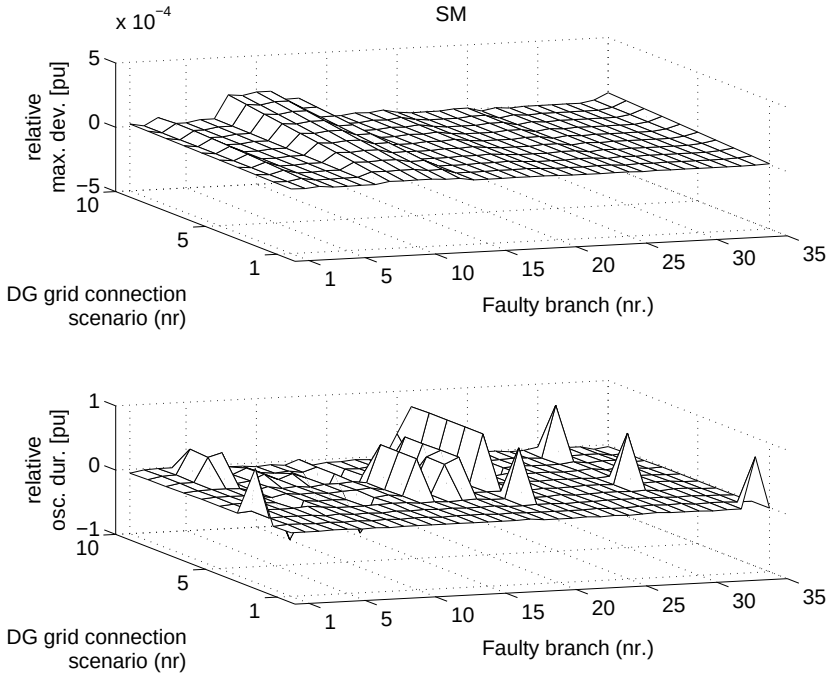

Figure 4.8: Relative value in system indicators (Scenario III-B minus Scenario III-A which means including resistance): maximum rotor speed deviations (upper graph); oscillation durations (lower graph) when DG is implemented as synchronous machines without grid voltage and frequency control (SM)

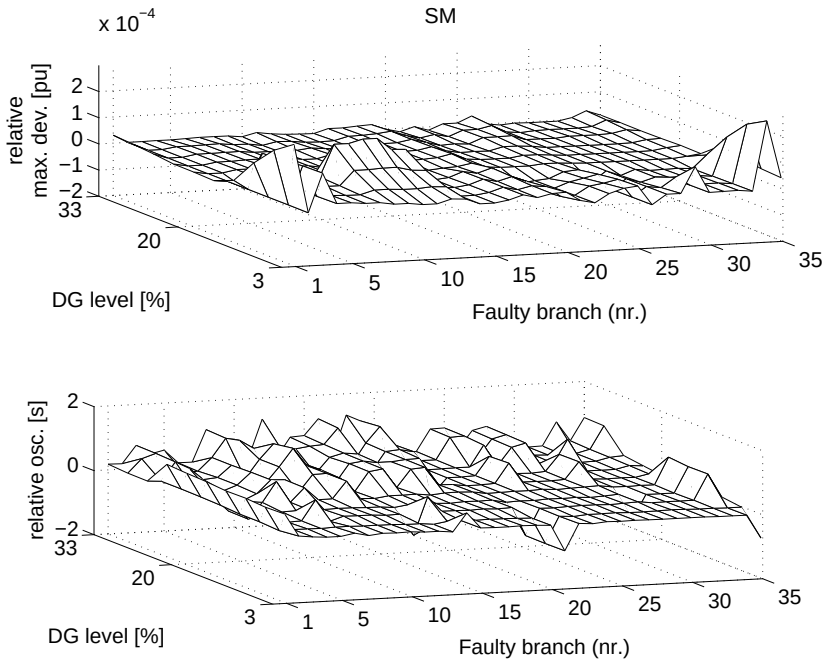

Figure 4.9: Relative value in system indicators (Scenario IV-A minus Scenario IV-B which means more spreading of DG): maximum rotor speed deviations (upper graph); oscillation durations (lower graph) when DG is implemented as synchronous machines without grid voltage and frequency control (SM)

4.3 DG Penetration Level and Technology Impacts

Although the results of Sections 4.1 and 4.2 show that some impact of raising DG penetration levels on the system stability can be generalized as regardless of the DG technologies implemented, some small differences were observed. This section investigates the impacts of raising DG penetration levels on the system transient stability with respect to the DG technology.

4.3.1 Simulation Scenario

The test system, the DG technologies and the DG topology are set according to the simulation setup described in Section 3.5, whereas DG penetration levels are varied in the similar way as in Section 4.1 with a minor difference. In Section 4.1.1 DG penetration level is raised in steps of 3.33% and the load increment is adjusted accordingly. In this section, the load is increased in steps of 5%, and the DG penetration level is adjusted accordingly.

4.3.2 Transient Stability Simulation

The transient stability of the test system is investigated by applying a permanent fault to a transmission line. The transmission line between buses 15 and 16 (Figure 3.7), carrying 315 MW and 150 Mvar in the pre-fault scenario with no DG implemented, is chosen arbitrarily. The fault is cleared by tripping the faulty line after a certain fault duration. Three fault durations are simulated: 100, 150 and 200 ms. The eleven penetration level scenarios are extended with three sub-scenarios based on the three fault durations. Furthermore, five DG technologies as described in Section 3.5.2 are simulated together with the eleven penetration levels and the three fault durations. To assess the system stability in these scenarios, the maximum rotor speed deviation and the oscillation duration are used again.

4.3.3 Simulation Results

At a first glance, the simulation results show that the implementation of DG in the test system (along with the increase in the loads) affects the transient stability differently depending on DG penetration level, DG technology, and fault duration. To investigate the results systematically, each of the five main DG technologies simulated in this section - the squirrel cage induction generator, the uncontrolled or controlled synchronous generator, and the DG coupled through an uncontrolled or controlled power-electronic interface - are commented on separately.

Induction Generator

Figure 4.10 shows the worst values of maximum rotor speed deviation (top) and oscillation duration (bottom) for large centralized generators, when DG with induction generator technology is implemented. The results are shown for three fault-time durations: 100, 150, and 200 ms.

When a 100 ms fault duration is applied, the maximum rotor speed deviation decreases when the penetration level increases from 0% up to 29%. However, increasing the penetration further, up to 33%, leads to growing maximum rotor speed deviations. When 150 and 200 ms fault clearing durations are applied, the maximum rotor speed deviations decrease when the penetration level rises from 0% up to 23% and they increase when the penetration goes further up to 33%. Overall, the relative changes of the maximum rotor speed deviations (either increasing or decreasing) are within 11% (at 100 ms fault clearing duration) and 14% (at 150 and 200 ms fault clearing durations).

Furthermore, when 100 and 150 ms fault clearing durations are applied, the oscillation durations tend to decrease. When the duration is 200 ms the oscillation duration tends to increase with increasing DG penetration level.

When the maximum rotor speed deviation and the oscillation duration of each large generator are displayed separately (Figure 4.11), a better insight is obtained. For the three fault durations applied, it can be observed that the maximum rotor speed deviation of each large generator tends to go up or down

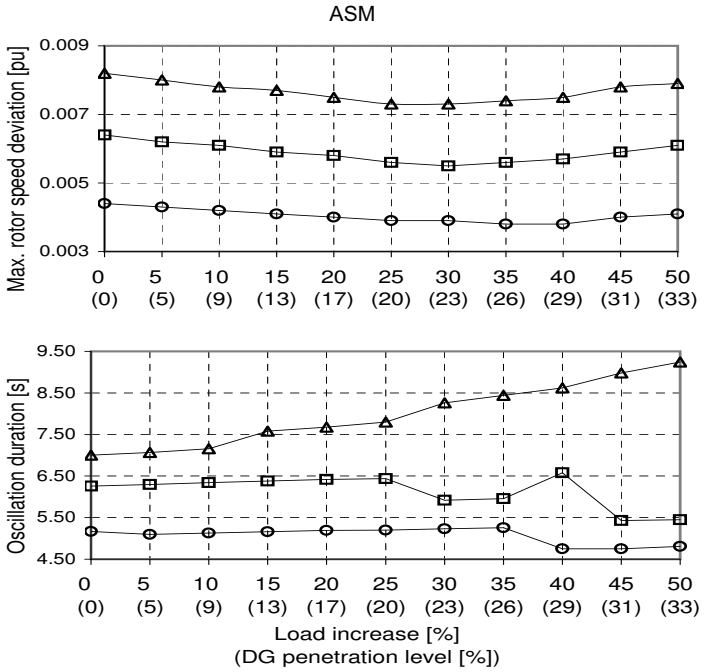

Figure 4.10: Maximum rotor speed deviation (top) and oscillation duration (bottom) using induction generator (ASM) DG technology, and fault clearing durations of 100 (○), 150 (□), and 200 ms (△)

consistently. The curves of the maximum rotor speed deviation in Figure 4.10 (first descending, then ascending) are thus made up by two generators: one with an increasing, and the other with a decreasing maximum rotor speed deviation due to the growing DG penetration level. A similar tendency is found for the oscillation duration.

These results may be explained as follows [47], [71]. The effect of induction generators on the power system stability depends on their distance to the synchronous generators:

- When they are located near the synchronous generators and the latter speed up during a fault, the stator frequency of the induction generators increases. This leads to a decrease in the slip frequency and thus in extra generated power, which in turn slows down the speeding up of the synchronous generators.
- When they are at a larger distance and more weakly coupled to the synchronous generator, its speeding up during the fault results in an increasing reactive power demand. This leads to a lower terminal voltage at the far away synchronous generator and thus in a decrease of the synchronizing torque and a faster increase in rotor speed.

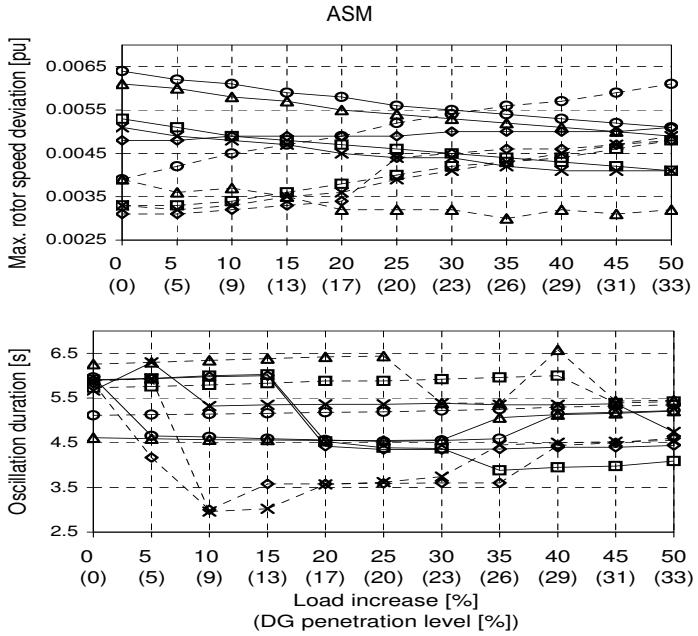

Figure 4.11: Maximum rotor speed deviation (top) and oscillation duration (bottom) for each large centralized generator when induction generator (ASM) DG technology is implemented and a 150 ms fault clearing duration is applied. Generator nr. 1 (G1) = dash-○; G2 = dash-△; G3 = solid-×; G4 = solid-□; G5 = solid-◊; G6 = solid-○; G7 = solid-△; G8 = dash-×; G9 = dash-□; G-10 = dash-◊

As an example, the synchronous generator 1 at bus 39 (Figure 3.7) is considered. From Figure 4.11, it is clear that generator 1 shows an increasing maximum rotor speed deviation with growing DG penetration levels. Since at buses 1, 2 and 9 no DG is implemented - i.e. generator 1 is not located close to DG - this result is what could be expected: a faster increase in rotor speed with growing DG penetration levels.

Synchronous Generator

The worst values of the transient stability indicators for the large centralized generators, in case that DG is implemented using uncontrolled or controlled synchronous generator technologies are displayed in Figure 4.12. The maximum rotor speed deviation consistently decreases when DG penetration level is increased. However, the oscillation duration is different when these two technologies are applied. While the oscillation duration tends to increase in case of uncontrolled synchronous DG, it tends to decrease in case of controlled synchronous DG.

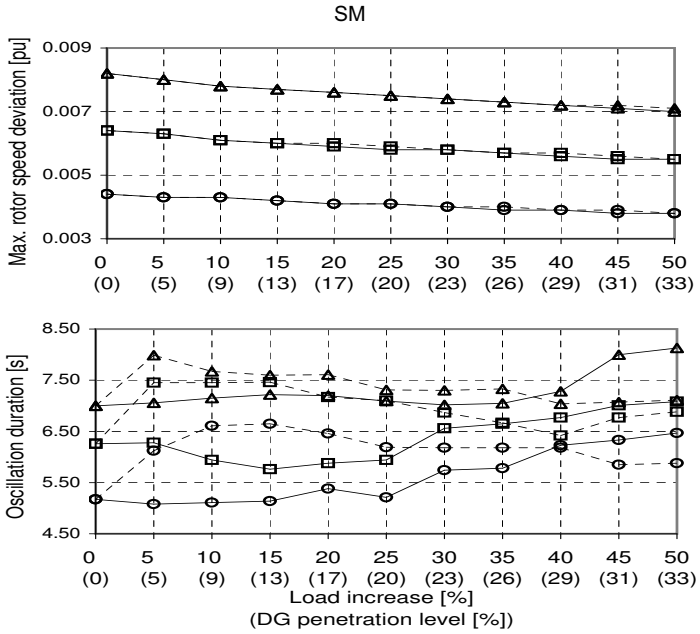

Figure 4.12: Maximum rotor speed deviation (top) and oscillation duration (bottom) when DG using uncontrolled, SM, (solid lines) and controlled, SMC, (dashed lines) synchronous generator technologies are implemented and fault clearing durations of 100 (○), 150 (□), and 200 ms (△) are applied

The results can be explained as follows. Both uncontrolled and controlled distributed synchronous generators are equipped with an excitation winding on the rotor, keeping the generators excited during the fault. When a fault occurs, the distributed generators supply the fault current and the voltage drop during the fault is not as severe as is the case without DG. Thus during the fault, a higher DG penetration level results in a higher terminal voltage and less overspeed.

Power-Electronic Converter

When DG is coupled through uncontrolled or controlled power-electronic converters, the maximum rotor speed deviation of the synchronous generators decreases consistently with increasing DG penetration levels (Figure 4.13). The oscillation duration shows different results. Along with increasing DG penetration levels, the oscillation duration of the synchronous generators tends to increase when DG is coupled through uncontrolled power-electronic converters. However, it tends to decrease slightly if DG is coupled through controlled power-electronic converters.

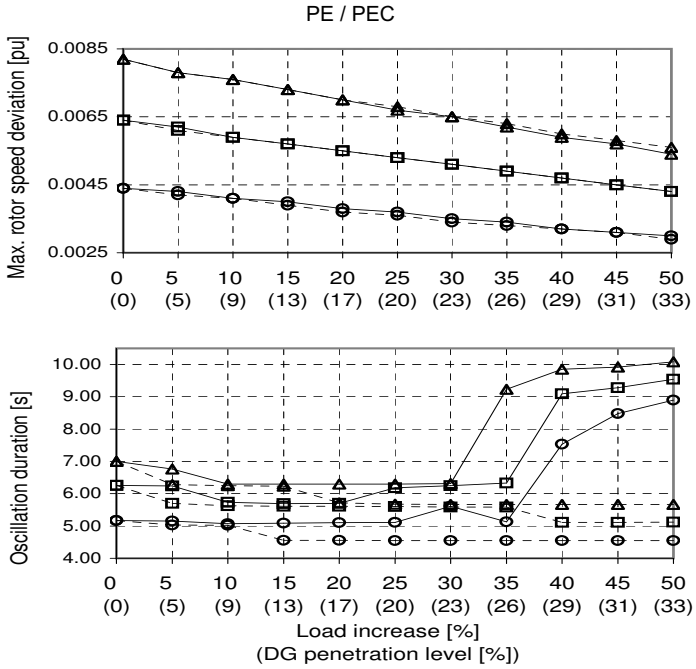

Figure 4.13: Maximum rotor speed deviation (top) and oscillation duration (bottom) when DG is coupled through a power-electronic interface without (solid lines) or with voltage and frequency control (dashed lines), and fault clearing durations of 100 (○), 150 (□), and 200 ms (△) are applied

The simulation results can be explained as follows. The protection systems applied, disconnect the distributed generators connected through a power-electronic interface as soon as the voltage level drops below 0.85 pu, e.g. during a fault. The protection system reconnects DG as soon as a recovery action is taken and when the voltage level increases again and passes 0.85 pu. Thus, during a fault, the distributed generators are lost and the rotor acceleration of the large synchronous generators is reduced. As the same protection schemes are applied for both controlled and uncontrolled power-electronic converters, the maximum rotor speed deviations are the same.

The different results found for the oscillation durations are caused by the frequency controller actions of the controlled power-electronic converter. When the distributed generators are grid-connected by means of a controlled power-electronic interface, the frequency controller damps the rotor oscillations of the centralized generators after the protection system reconnects the DG.

4.3.4 Remarks

The computations in this section show that the impact of DG on the system stability depends on both DG technology and penetration level. The maximum rotor speed deviation for most of the synchronous centralized generators decreases with increasing DG penetration levels for the main DG technologies, either controlled or uncontrolled. However, when induction generator based DG is implemented, this is only true for generators located in the vicinity of the DG. The results for the oscillation duration are ambiguous, although it appears that the oscillation duration tends to decrease with increasing DG penetration levels when a DG technology equipped with controllers (Section 3.4.1) is applied. This suggests that the performance of the system can be improved by enhancing the control capabilities of the DG technology.

4.4 Protection of Power-Electronics Impacts

In this section, the impact of implementing power-electronic interfaced DG on the system stability is further investigated, with the focus on the two protection systems: DG that disconnects from the network automatically when the voltage drops below a certain level, and reconnects as soon as the voltage recovers and DG that remains connected to the power network during a fault (ride-through-capability [42]).

4.4.1 Simulation Scenarios

The test system and the DG topology are again set according to the simulation setup described in Section 3.5.

DG connected to the grid via a power-electronic converter without grid voltage and frequency control (PE) (Sections 3.4.1) is simulated.

The DG penetration levels in the test system are varied in the same way as in Section 4.1 (*Scenario I*, eleven (sub)scenarios). The DG connected to each load bus produces an amount of active power equal to the increased real power consumption of the load at that particular bus.

Two protection schemes for DG are applied:

- DG is disconnected from the power network when the voltage level of the system drops below 0.85 pu and reconnected as soon as the voltage level passes 0.85 pu (*Protection I*).
- DG remains connected to the network during a fault. However, due to limitations of the components of a power-electronic interface, it is assumed that the current through the power-electronic interface is limited to a maximum value of 1.2 pu. Thus, in case the voltage level drops during the fault, the power supplied by the DG drops accordingly, whereas the current is constant and limited to its maximum value (*Protection II*).

Figure 4.14 shows an example of the different active power output values of converter-connected DG (PE) in case of Protection I (top) and Protection II (middle). The fault occurs between the buses 15 and 16, and both protection schemes, Protection I and Protection II, are applied. The bottom graph shows the voltage of the corresponding bus obtained from the case without voltage and frequency control and Protection I. The case of Protection II results in a slightly different value of the corresponding bus voltage. Yet it is quite comparable to the case of Protection I. The x-axis represents the time and the y-axis represents the DG unit. The z-axis, represents the value of the active power output of the DG unit (top and middle) and the value of the corresponding bus voltage (bottom).

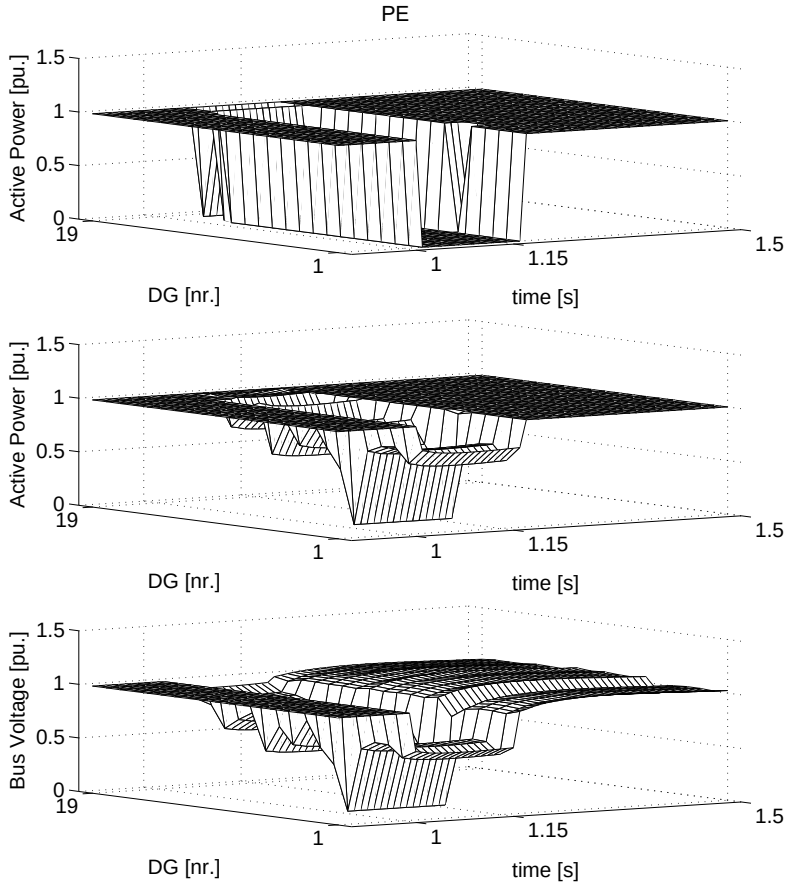

Figure 4.14: DG active power outputs when implemented via a power-electronic interface without grid voltage and frequency control (PE) in the case of Protection I (top) or Protection II (middle) at a DG penetration level of 33.33% and the corresponding bus voltages of Protection I case (bottom)

4.4.2 Transient Stability Simulation

The transient stability of the test system is investigated by applying a permanent three-phase fault, cleared after 150 ms, to all possible branches. The maximum rotor speed deviation and the oscillation duration are again applied.

4.4.3 Simulation Results

To investigate the impact of both protection schemes, the simulation results of both schemes are compared. The values of the indicators in Protection scheme II are generally higher than that of Protection scheme I, especially when DG is implemented without grid voltage and frequency control (PE) (Figure 4.15). This can be explained as follows.

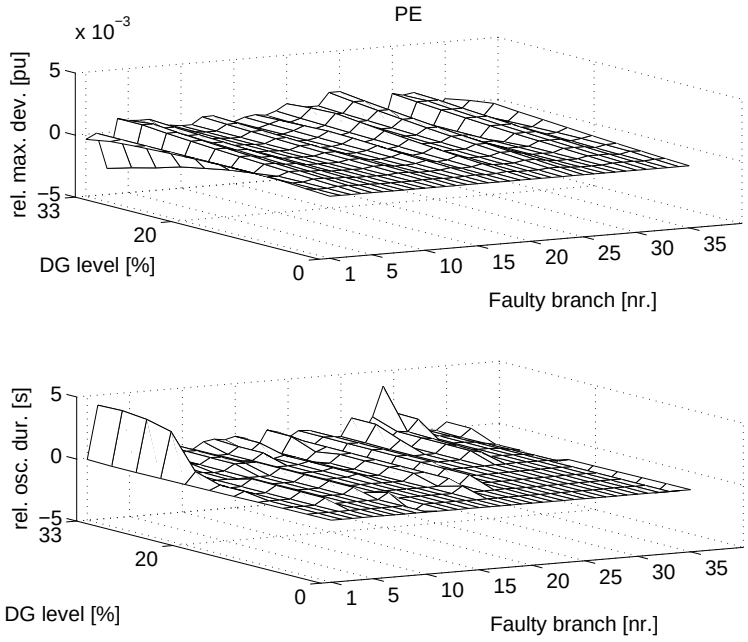

Figure 4.15: Relative values in maximum rotor speed deviations (top) and relative oscillation durations (bottom), i.e. the results of Protection scheme II minus Protection scheme I. DG is connected via a power-electronic interface without grid voltage and frequency control (PE).

In case DG remains connected (Protection II) to the system, DG covers part of the power consumption. As a result, the CG electrical power output, P_e is lower (accelerating power, P_a, is larger then) than when the DG disconnects (Protection I) from the system. In other words, when DG disconnects from the system (Protection I), the part of the power consumption that in Protection

scheme II would be covered by the kept-connected DG is covered by CG. This results in a higher electrical power output, P_e, and less accelerating power, P_a.

4.4.4 Remarks

This section shows that when the power-electronic interfaced DG remains connected to the network during the fault, higher generator speeds result (i.e. reduced transient stability) than in case DG disconnects during the fault. However, from the power supply point of view, it may be important to keep (parts of) the DG connected to the system during a fault in order to supply power to the less involved areas. In this case, a rule could be applied that prescribes when the DG disconnects from the system or when it remains in the system during a fault. As an example, a rule based on the voltage level can be used for this purpose.

4.5 Conclusions

It is well-known that the implementation of DG influences the technical aspects of the distribution grids. However, the impact of a small amount of DG connected to the grid on the power system transient stability has not been treated so often. When the penetration level of DG increases, its impact is no longer restricted to the distribution network, but begins to influence the whole system [76].

In this chapter therefore the DG penetration level on the power system transient stability is analyzed. Several factors are analyzed such as load scenario, DG grid connection strength, DG technology, and the protection scheme of power-electronic interfaced DG. When load is increased and DG is implemented in the distribution grid, the active power generated by the DG is consumed directly by the load at the same feeder and the active power flows on the transmission lines are more or less constant instead of increasing active power flows when CG needs to cover the increased load. In contrast, the active power flows in the transmission lines decrease when DG covers also part of the existing load. Less power flows should intuitively result in a more stable system, and in this work, as the system stability indicators show less maximum rotor speed deviation and shorter oscillation duration. Although a mathematical proof is not established, [31] supports this correlation, and results in this chapter support this as well. It is also found that the values of the stability indicators show a tendency to increase slightly when the impedance between DG and the transmission system is raised. Furthermore, taking into account the resistance of the distribution system in which DG is implemented results in slightly higher stability indicators than when the resistance is neglected.

It is found that the maximum rotor speed deviation for most of the synchronous centralized generators decreases with increasing DG penetration levels for all DG connection technologies, either controlled or uncontrolled. However, when induction generator based DG is implemented, this is only true for gener-

ators located in the vicinity of the DG. The results for the oscillation duration are ambiguous, although it appears that the oscillation duration tends to decrease with increasing DG penetration levels when a DG connection technology equipped with controllers is applied. This suggests that the performance of the system can be improved by enhancing the control capabilities of the DG technology.

It is also found that when the power-electronic interfaced DG remains connected to the network during and after a fault, higher generator speeds appear than in case DG disconnects during the fault (i.e. reduced transient stability). However, from the power supply point of view, it is important to keep (parts of) the DG connected (ride-through-capability) to the system during a fault in order not to loose too much power in the system. In that case, a rule could be applied that prescribes when the DG disconnects from the system or when it remains in the system during a fault, for example based on the voltage level to which it is connected [20].

In general, there appear no significant stability problems up to the 30% DG penetration level examined. Higher DG penetration levels have not been tested in this chapter. Note that in this chapter, all centralized generators remain in the system - as well as their active and reactive power controls - along with the increasing DG penetration levels.

Chapter 5

'Vertical to Horizontal' Transformation of Power Systems

A large-scale implementation of DG may be expected in future. Eventually, the high amount of DG in a power system may cause a number of centralized generators (power plants) to be shut down for efficiency (or environmental) reasons. This results in a gradual transition from the current 'vertical' into a future 'horizontal' power system (Section 1.3). Figure 5.1 illustrates the concept of a 'vertical' and a 'horizontal' power system (redefined from Figure 1.3).

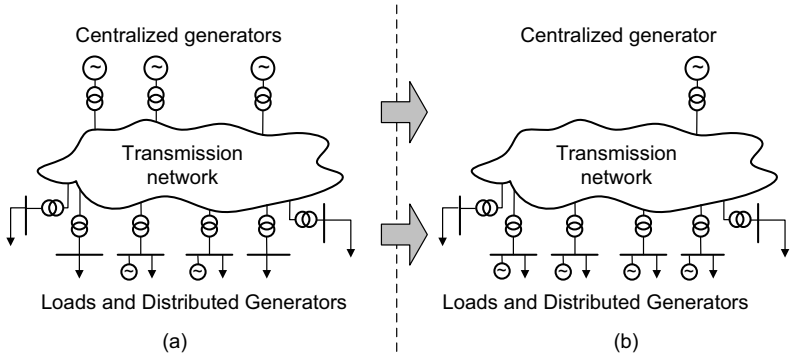

Figure 5.1: Illustration of the 'vertical' (a) and the 'horizontal' power system (b)

In Chapter 4, all centralized generators and their corresponding inertias and control functions remain in the system when the DG level is increased. However, a 'vertical-to-horizontal' transformation of power systems results in

less centralized generators in service and, correspondingly, reductions of their control functions alongside with the increasing DG level. Moreover, the use of large-scale power electronic-interfaced DG units implies a reduction in the rotating masses (inertia) in the system. In this chapter, the impact of such 'vertical-to-horizontal' transformation of power systems on transient stability is investigated.

Simplifications are assumed in shutting down the centralized generators. The main idea is to give a consistent sequence of shutting them down. A simple economic dispatch program is used for the remaining units in service.

The results of this chapter show that based on power system transient stability constraints, a limit of DG penetration level in a power system can be reached.

Some remedies to improve the stability of the system that goes through the 'vertical-to-horizontal' transition are also discussed (Sections 5.3 through 5.5).

5.1 Simulation Setup

Test system, load modeling and DG topology for simulations in this chapter are set according to the simulation setup defined in Section 3.5.

DG is implemented as power-electronic interfaced DG without grid voltage and frequency control (modeled as a constant PQ-source; Section 3.5.2).

The transformation from a vertical to a horizontal power system is done in the following way:

- Both the active and reactive power of all loads are kept constant.
- The penetration level of DG is raised by increasing the fraction of the total load in the test system served by DG.
- DG is connected to every load bus via a j0.05 p.u. impedance at the 100 MVA system base. The fraction of the total load served by DG is distributed among the modeled DG units proportional to the active power consumed by the load at a particular bus.
- The remaining power is divided among the (dispatchable) centralized generator (CG) units by considering the economic operation of the power system, where some CG units, if necessary, are taken out of service.

The DG penetration level in the system is defined as

$$\%DG_{level} = \frac{P_{DG}}{P_{Load,Total}} \times 100, \tag{5.1}$$

a modified version of the definition of DG penetration level used Chapter 4. $P_{Load,Total}$ is the total amount of active load within the test system and P_{DG} is the total amount of active power generated by DG.

Minimum and maximum loading limits of the CG units are assumed. All centralized generators are initially dispatchable and have a piece-wise linear cost curve [53]

$$f_i = a_i P_{CGi} + b_i, \tag{5.2}$$

with f_i the cost of CG unit i to generate an amount of active power P_{CGi}. In (5.2), a_i (incremental cost) and b_i (start-up cost) are constants corresponding to the CG unit i. To differentiate the economic efficiency of each CG, and thus give a consistent sequence of taking out of service centralized generators, the constants a_i and b_i are defined as

$$a_i = \alpha c_i, \tag{5.3}$$
$$b_i = \beta c_i, \tag{5.4}$$

with α and β constant, and c_i defined as

$$c_i = \{c_1 + \gamma(i-1) | i = 2, \ldots, 10, \gamma \in \mathbb{R}_+\}. \tag{5.5}$$

In this way, P_{CGj} is higher than the $P_{CG(j-1)}$ (e.g, in the test system CG nr. 10 is more expensive than CG nr. 9, CG nr. 9 is more expensive than CG nr. 8, and so forth). An optimal power flow (OPF) program, with *objective function to minimize the fuel cost* is then run each time the DG penetration level is raised. As the main constraint, the voltage limits with 5% margin are set in this OPF program. The most inefficient CG unit whose power output falls below its minimum loading limit, is taken out of service, and a fixed shunt device is implemented at the location of the shut down CG to compensate the former's reactive power generation. The optimal power flow program is then re-run. In this way, the 'vertical-to-horizontal' transformation of the power system, is simulated. The flowchart of Figure 5.2 illustrates this process. In this study, the value used for increasing the DG level in each simulation is 5%, and a DG level of 90% is set as maximum. A 90% maximum DG_{level} is chosen so that in all scenarios at least one centralized generator remains in operation when the optimal power flow is performed. This generator is necessary to provide a reference frequency for all power electronic converters of the DG units. The stability of these last centralized generators that remain connected determines the stability of the system as a whole.

The transient stability of the test system is investigated by applying a permanent fault to the (arbitrarily chosen) transmission line between buses 15 and 16 . A single line diagram of the test system is shown in Figure 3.7, and detailed in Appendix B. It is assumed that the fault is cleared by tripping the faulty line after 100 ms.

The protection system applied disconnects the power-electronic interfaced DG units as soon as the voltage level drops below 0.85 pu, e.g. during a fault, and it reconnects the DG as soon as the voltage level increases again above (or equal to) the 0.85 pu level (Section 3.4.1) after the fault is cleared. In Section 5.5, DG with "ride-through" capability is applied. In that case, the rated current of the DG converter is limited to 1.2 pu of the power electronic connected DG.

To assess the transmission system stability, two transient stability indicators, maximum rotor speed deviation and oscillation duration (Section 3.3), are used to observe the rotor angle stability and to quantify the severity of the rotor

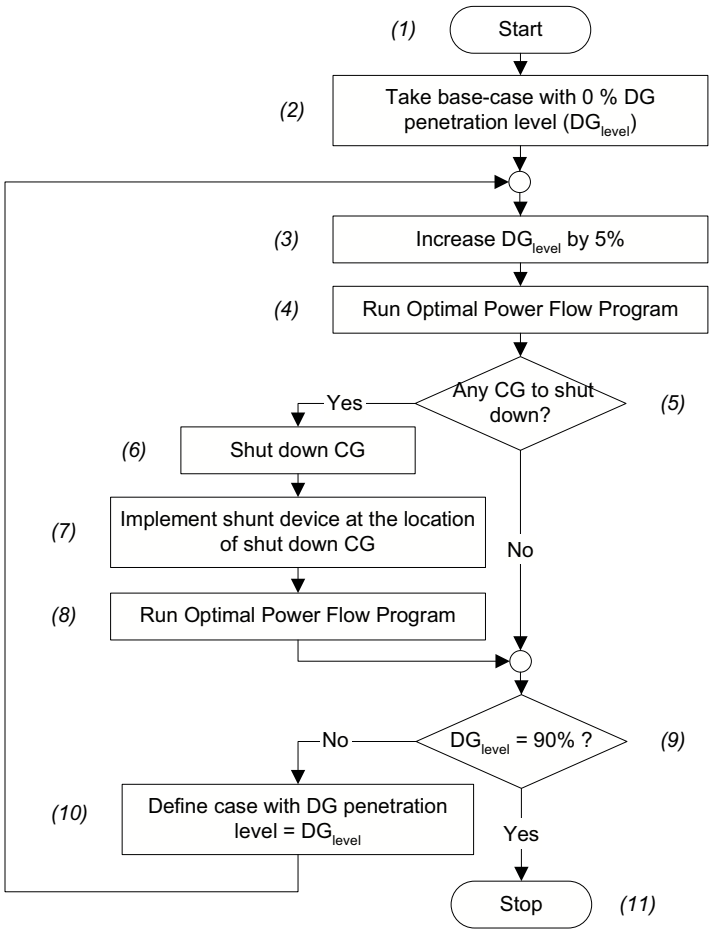

Figure 5.2: Flowchart depicting 'vertical-to-horizontal' transformation process

speed oscillations of the remaining centralized generators. The transient stability performance of the cases within the vertical-to-horizontal transformation scenario is compared based on these indicators.

5.2 Simulation Results Case I

The approach depicted in Figure 5.2 results in a number of simulations for a power system that goes trough the 'vertical-to-horizontal' transformation. As a result of performing the optimal power flow, CG units are taken out of service as the DG penetration level increases. The result of this process is illustrated in Figure 5.3. In this research, each shutdown CG unit is replaced by a fixed (at

one value) reactive shunt device (cheaper than the more sophisticated variable switched shunt devices or FACTS devices). With this approach, the power flow program keeps 4 centralized generators in operation. Note that due to the small values, in Figure 5.3 the output power generated by CG nr. 2 and CG nr. 4 are not clearly visible. This is called *Case I.*

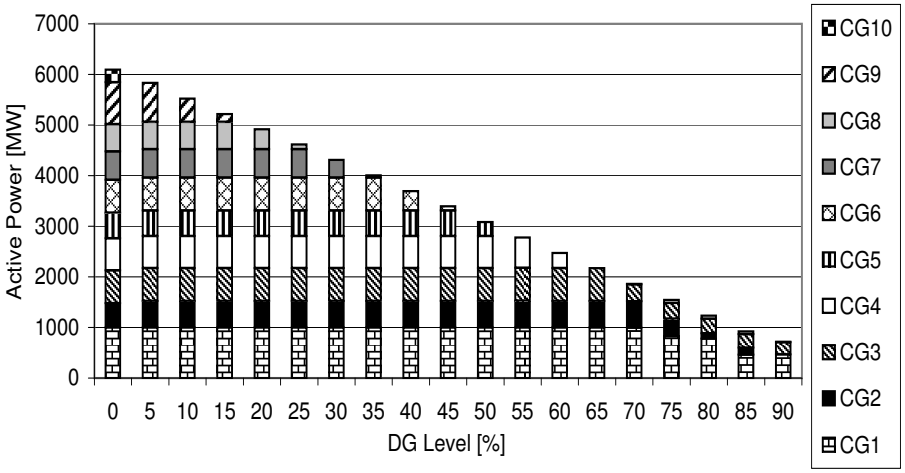

Figure 5.3: Dispatched CGs as a function of the DG penetration level (Case I)

Figure 5.4 shows both stability indicators as a function of the DG level, when a permanent fault to the transmission line between buses 15 and 16 is applied. More detailed values are given in Table 5.1.

It can be observed from Figure 5.4 and Table 5.1, that up to 45% DG level the indicators do not change much. The indicators significantly increase when the DG level rises beyond this value. At 60%-75% DG penetration levels the applied fault causes instability. When DG levels are increased even further (80%-90%), the applied fault does no longer cause instability, although the indicator values are high compared to the values resulting from 5%-45% DG levels.

This result can be explained by considering the fact that two competing mechanisms play a role in influencing the transient stability behavior of the system in this 'vertical-to-horizontal' transformation:

- The total inertia (i.e. stored kinetic energy) within the rotating masses of the machines in the system decreases, so stability decreases.
- The branch flows, in particular in the faulty branch, decrease so stability increases.

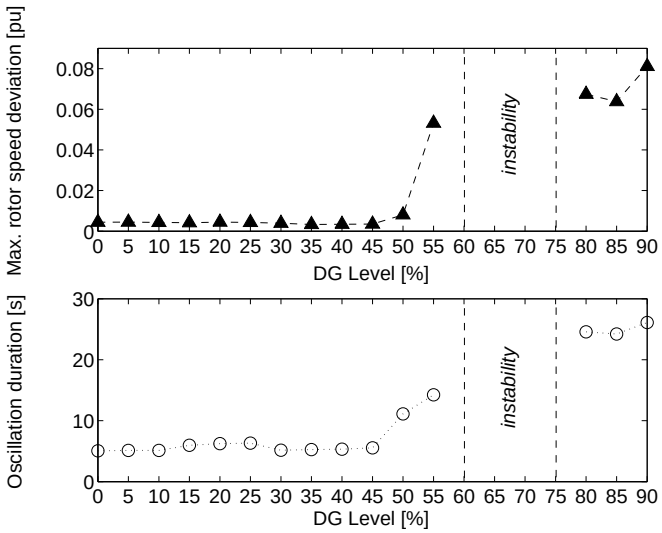

Figure 5.4: Transient stability indicators: maximum rotor speed deviation (top) and oscillation duration (bottom) as function of DG penetration level. Note that at DG levels of 60% through 75% the simulation shows that the applied fault causes instability in Case I

Table 5.1: Stability indicators as a Function of the DG Level (Case I)

DG Level Scenario(%)	Max. Rotor Speed Deviation (pu)	Oscillation Duration (s)
0	0.0044	5.05
5	0.0045	5.13
10	0.0043	5.12
15	0.0042	5.96
20	0.0045	6.23
25	0.0043	6.31
30	0.0039	5.16
35	0.0033	5.25
40	0.0034	5.32
45	0.0035	5.54
50	0.0080	11.12
55	0.0532	14.24
60	*unstable*	*unstable*
65	*unstable*	*unstable*
70	*unstable*	*unstable*
75	*unstable*	*unstable*
80	0.0674	24.57
85	0.0638	24.22
90	0.0811	26.11

In this study, we assume that all centralized generators are of the same type and technology. The inertia constants of all centralized generators in per unit thus are equal. Using the inertia constant H (3.4) and using the dispatched CG values found from the optimal power flow simulation as shown in Figure 5.2, we obtain the total stored kinetic energy of the system at synchronous speed as shown in Figure 5.5. With H the same for all generators, the plot in Figure 5.5 is equivalent to the plot of the sum of machine ratings for the generators connected. The circles (solid line) and their data labels mark the stored kinetic energy (in per unit) at the speed of the moment immediately following fault clearing ($\sum_{i=1}^{n_{CG}} H_i(\omega_i^{pf})^2$; pf stands for post-fault).

The total stored kinetic energy of the system decreases consistently as the DG level increases up to 55% and remains constant thereafter because the minimum of four CGs are kept in the system.

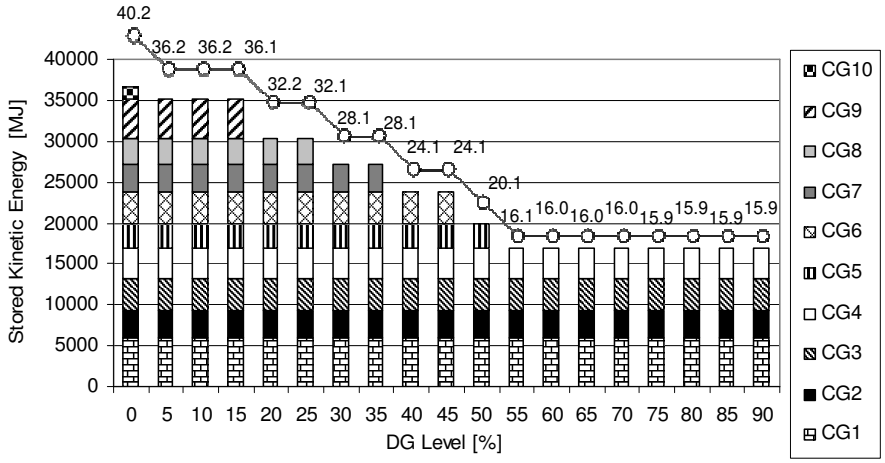

Figure 5.5: Total stored kinetic energy in the system at synchronous speed in Case I. The circles (solid line) and their data labels mark the stored kinetic energy at the speed of the moment immediately following fault clearing

The sum of active power flows in all grid lines, as well as the power flow in the branch between buses 15-16, are shown in Figure 5.6.

The load flow in the test system, particularly the active power flow in the branch between buses 15 and 16 where the fault is applied, behaves differently. This flow initially decreases when the DG level is raised from 0% to 45%. Later, it increases when the DG level is continuously raised up to 70% and decreases again when the DG level increases further to 90% (Figure 5.6). This is due to the combination of implementing DG and taking out of service of CG units during the 'vertical-to-horizontal' transformation of the power system. It can be concluded that in the first place, the decreasing total inertia of the system (total

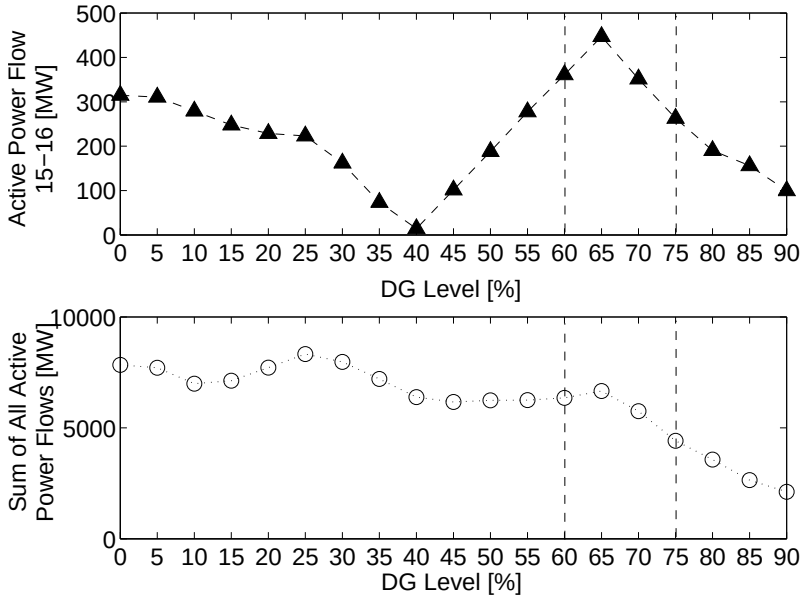

Figure 5.6: Active power flow in the branch between buses 15-16, where the fault is applied in the simulation (top) and the sum of all active power flows in the grid lines of the test system (bottom) in Case I

stored kinetic energy in the system) that occurs when the DG level increases from 0% to 45% is 'compensated' by the decreasing active power flow, so that the stability performance of the system with a DG level up to 45% does not vary much. However, when the DG level increases further, high(er) transient stability indicators for the cases of 50% and 55% DG level are observed, after which instability occurs for 60%-75% DG levels. With 80%-90% DG levels, the system is again stabilized, although the transient indicators for these cases are quite high (Figure 5.4). The reason is that the total inertia of the system is not changed when the DG levels are increased from 55% to 90% (Figure 5.5), while the active power flow in the branch where the fault is applied, experiences its maximum at the 70% DG level (Figure 5.6). Note that in Figure 5.6 the sum of all flows in the system does not experience a monotonic decrease as the DG penetration level goes up, because the objective function of the OPF is to minimize the fuel cost rather than to minimize the branch flows. Therefore, it seems that in the case of 55% and 80%-90% DG levels, the small active power flowing in the branch where the fault is applied 'compensates' for the low total inertia of the system, so that the applied fault does not cause instability (unlike in the case of 60%-75% DG levels with the high active power flowing in the faulty branch and the low total system inertia).

5.3 Rescheduling Generation Case I

Figures 5.4 through 5.6 show that a combination of the smaller total system inertia and the increased power flow for 60%-75% DG levels (compared to 0%-55% and 80%-90% DG levels) results in system instability. Therefore, a logical remedy to eliminate the instability is optimizing the load flow in case of reduction of the total system inertia.

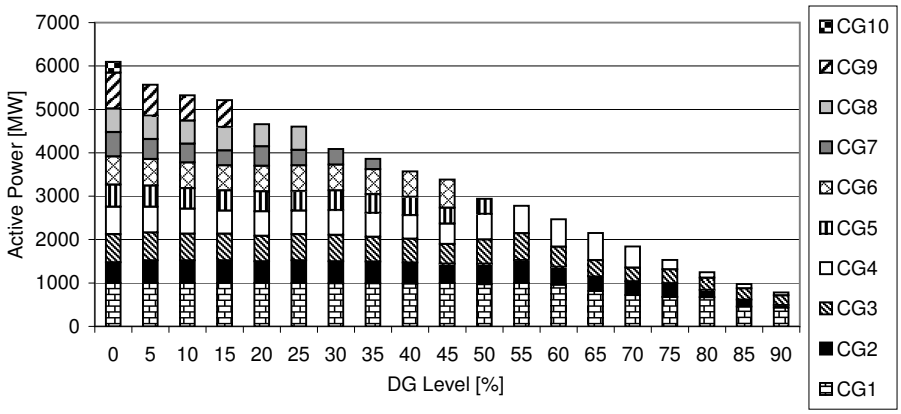

Figure 5.7: Dispatched CGs as a function of the DG penetration level, Case I after CG outputs are rescheduled

In this section, the outputs of the remaining centralized generators (CGs) in the system are rescheduled to alleviate instability problems. For this purpose, after the approach depicted in Figure 5.2 is performed in which some CG units are taken out of service, an OPF program is run, with the objective function set to minimize the losses, so that the sum of all branch flows and the flow in branch 15-16 are more or less minimized. Figure 5.7 shows the dispatched CG units as a function of the DG levels after the CG outputs are rescheduled. Figure 5.8 shows the corresponding sum of all branch flows and the flow in branch 15-16. As may be expected, after the load flow is optimized, the instabilities for cases with 60%-70% DG levels are eliminated (Figure 5.9). It is not obvious that in all cases rescheduling of generation is effective enough, but here it is.

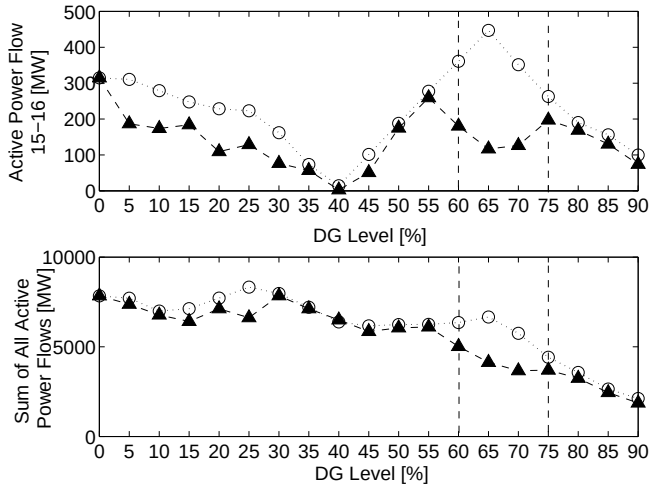

Figure 5.8: Active power flow in the branch between buses 15-16 where the fault is applied in the simulation (top) and the sum of all active power flows in the grid lines of the test system (bottom). The triangles (dashed line) mark the results of rescheduling CG outputs and the circles (dotted line) mark the original Case I

5.4 Simulation Results Case II

In Section 5.2, if a CG unit is taken out of service, a fixed switched shunt device is used to replace it and to provide reactive power (Figure 5.2, step No. 7). When the gradual transition is continued, once a CG unit is taken out of service, the topology and reactive power balance of the test system are changed. Since this fixed switched shunt device has no flexibility of supporting the voltage in the system, unlike the replaced CG units, the power flow program forces the 4 generators to keep running, in order to fulfill the reactive power demand changes within the system and to hold the voltage in between specified margins.

To avoid this constraint, in this section, instead of using a fixed switched shunt device, a variable switched shunt device is used in the process No. 7 of the flowchart depicted in Figure 5.2. In this way, the reactive power supplied by the shunt device is adjusted at every step of the gradual transition in such a way that the voltage at the bus is kept between 0.95–1.05 pu. As a result, when the DG level increases up to 90%, the load flow program can manage up to only 2 generators running (8 CG units are taken out of service). This is called *Case II*. Figure 5.10 shows the resultant dispatched CG. The corresponding inertias of the CG units are shown in Figure 5.11.

Applying the 100 ms permanent fault clearance on the line between bus 15-16 results in the indicators shown in Figure 5.12. In Case II, rescheduling the output power of CG units only improves the indicator at a DG level of 60%.

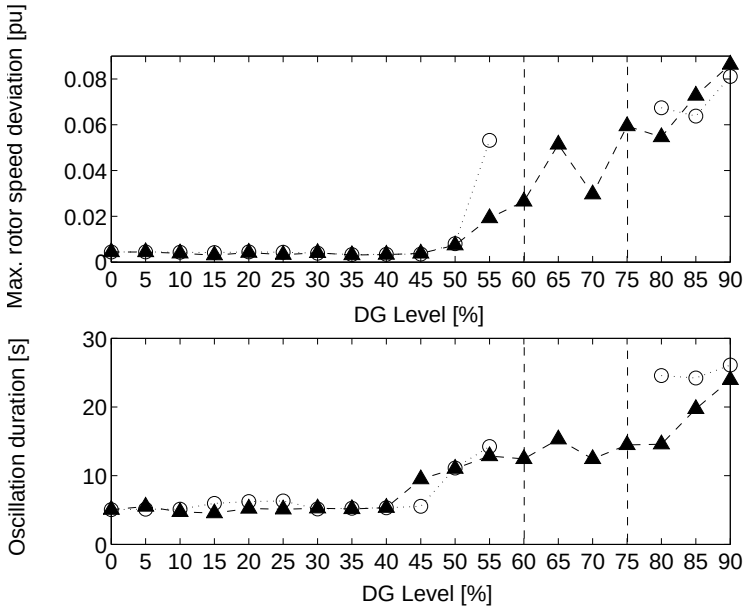

Figure 5.9: Transient stability indicators: maximum rotor speed deviation (top) and oscillation duration (bottom) as a function of the DG penetration level. The triangles (dashed line) mark the results of rescheduling CG outputs and the circles (dotted line) the original case. Note that by rescheduling CG outputs, the applied fault does not cause instability at DG levels of 60% through 75%

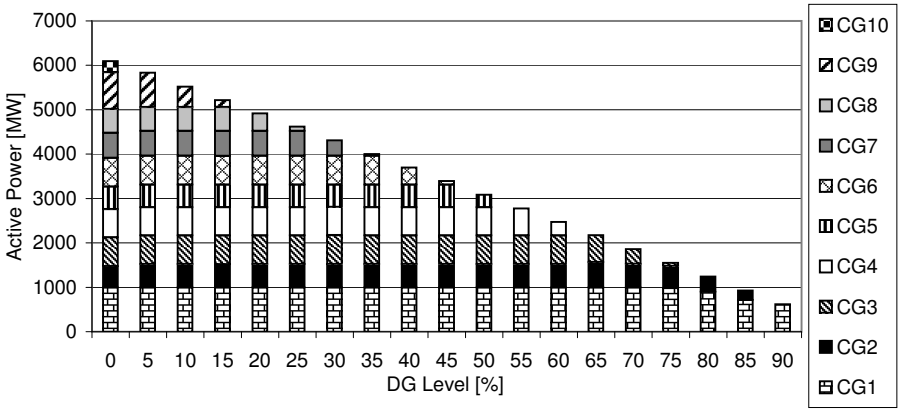

Figure 5.10: Dispatched CGs as a function of the DG penetration level when variable, instead of fixed, shunt devices are used (Case II instead of Case I)

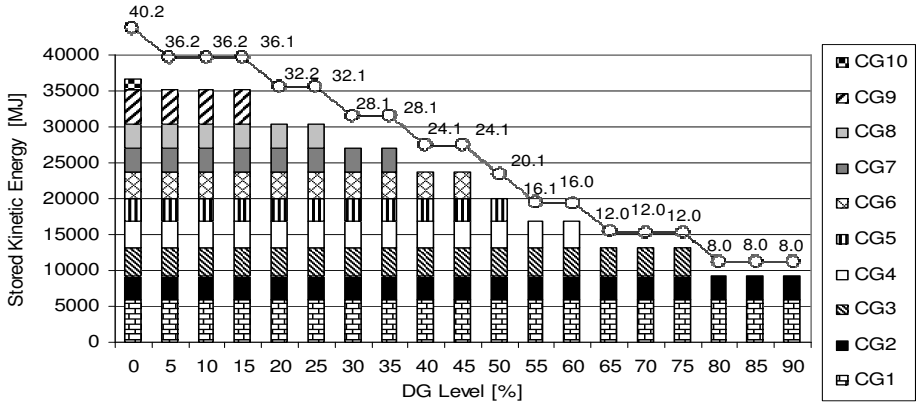

Figure 5.11: Total stored kinetic energy in the system at synchronous speed, as a function of the DG penetration level in Case II. The circles (solid line) and their data labels mark the stored kinetic energy (in per unit) at the speed of the moment immediately following fault clearing

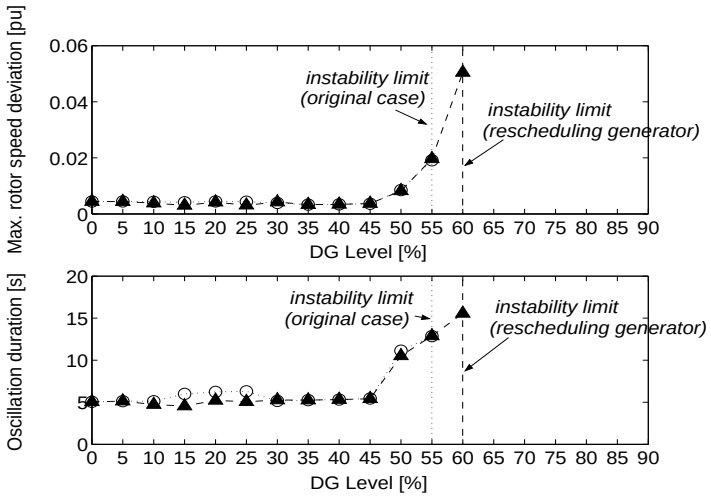

Figure 5.12: Transient stability indicators: maximum rotor speed deviation (top) and oscillation duration (bottom) as a function of the DG penetration level. The circles (dotted line) mark Case II and the triangles (dashed line) the results of rescheduling CG output in Case II. Note that by rescheduling CG outputs, the applied fault does not cause instability at DG levels of 60%

As shown in Figure 5.13, the load flow in the case of 60% DG level with rescheduling CG units is much improved compared to the original one of 60% DG level. At higher DG level rescheduling CG does not help, although the load flow still decreases. This result is logical when the inertia decreases. This leads to the conclusion that there is a limit to the DG penetration level in power systems for the test system used.

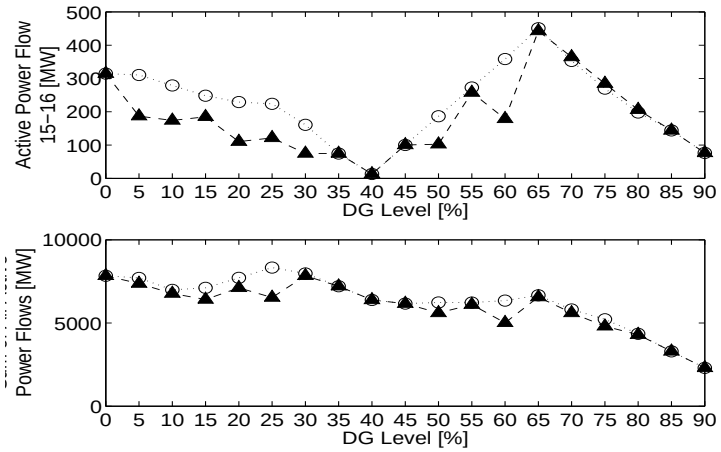

Figure 5.13: Active power flow in the faulted branch (top) and sum of all active power flows in the grid lines of the test system (bottom) in Case II. The triangles (dashed line) mark the results of rescheduling CG outputs and the circles (dotted line) the original Case II

This is interesting as so far the DG penetration level is mostly straightforwardly used without a limit. This, however, does not explicitly take into account how many CG units still are in operation to provide the inertia or reactive power service to the system. Therefore, this result suggests another way of defining the limit of DG penetration level. This new approach must be based on the stored kinetic energy provided by the system. Like the example in this section, the DG level is limited when the system has a total inertia of 30% or less compared to the original one. But, the availability of reactive power support can influence this limit.

The limit obtained in this section is sensitive to the network/test system and vertical-to-horizontal scenario. However, the merit of this section is in showing that, in order to determine the DG limit for a given system, analysis has to be done on the network. Similar remedial actions might be needed as discussed here. This requires the specific sequence of shutting down the CG units, and identifying if certain unstable situations are correctable by re-scheduling the remaining generation. Of course all possible faults and branches in the system have to be taken into account in such an analysis.

5.5 DG with Ride-Through Capability

In this section, DG with ride-through capability is applied to the simulation setup of Section 5.4. The rated current of the DG converter is limited to 1.2 pu of the power electronic connected DG.

As loads are equally divided in constant impedance, constant power and constant current, it is shown that the use of ride-through capable DG results in an improved voltage support for the system, and hence in system stable operation even up to 80% penetration levels. Figure 5.14 shows the results of system indicators when ride-through DG is used. Figure 5.15 shows the voltage level at a certain bus in the system for 50% and 55% DG respectively. This result again proves that the limit of DG penetration level is influenced by a number of factors such as system inertia, reactive power support, and protection mechanism of the power-electronic interfaced DG.

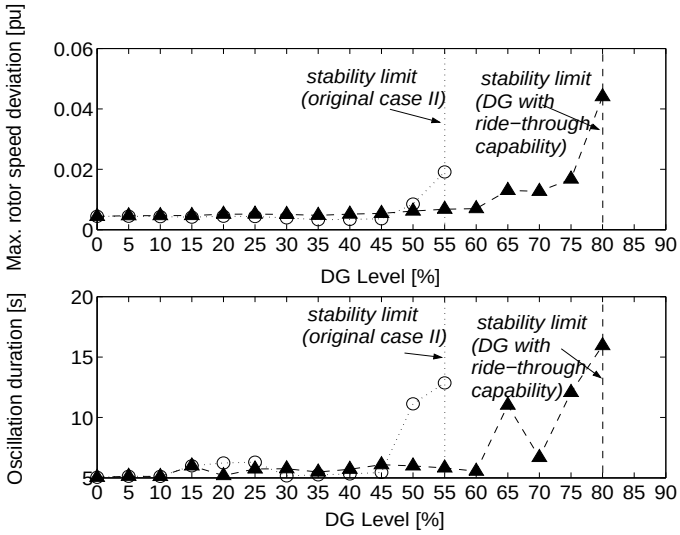

Figure 5.14: Transient stability indicators: maximum rotor speed deviation (top) and oscillation duration (bottom) as a function of the DG penetration level. The circles (dotted line) mark the original Case II and the triangles (dashed line) the results of applying DG with ride-through capability in this case. Note that by applying DG with ride-through capability, the applied fault does not cause instability at DG levels of 60% through 80%

The results shown in Figure 5.14 are consistent with those of Chapter 4. When the penetration level of DG is low, disconnecting DG from the system during fault acts like introducing a resistive load to the system, damping the synchronous machine oscillations (higher indicators values at DG level up to 50% when DG is kept connected). However, in the higher level, when DG is supporting the voltage, it improves system stability.

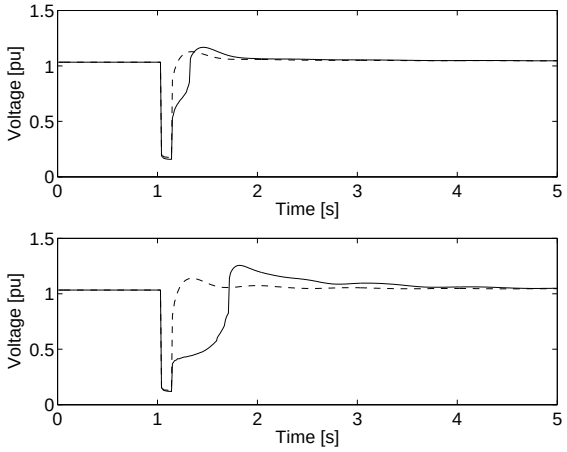

Figure 5.15: Node voltage of bus 16 at 50 % DG level (upper graph) and 55% DG level (lower graph). The solid lines correspond to the original Case II (i.e. DG is disconnected during the fault), the dashed lines to the case where ride-through capability DG is used

5.6 Remarks

In this section, it is assumed that all power electronic interfaced DG units require a reference frequency for their proper operation, i.e. the power electronic converters need a frequency reference taken from the grid. Therefore, within this chapter, the 'vertical-to-horizontal' transformation is limited until at least two centralized generators are still running (Section 5.4). The remaining CG units albeit small in percentage (e.g., only 2 units) are crucial for the operation of the DG units and thus the whole system to give the frequency reference to the power-electronic interfaced DG. When these machines are unstable, they cannot be simply disconnected from the system. Moreover, when these CG units provide additional reactive support, it is even more important not to lose these units.

5.7 Conclusion

Higher penetration levels of DG leads to taking out of service of centralized generators. In this way, an increase in DG penetration level is followed by a decrease in inertia and reactive power support ability in the system. Power system inertia and the respectively stored kinetic energy of the total generation system is an important component influencing power system stability [43]. Therefore, intuitively when the increasing penetration level of converter connected DG that adds no inertia to the system is in parallel with the decreasing

inertia due to taking out of service of centralized generators, the system will be more vulnerable to disturbances [48]. This chapter examines the impact of such a change in supply structure on the system transient stability. Studies on the impact on the power system with DG and limited inertia have been presented in literatures [38], [44]. Yet, the contribution of this work is the more fundamental approach of transforming a power system from the classical 'vertically-operated power system' supported mainly by several large centralized generators into a 'horizontally-operated power system', having a large number of small to medium-sized distributed generators, that is where the simultaneous effects of increasing DG and decreasing system inertia occurs.

It is then found that a limit to DG penetration level in a given power system can be reached. This limit is based on the total kinetic energy remaining in the system and the reactive power support scheme adopted. This finding is interesting since DG penetration level is classically defined as a share of active power output generated by DG units compared to the total active power generated by all generators in the system, or as a share of the active power output generated by DG units compared to the total load. The transient stability analysis results that the ability of centralized generators to supply supporting services like system inertia and reactive power, is of most importance. Therefore a limit in DG penetration level cannot solely be set based on the proportion of the active power production of DG.

Reactive power support depends significantly on the network topology and the optimal power flow strategy. Therefore, the limit obtained is sensitive to the network analyzed and the vertical-to-horizontal scenario. Therefore, to determine the DG penetration limit for a specific case, detailed analysis has to be done on the network. Furthermore, both the sequence of shutting down CG units and the strategy for substituting reactive power support have to be specified.

A straightforward remedy for instability problems that may occur could be advocated by assigning certain "must-run" CG units that provide inertia to the system and, in addition, the reactive power support required. Another approach as suggested in literature could be for instance to equip the converter connected generators with control system such that generators contribute in stabilizing the system [37], [43].

If higher DG penetration levels are wanted, sufficient inertia and voltage support must be installed. Doing so, in theory one could consider aiming for 100% DG. This is the subject of the Chapter 7.

Chapter 6

Stochastic Approach to Transient Stability of Power Systems with DG

In Chapters 4 and 5 the transient stability of the power systems is investigated based on a deterministic approach. In this approach, power system parameters are set at the rated values. It is found that the transient stability performance of power systems depends on the (pre-fault) load flow in the system.

It is well known, however, that some parameters of a power system do not behave in a deterministic way. For example, demand fluctuates due to the behavior of customers, that is by definition stochastic. The implementation of renewable–energy–source–based DG also implies a more stochastic approach on the electricity generation side (Chapter 2). This stochastic behavior impacts, among other things, the load flow within the system. Therefore, one may think of analysis methods that incorporate the stochastic nature to investigate the transient stability of the power systems. In fact, this approach is more comprehensive than the deterministic one.

In this chapter, we extend the transient stability analysis to and focus more on the stochastic approach. As the stochastic behavior of a power system is, by nature, extremely complex, we restrict ourselves to the study of the stochastic behavior of the DG output (Chapter 2). Throughout the analysis we assume that every DG unit is a customer-owned synchronous generators; i.e. the owners decide whether the units operate or not. Even though the DG units are now in essence "deterministic" they still characterize stochastic generation. The results from this approach show that the inclusion of the stochastic nature of DG leads to a more complete and detailed view of the system transient stability.

We begin our discussion with the impact of stochastic behavior of DG on the load flow in Section 6.1. The impact on the system transient stability is discussed in Sections 6.2 and 6.3.

6.1 Stochastic Load Flow

In the classical "vertically-operated" power system there is only a "small" number of large centralized generators "dispatchable", i.e. controllable to meet the demand. In the "horizontally-operated" power system, the DG units in the "active" distribution networks, (called Active Distribution Systems (ADS)), are basically "non-dispatchable". This non-dispatchable behavior results from the fact that certain DG units generate power from primary energy sources with inherently stochastic characteristics, such as wind and solar energy (Chapter 2). Even when DG units are in essence "deterministic", if they are customer-owned units, the owners can decide whether the units operate or not. In both cases DG possesses a stochastic generation characteristic, and the modeling discussed in the previous chapters needs be adjusted to account for this.

The power flow solution of a system with stochastic DG is computed by including the stochastic behavior of the parameters of the specified active and reactive power of each bus representing ADS in a power system. With DG implemented in every load bus, each load bus (i.e. distribution network) contains both consumption and generation (modeled as negative consumption) in the steady-state simulation. Therefore, seen from the transmission level, each active distribution system (ADS) can be represented by an aggregated load in parallel with aggregated generation

$$P_{ADS(i)} = \sum_{j=1}^{N_{L_i}} P_{L(i,j)} - \sum_{k=1}^{N_{DG_i}} P_{DG(i,k)}, i = 1, \ldots, N_{ADS}, \tag{6.1}$$

with N_{ADS} the number of ADS, N_{L_i} the number of loads and N_{DG} the number of DG in ADS i. $P_{ADS(i)}$ is incorporated in the load flow algorithm (i.e., as the corresponding $P_{i,sch}$ in the Newton Rhapson algorithm described in Appendix D, by considering that both the rigth-hand side terms of equation (6.1) contain stochastic elements and a stochastic load flow results.

6.2 Stochastic Transient Stability Analysis

A method is proposed to investigate the impact of a large-scale DG implementation on the power system transient stability in which both the stochastic behavior of the DG units and the loads are taken into account. The test system and the simulation setup are set according to Section 3.5.

6.2.1 Simulation Scenario

A 50% DG level is considered, whereas the total load of the test system is kept constant. The fraction of the total load served by the DG is distributed among the DG units, proportional to the active power consumed by the load at that particular bus. The remaining power generation is divided among dispatchable CG units by considering the economic operation of the power system, similar

to the approach done in Chapter 5. Minimum and maximum loading limits, as well as the cost models of the CG units are chosen in such a way that the higher-numbered CG units are more expensive than the lower-numbered ones (e.g. power production with CG_3 is more expensive than with CG_2). An optimal power flow program, whose objective function is to minimize the fuel cost, is run with a DG penetration level increased to 50%. The most inefficient CG units whose power output falls below their minimum loading limits are shut down and switched shunt devices are implemented at the location of the shut down CG units to compensate for the former reactive power generation. In this way, 5 CG units are shut down (i.e CG nr. 6 to 10; see Appendix B).

The DG units are modeled as synchronous generators without grid voltage and frequency control (Chapter 3). A DG unit is connected to every load bus via a j0.05 pu impedance on the 100 MVA system base, and represents the aggregate active power generation of all DG units in an ADS [18]. Customer-owned DG units that are installed in the ADS supply only active power (1 MW rated active power each) and no reactive power. The owners decide whether the units are running or not: i.e. the DG units are randomly connected to and disconnected from the network. Therefore, the aggregated DG unit is stochastically calculated as a binomial distribution where each DG unit within the DES is connected to the system with a probability $p_{(DG=on)}$. We set that $p_{(DG=on)} \times \sum_{k=1}^{N_{DG_i}} P_{DG(i,k)}$ is equal to the load value at bus i. Thus, the maximum DG capacity installed in one load bus ($\sum_{k=1}^{N_{DG_i}} P_{DG(i,k)}$) can be $1/p_{(DG=on)}$ times the rated value. The loads are following a normal distribution, where the mean values equal the rated values (Appendix B), and the standard deviations equal σ. Several scenarios are developed in which both parameters $p_{(DG=on)}$ and σ are varied according to Table 6.1.

Table 6.1: Scenario cases

Case (nr.)	Loads' standard deviation (σ)	Probability that DG unit is turned on ($p_{(DG=on)}$)
1	0.01	0.8
2	0.03	0.8
3	0.05	0.8
4	0.03	0.5
5	0.03	0.7
6	0.03	0.9

A Monte Carlo simulation (MCS) is used to generate samples of aggregate DG output power and load at each load bus. 10,000 samples are generated in each scenario. These 10,000 samples are considered to be sufficient since the MCS converges after 10,000 samples.

6.2.2 Monte Carlo simulation (MCS) Samples

Figure 6.1 shows the MCS generated samples of the active power consumption of each load. The loads are normally distributed functions, where the mean values equal the rated values and the standard deviations σ vary according to scenario nr. 1, 2 and 3 in Table 6.1. The reactive load samples are generated based on the MCS samples of the active load data, by keeping the active and reactive power ratio (P_i/Q_i) at each load bus (bus i) constant. From Figure 6.1, one can observe larger spread around the rated load values in case of an increasing standard deviation (σ).

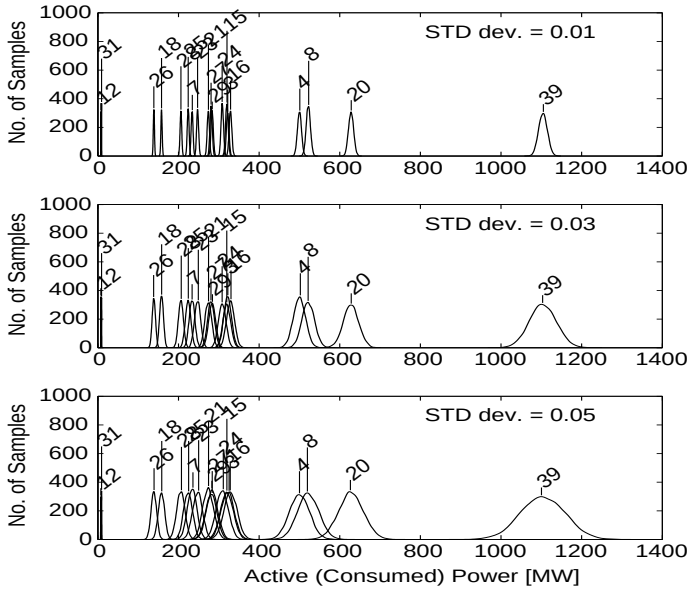

Figure 6.1: MCS generated samples of the active power consumption of each load bus (Numbers in the graphs indicate the number of the load bus)

Figure 6.2 shows the MCS generated samples of the DG power generation at each load bus (except for bus nr. 12 and 31, not displayed due to small values). Figure 6.2 indicates that the spread of the MCS samples of the DG power generation decreases along with a rising probability $p_{(DG=on)}$. The reason is because we set the average power output of the DG units as the rated. Therefore, if each DG unit has a lower probability to be connected to the grid, more DG units will be implemented in order to generate the average power equal to the rated value.

For each MCS sample, the transient stability of the test system is investigated by applying a fault to the transmission line between the buses 15 and 16 of the test system. After 150 ms, the fault is cleared by tripping the faulty line. None of the CG or DG is disconnected during the fault.

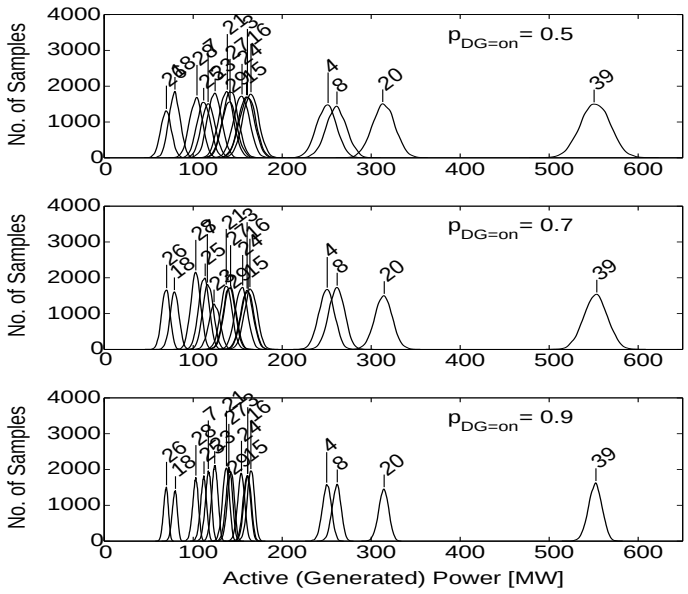

Figure 6.2: MCS generated samples of the DG power generation at each load bus (Numbers in the graphs indicate the number of the load bus)

To assess the transmission system stability, two indicators are applied to quantify the rotor speed oscillations of the CG in the system: maximum rotor speed deviation and oscillation duration (Chapter 3).

Algorithm 4 shows the stochastic transient analysis of power systems with DG in an ADS.

6.2.3 Simulation Results

We run Algorithm 4 for all cases given in Table 6.1. The results are shown in Figures 6.3 and 6.4.

For Cases No. 1–3 the computations show that the spread of the total active power flow in the lines becomes larger with increasing spread in the load (Figure 6.3 (left)). An immediate consequence of this growth is an increase of the spread of probability distributions of the maximum rotor speed deviation (Figure 6.3 (right)). It is obvious from these results that large power flows have a detrimental effect on the damping of oscillations. This is in accordance with what already explained in Chapters 4 and 5.

In Figure 6.4 (left), the spread of the stored kinetic energy is shown for Cases 4–6. Down from Case 6 to 4, the spread of the stored kinetic energy in the system rises as the probability of the DG units to be connected to the grid decreases and only the rotating masses of the connected DG units contribute to the total stored kinetic energy in the system. Due to this effect, the spread

Algorithm 4 Stochastic transient stability analysis

1: Set test system parameters, with $i = 1, \cdots, N$ the number of buses
2: Set DG_{level}, the mean (rated value) μ_i and the standard deviation σ_i
3: Set the number of generators connected in each bus-i $N_{DG,i}$ and the probability of DG being connected $p_{(DG=on)}$
4: Set $N_{MCS} := 1000$
5: **for** $k = 1, \ldots,$ until convergent **do**
6: **for** $j = 1$ to N_{MCS} **do**
7: Generate normal random numbers for P_i and Q_i with μ_i and σ_i
8: Generate random numbers for $P_{DG,i}$ from the binomial distribution with parameters $N_{DG,i}$ and $p_{(DG=on)}$
9: Simulate a permanent fault 150 ms (t_{fault})
10: Calculate maximum rotor speed deviation and oscillation duration
11: **if** MCS convergent with N_{MCS} samples **then**
12: Calculate probability distribution function (pdf) of maximum rotor speed deviation and oscillation duration
13: **quit**
14: **end if**
15: **end for**
16: $N_{MCS} := N_{MCS} + 1000$
17: **end for**

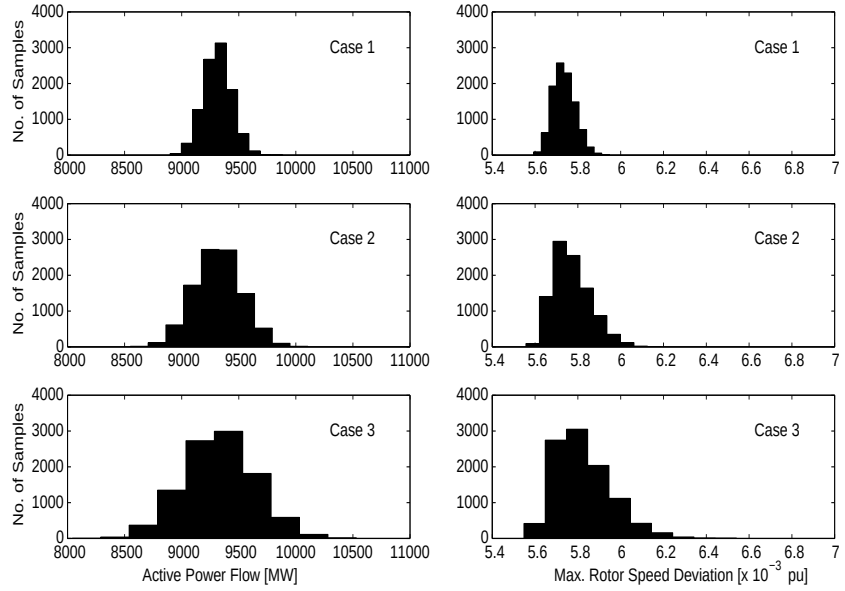

Figure 6.3: Total active power flows (left) and maximum rotor speed deviations (right) in the system in Case 1 (upper), Case 2 (middle) and Case 3 (lower)

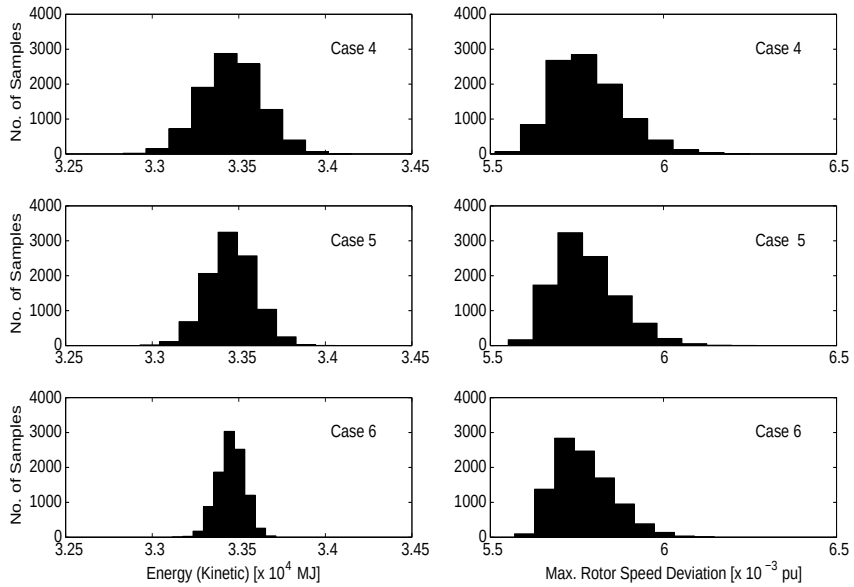

Figure 6.4: Total stored kinetic energy (left) and maximum rotor speed deviations (right) in the system in Case 4 (upper), Case 5 (middle) and Case 6 (lower)

of the probability distributions of the maximum rotor speed deviation increases slightly (Figure 6.4 (right)). Hence, the lower the stored kinetic energy in the system (i.e. inertia) becomes, the more vulnerable the system is in terms of transient stability (e.g. due to disturbance) [25], [33] (Chapters 4 and 5).

The stochastic behavior of consumption and generation within an ADS results in stochastic power flows in the lines. In addition, the stochastic behavior of connecting/disconnecting DG units results in a stochastic amount of stored kinetic energy in the system. Accordingly, the transient stability analysis does not result in a single value of the stability indicators, but in a probabilistic distribution of the stability indicators. In other words, in stead of a black-and-white statement on the system stability, a more nuanced result is obtained.

Table 6.2 gives a comparison of the indicators obtained from the deterministic approach and the ones (average values) obtained from the stochastic approach. Especially the average values of the oscillation duration are significantly higher than the ones obtained from the deterministic approach, which gives an indication that the system tends to be more unstable when the stochastic behavior of the ADS is taken into account.

Table 6.2: Maximum rotor speed deviations (max. dev.) and oscillation durations (osc. dur.) that result from both deterministic and stochastic stability analysis

Case nr.	Deterministic approach		Stochastic approach (average value)	
	Max. dev. [pu]	Osc. dur. [s]	Max. dev. [pu]	Osc. dur. [s]
1	0.0057	7.16	0.0057	7.16
2	0.0057	7.16	0.0058	7.25
3	0.0057	7.16	0.0058	7.48
4	0.0057	7.16	0.0058	7.30
5	0.0057	7.16	0.0058	7.26
6	0.0057	7.16	0.0058	7.23

An advantage of the stochastic transient analysis is that it does not result in a single value of the stability indicators, but in a probabilistic distribution of the stability indicators. Although the average values of the maximum rotor speed deviations are almost equal to the deterministic ones (Table 6.2), the probability that the value of the indicators obtained from the stochastic approach is larger than the ones obtained from the deterministic approach can be quite high (Table 6.3). This means that it gives a more complete picture of the transient stability of a system with DG in ADS.

Table 6.3: Probability that the values of the stability indicators that result from the stochastic approach are larger than the ones from the deterministic approach

Case nr.	Probability [%]	
	Maximum rotor speed deviation [pu]	Oscillation duration [s]
1	38.0	1.3
2	55.6	70.8
3	68.4	92.4
4	58.0	82.3
5	55.2	85.0
6	51.2	70.8

6.3 Stochastic Transient Stability Study with Increasing DG

The stochastic approach is used in this section to investigate the transient stability of power system that goes through a 'vertical-to-horizontal' transformation (Chapter 5).

6.3.1 Simulation Scenario

A 'vertical-to-horizontal' transformation is obtained by gradually increasing the DG penetration level, i.e. by increasing the fraction of the total load in the test system served by DG in steps of 10% up to 50%. The remaining power is divided among the dispatchable CG units by considering the economic operation of the power system, similar to the approach in Chapter 5. As in Section 6.2, a scheme of minimum and maximum loading limits and the cost models of the CG units are taken in such a way that the higher-numbered CG units are the more expensive ones. An optimal power flow program, with objective function to minimize the fuel cost, is run with a DG penetration level from 10% to 50%. The most inefficient CG units whose power output falls below their minimum loading limits are shut down. Switched shunt devices are implemented at the location of the shut down CG units to compensate for the reactive power lost.

6.3.2 MCS Samples

The total (aggregated) customer-owned DG is stochastically calculated as a binomial distribution where each DG unit within the distribution network is connected to the system with a probability (p_{on}) equal to 0.8. The penetration level of DG is defined as: $(\frac{(p_{on} \times P_{DG,installed})}{P_{load,nominal}}) \times 100\%$. Thus, the maximum capacity of DG installed at one load bus can be 125% of the rated load value (i.e. when 100% DG is supposed). The DG units supply only active power (1 MW rated active power each) and no reactive power. The loads are following a normal distribution, where the average is the rated load (Appendix B), and the standard deviations equal 2.5%. 5,000 Samples are generated for the aggregate DG output power and the load at each load bus, in every scenario of increasing DG penetration level. These 5,000 samples are considered to be sufficient since the MCS converges after 5,000 samples.

Figure 6.5 shows the contours of the histograms of the MCS generated samples representing the DG power generation at each load bus, (except at bus nr. 12 and 31, not shown due to small values), at 10 to 50% DG penetration level.

The transient stability of the test system is investigated by applying a permanent fault to the transmission line between buses 15 and 16 for each MCS sample. The fault is cleared by tripping the faulty line after 150 ms. To assess the transmission system stability, two indicators are applied to quantify the rotor speed oscillations of the CG in the system, maximum rotor speed deviation and oscillation duration (Chapter 3).

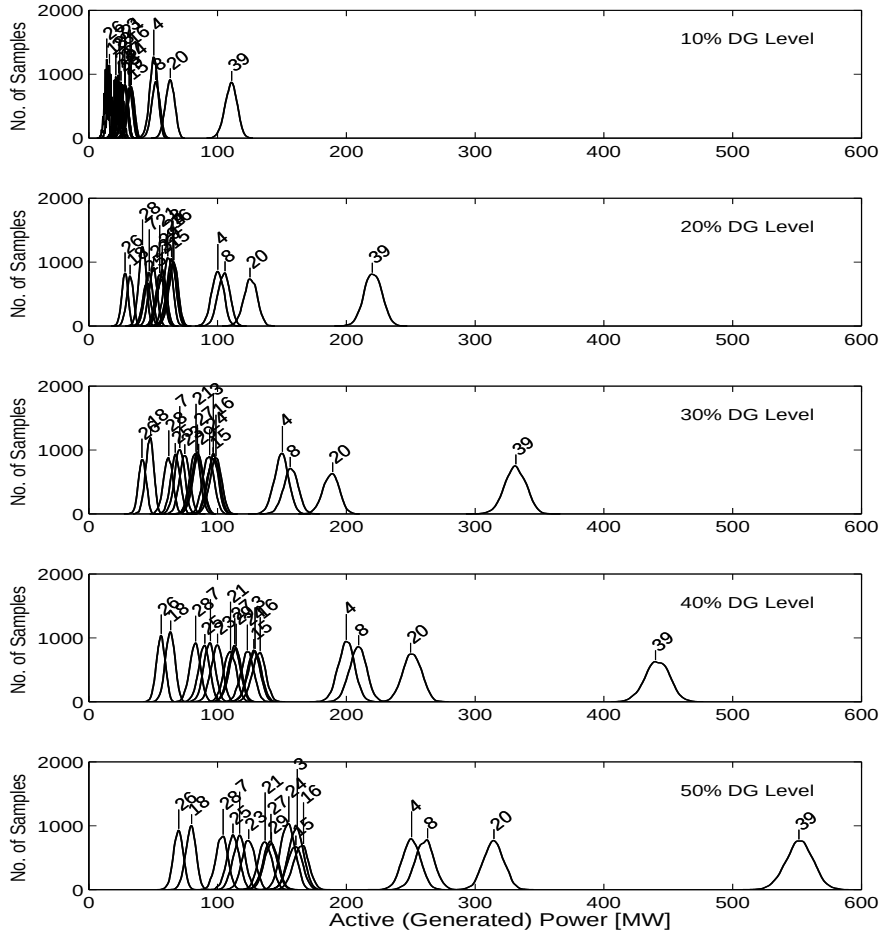

Figure 6.5: MCS generated samples representing the DG power generation at each load bus at a 10%, 20%, 30%, 40% and 50% DG penetration level

6.3.3 Simulation Results

Figure 6.6 shows a number of scenarios of the 'vertical-to-horizontal' power system transformation. It can be observed from Figure 6.6 that there are five CG units operating within all scenarios (DG penetration level from 0% to 50%): CG nr. 1, 2, 3, 4, and 5 (i.e. the lowest 5 bars of fig. 6.6). To compare the transient stability performance in the different scenarios, the transient stability indicators are applied on these five CG units.

The values of both stability indicators, i.e. the average value in case of the stochastic approach and the deterministic value in the deterministic approach, are shown in Table 6.4.

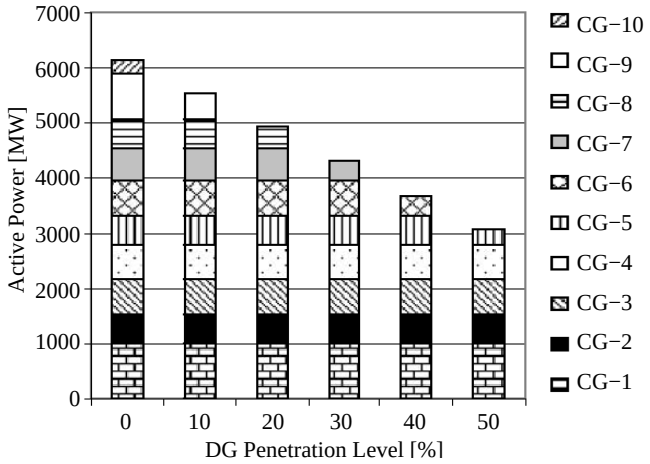

Figure 6.6: Dispatched CGs as a function of the DG penetration level

Table 6.4: Maximum rotor speed deviations and oscillation durations resulting from the deterministic and the stochastic (average) approaches of all MCS simulations at the five DG penetration levels

DG level Scenario (%)	Deterministic approach		Stochastic approach	
	Max. rotor speed deviation [pu]	Oscillation duration [s]	Average of the max. rotor speed deviation [pu]	Average of the oscillation duration [s]
10	0.0053	6.31	0.0053	6.32
20	0.0055	7.09	0.0055	7.09
30	0.0055	7.36	0.0055	7.07
40	0.0055	6.31	0.0055	6.86
50	0.0063	6.88	0.0063	7.20

From Table 6.4, it can be concluded that the stochastic approach and the deterministic approach result in the same average maximum rotor speed deviation. The oscillation duration is, however, different for both approaches. The latter fact gives an indication that the results obtained from the deterministic approach may give either too pessimistic (e.g. at the 30% DG penetration level) or too optimistic (e.g. at the 40% and 50% DG penetration level) results compared to the results obtained from the stochastic approach.

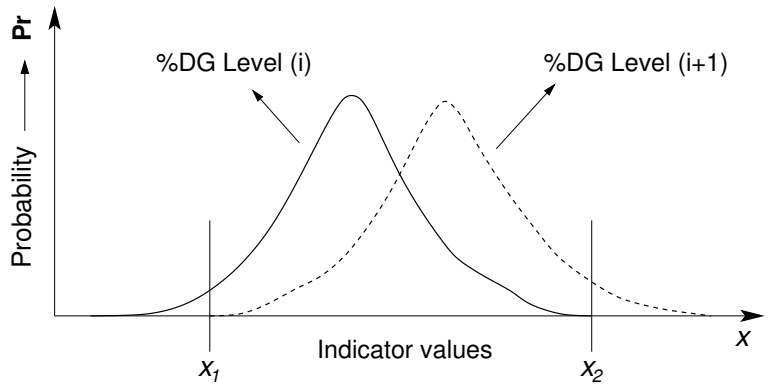

Figure 6.7: Probability distributions of stability indicators overlap

Furthermore, with the stochastic approach proposed in this section, the probability distributions of the stability indicators are obtained and contain additional information. First of all, the black-and-white statement that the system becomes more unstable when e.g. the DG penetration level increases from 10% to 20% can be more nuanced. Equation (6.2) and Figure 6.7 illustrate the use of this approach. In Figure 6.8, for example, is shown that the probability distributions of the maximum rotor speed deviations overlap in some ranges.

$$P_r(g_1(x) > g_2(x)) = \int_{x_1}^{x_2} g_1(x) \left(\int_{x_1}^{x} g_2(y)\ dy \right) dx. \tag{6.2}$$

Discretizing and applying (6.2) to the results obtained from the stochastic approach, leads to Table 6.5.

Table 6.5: Probability that the indicators resulting from the scenario with lower DG level surpass the indicators resulting from the scenario with the one-step-higher DG level

%DG level		$P_r(g_1(x) > g_2(x))$	
$g_1(x)$	$g_2(x)$	x = indicator of max. rotor speed deviation	x = indicator of oscillation duration
10%	20%	0.0043	0
20%	30%	0.1406	0.3984
30%	40%	0.3211	0.6942
40%	50%	0	0.2413

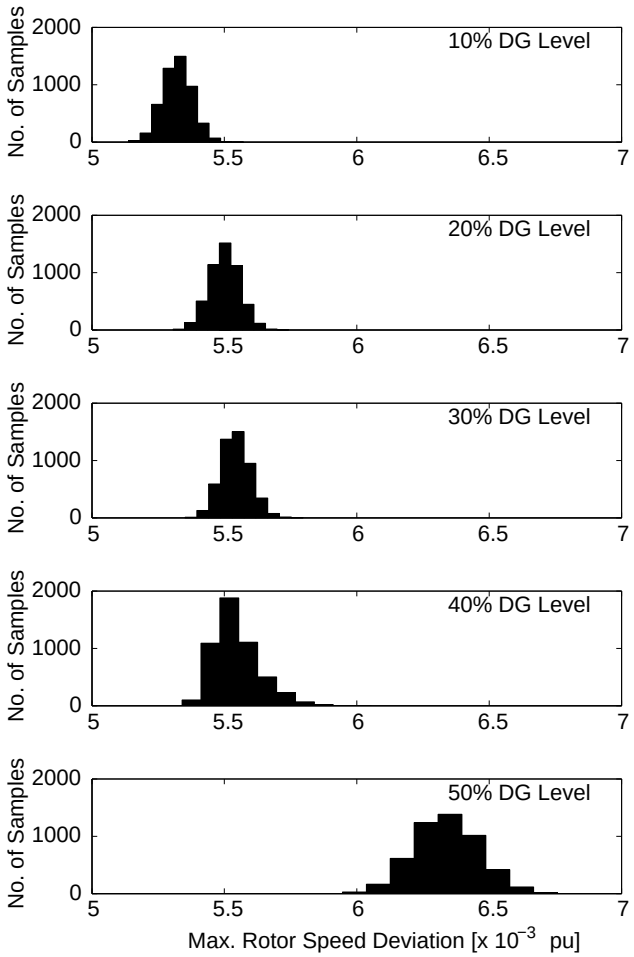

Figure 6.8: Histograms of the maximum rotor speed deviations (in 10^{-3} pu). Note that the x-axis and y-axis of all graphs are adjusted to be uniform

6.4 Conclusions

Results from the preceding chapters suggest that the transient stability performance of power systems depends on the (pre-fault) load flow within the system. Moreover, the implementation of DG, based on renewable energy sources, implies more stochastic behavior of the electricity generation. Therefore, stochastic approach should be considered to study the transient stability of power systems.

This chapter deals with examining the consequences of a stochastic approach on the system transient stability. The study is mainly focused on the stochastic behavior of the DG output, that is simulated using Monte Carlo Simulation method, within the framework of the "vertical-to-horizontal" transformation.

It is shown that although many simplifications are applied for the stochastic parameters, the inclusion of the stochastic behavior of DG leads to a more complete and detailed view of the steady state situations. When the transient response of the system is simulated, the average values of the stability indicators obtained from the stochastic approach may be the same as the indicators obtained from the deterministic approach. Yet, in the stochastic approach, also the probability distributions for the indicators are estimated. When compared to the single result of the deterministic approach, it is shown that the deterministic approach may give either under-valued or over-valued results.

The probability distributions of the stability indicators of two different DG penetration levels may overlap. Therefore, the deterministic statement that a system becomes more stable (or unstable) when the DG penetration level is increased can be more nuanced as that the system becomes more stable (or unstable) to certain degrees.

The merit of stochastic stability studies is evident even in the case of a relatively simple example studied here. Therefore, a stochastic approach becomes a necessity when, e.g. DG units depend on highly intermittent energy sources (e.g. wind and solar energy), or when the dependence between the generation of DG units and the loads becomes important.

Chapter 7

Maintaining Power Balance with Active Distribution Systems

This chapter investigates the situation when the power system is pushed towards a scenario, where DG penetration reaches a level that covers the total load of the original power system (100% DG implementation in the system).

The assumption is that all DG units are implemented via power-electronic converters within active distribution systems (ADS). The ADS are connected to the transmission system also via power-electronic interfaces. The power system is still connected to one source that provides a constant 50 Hz voltage. This can be, for example, a connection (tie line) to a strong external system. This source is meant only to gives a (system) frequency reference for the other generators and generates no power at steady state. Therefore, any power imbalance in the power system must be compensated by generators in the ADS.

Due to the power-electronic interfaces, the output power of all generators within the ADS are decoupled from the system frequency. Therefore, voltage deviations are proposed to detect power imbalances in the system. Remedies to eliminate the negative consequences of using the voltage deviations to detect the power imbalances are discussed and appropriate control systems are suggested. Figure 7.1 shows an illustration of the power system with ADS.

7.1 Background

The implementation of the distributed generation (DG) turns the current *passive* distribution network into an *active* one (Chapter 1). This active distribution network does not only consume, but it also generates power and supplies it to the transmission system [41], [55]. In this way, power can be transferred from one distribution network to another. When we reflect further on this issue to the

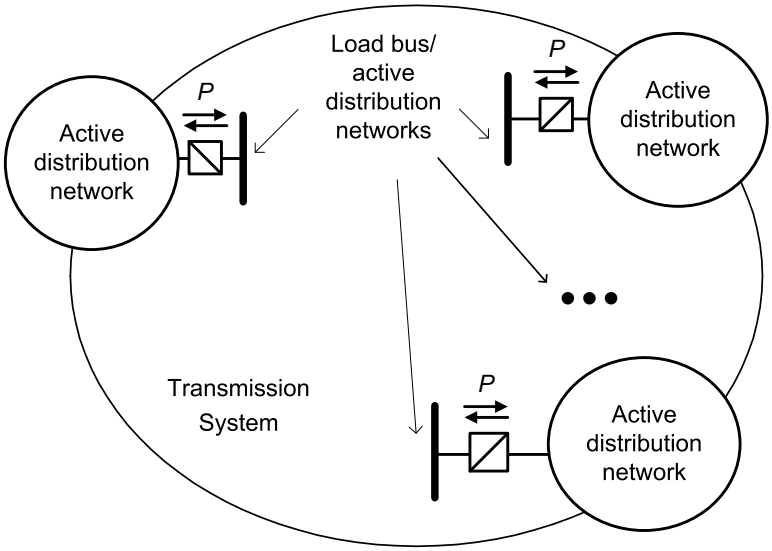

Figure 7.1: Illustration of the power system with ADS

extreme, we could imagine that at a certain moment in time the electrical power generated by the DG within the distribution networks may become sufficient to cover the total demand in the transmission system.

Most of the DG implementations based on renewable energy sources or environmentally-friendly technologies are connected to the grid via power electronic converters (Chapter 2). Moreover, when the distribution networks evolve to become more hybrid, including AC-DC, and with flexible storage systems, it is envisaged that connecting these distribution networks to the transmission system via power electronic interfaces will be an interesting option [19].

7.2 Power Balance

One of the primary tasks of power system operation is to balance the electricity supply from generators and loads including the losses in the network at any time. However, a disturbance may occur in the system that causes a power imbalance. It is important that the power system can restore the power balance and return to a stable state after this disturbance, called *power system stability* [34] (Chapter 3).

In this chapter, all generators within the ADS are 'hidden' behind power-electronic interfaces. The output power of the generators are decoupled from the grid frequency. On the other hand, the source that provides the constant 50 Hz voltage is meant only to give a frequency reference for the other generators (in the ADS) and not meant to generate power at steady state. Therefore, any

power imbalance in the power system must be compensated by generators in the ADS. However, as a result of the decoupling between the output power and the grid frequency in the ADS, the power imbalance cannot be detected by the ADS in the classical way, as an altered system frequency. Therefore in this chapter, the use of *voltages* to detect a power imbalance in the transmission system with active distribution systems is proposed.

Traditionally, however, two problems may arise from using the voltages to detect a power imbalance in a power system. Firstly, the voltage (magnitude) at a bus is affected by the flow of the reactive power. Secondly, the voltages at the buses throughout a power system are not the same (in contrast to the system frequency). Therefore in the following sections, remedies to eliminate these problems are presented. Assumptions are applied on the model of the power system with ADS to eliminate the first problem as it is not essential. To deal with the latter problem, several control systems are proposed and simulated.

7.3 Model of Power System with ADS

7.3.1 Assumptions

To decouple the changes of the voltages with the changes of the reactive power, some assumptions are applied on the model of the power system as the following:

- The distribution networks are equipped with reactive power sources. The reactive power source is sufficient to fulfill the reactive power needs within the distribution networks.
- The (active) distribution networks are connected to the transmission system via power electronic interfaces. The power electronic interface is assumed to permit only active power to flow (bi-directional).
- The reactances of the transmission lines are compensated, in such a way that they behave like resistive lines.

7.3.2 Model of ADS

This chapter focuses on functioning of the ADS to maintain the power balance in the systems. The ADS are considered as follows:

- The (distributed) generators are connected via power electronic converters and generate only active power. The generators are initially set to balance active power demand.
- The loads demand active and reactive power. They are modeled as constant impedance and constant power. Electrical motors and the corresponding inertias are hidden behind power electronic interfaces from the grid; therefore, electrical motors, if any, are assumed to be included in the constant power model of the loads.
- The reactive power is supplied by dedicated reactive power sources. The reactive power sources are preset to balance the reactive power demand.

- A power imbalance is simulated by changing the active power demand of the load. A reactive power imbalance is not simulated. Therefore, only active power flows between the ADS and the transmission system. Furthermore, to balance the reactive power within the ADS, reactive power sources are applied and modeled as shunt devices.

Thus in the simulation, each ADS is modeled as shown in Figure 7.2.

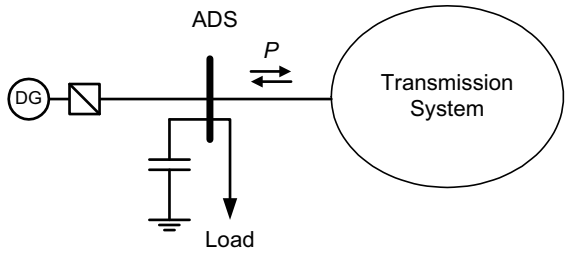

Figure 7.2: Model of ADS used in the simulation of maintaining the power balance in the system

7.3.3 Generator Models

In the power system with ADS, generators perform the following functions:

- One central generator operates as a reference. It serves as voltage and frequency reference for the other generators in the system and generates no power at steady state.
- The distributed generators operate as active power sources. They only supply active power.
- One (or more) central or decentralized generator serves as a 'slack' generator that either supplies or absorbs any deficit or surplus of active power in the system. This generator is assumed to have no current limiter and to be equipped with sufficient (energy) storage.

Three converter connected generator models are used:

- A constant voltage source is used to represent the generator providing voltage and frequency reference. Figure 7.3 shows the representation of this generator, where U_s is the constant (reference) voltage with a fixed frequency, and Z_s is a source impedance.
- A constant current source that generates a current in phase with the terminal voltages U_t of the generator (a Phase Locked Loop, PLL, is used for this purpose) is used to represent the distributed generator that supplies active power. Figure 7.4 shows the representation of this generator.
- A controlled current source is used to represent the generator serving as the 'slack' generator (Figure 7.5).

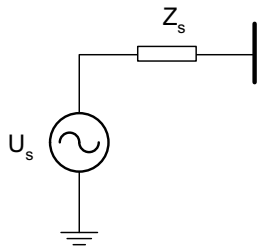

Figure 7.3: Constant voltage source model

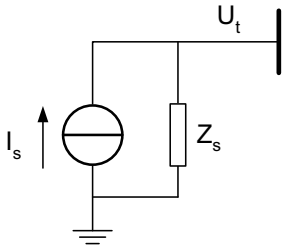

Figure 7.4: Constant current source model

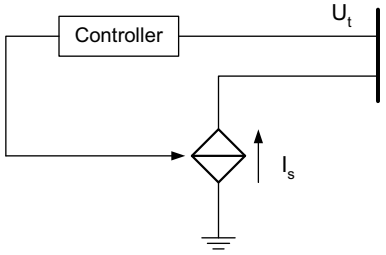

Figure 7.5: Controlled current source model

A remark should be made that power electronic interfaces driving the output of converter-connected (distributed) generators basically represent a voltage source converter, as mostly used nowadays [70]. Yet, the use of constant current sources to represent converter-connected generators in this simulation is supported by the following assumptions (Chapter 3):

- A converter is actually a voltage source converter, but it behaves like a current source, so that current source models can substitute voltage source converters when simulations are made in large systems [42].

- It is usual to model the sources as PQ-sources in studies of large systems [69]. A constant current source generating a current in phase with the (terminal) voltage represents a PQ-source generating constant active power (P) and zero reactive power ($Q = 0$), as long as the terminal voltage of the generator is constant.
- In practice, a converter is equipped with a current limiter. When the terminal voltage drops, the converter supplies less active power. Thus, the use of a constant current source corresponds to a converter whose current is limited to the rated value (in practice, 100% up to 120% of the rated value).
- When the terminal voltage raises temporarily, the use of the constant current source can be justified by assuming that the generator is equipped with energy storage so that the generator can supply extra active power for a short period of time.

7.4 Basic Controller Model

The function of maintaining the power balance is supposed to be done by the controller-block of the 'slack' generator(s). The 'slack' generator(s) represented by the controlled current source(s) (Figure 7.5) must supply or absorb any deficit or surplus of active power in the system. The basic functionality of the controller-block is highlighted hereunder.

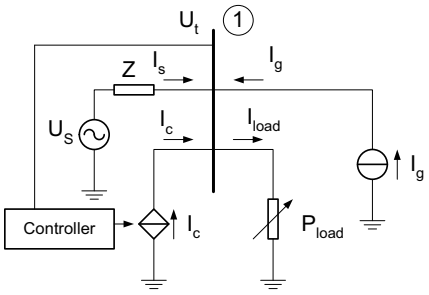

Figure 7.6: Basic controller idea applied at a single-bus test system

In Figure 7.6, three types of converter-connected generators - a constant voltage source providing a reference voltage (U_s), a constant current source generating a constant current (I_g) and a controlled current source supplying a changeable current (I_c) - and an active load consuming active power (P_{load}) are implemented.

In steady state, the current of the voltage source (master generator providing a reference voltage and frequency) should be zero ($I_s = 0$), so that there is no voltage drop across the impedance Z. Hence, the terminal voltage (U_t) of bus-1 is equal to the reference voltage U_s.

Any power imbalance should be eliminated by controlling the current I_c generated by the controlled current source. This controlled current source represents the 'slack' generator. When, for example, the active power consumption of the load P_{load} increases, the current flow to the load (I_{load}) rises. Both generators modeled as current sources do not react (yet) and the voltage source starts to supply active power in order to balance the power. The voltage source, representing a strong source acting as the frequency reference, takes care of the primary action. This source, however, is meant to provide the frequency reference only: the source should not generate active power at steady state. Therefore, as I_s increases and causes a voltage drop across Z so that U_t decreases, a secondary action is taken. The controller of the controlled current source should detect this voltage drop. As a result, the controlled current source supplies more active power, i.e. it injects more current I_c, until the power balance is restored.

The controller used in the basic model is a proportional-integral controller (PI controller), a common feedback loop component in industrial control applications. The controller compares a measured value from a process with a reference setpoint. The difference or "error" signal is processed to calculate a new value for a manipulated process input, in which the new value brings the process measured value back to its desired setpoint. Unlike simpler control algorithms, the PI controller can adjust process inputs based on history and rate of change of the error signal, which gives a more accurate and stable control. It can be shown mathematically that a PI loop produces accurate stable control in cases where other control algorithms would either exhibit a steady-state error or cause the process to oscillate. The mathematical form of PI controller can be shown as [46]

$$U(t) = K_P E(t) + K_I \int E(t)dt, \tag{7.1}$$

where $U(t)$ is output of the controller, $E(t)$ is error signal (difference between desired and real output), K_P is proportional and K_I integral term.

To verify the basic controller model, a load jump is simulated to cause a power imbalance in the system (Figure 7.6). The system voltage is set at 10 kV. The load demands 60 MW of active power (P_{load}) initially, equally divided in constant impedance and constant power. The constant current source supplies initially all demand. The currents generated by the constant voltage source (I_s) and the controlled current source (I_g) are zero. A load jump is applied by increasing the load modeled as the constant impedance by 30 MW.

Figures 7.7, 7.8 and 7.9 show transients of voltages, currents and active power when the load jump occurs. Note that the $P_{`constantactivepower'generator}$, $P_{`slack'generator}$, and $P_{`master'generator}$ represent the active power supplied by the constant current source, controlled current source and constant voltage source of the system in Figure 7.6 respectively. Simulations are performed on a Real Time Digital Simulator (RTDS) with a time step of 50 μs.

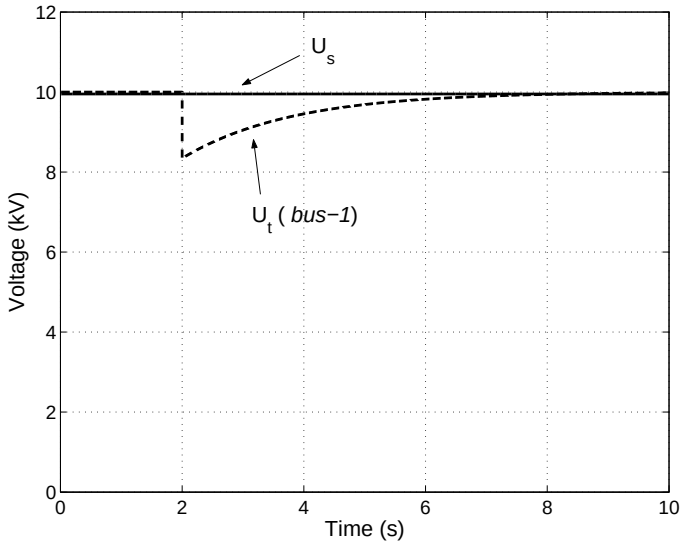

Figure 7.7: Transients of the voltages when a 30 MW load jump is applied at bus-1 of the system shown in Figure 7.6

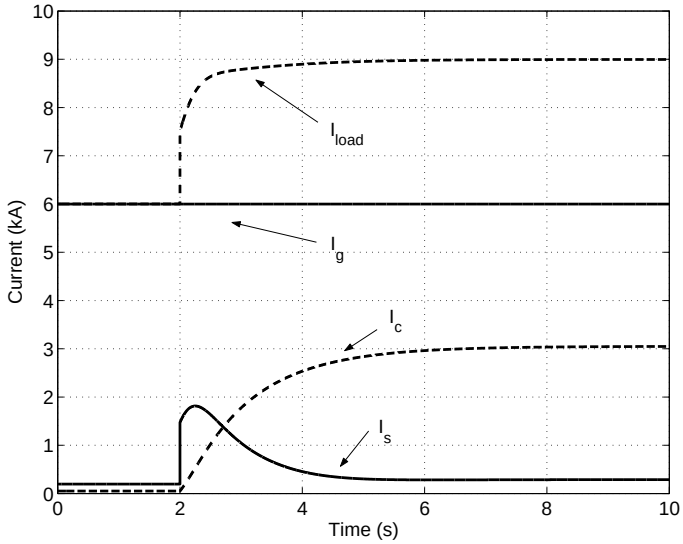

Figure 7.8: Transients of the currents when a 30 MW load jump is applied at bus-1 of the system shown in Figure 7.6

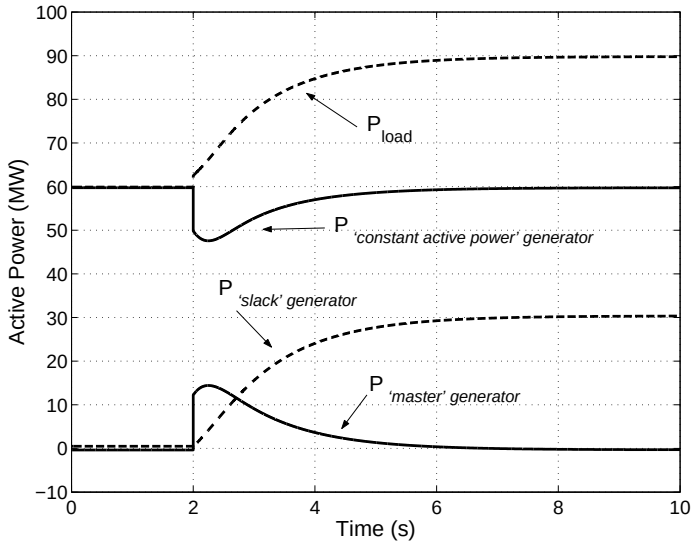

Figure 7.9: Transients of the active power when a 30 MW load jump is applied at bus-1 of the system shown in Figure 7.6

We can see from these figures that, following the load jump, the power balance is restored, and the 'extra' power demand is finally supplied at the steady state by the 'slack' generator (increasing current I_c and active power $P_{'slack'generator}$ in Figures 7.8 and 7.9). The voltage level of the bus also restores to the steady-state value that lies within a +/-5% margin of the rated voltage.

7.5 ADS Control Systems

Practically, a power system consists of more than one bus. In this case, the system is decoupled and no longer linear, due to the interdependency of the buses. In addition, the voltages at the buses throughout the system are not the same (Section 7.2). Consequently, applying the basic control model of Section 7.4 to each bus gives potential difficulties, since the basic control model is linear.

In this section, three existing control system methods are proposed [46]:

- *Stand-alone master controller.*
- *Decentralized-controller with single reference.*
- *Decentralized-controller with hysteresis.*

To verify these control systems, a simple test system that consists of 3 buses is defined (Figure 7.10). Tables 7.1 and 7.2 show respectively the component parameters used and the load flow settings and computed results in the 3-bus test system. Note that G_{ref} refers to the reference ('master') generator. G_j refers to the constant-power generator at bus-j, $Load_j$ to the load at bus-j

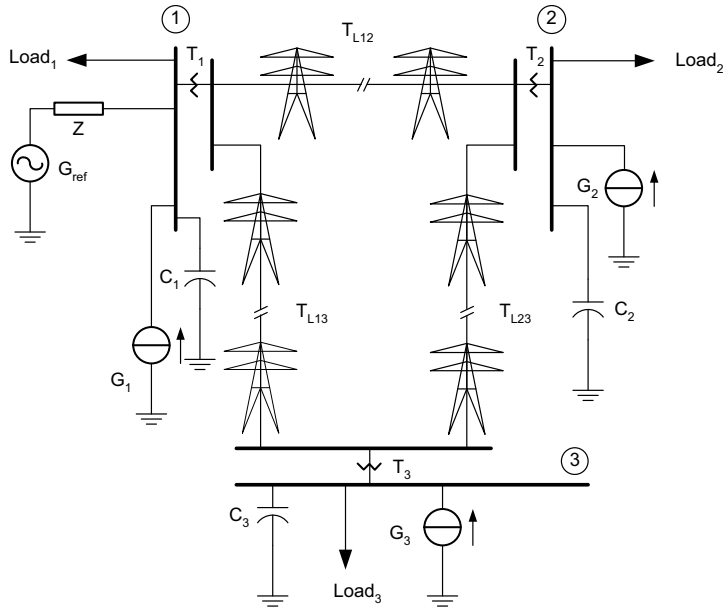

Figure 7.10: A simple 3-bus test system

and C_1 to the reactive power source at bus-j. Also note that the transmission lines introduce quite some capacitance in the system; each transmission line generates around 16 Mvar. T_j indicates the transformer at bus-j and T_{Ljk} the transmission line between bus-j and bus-k. In Table 7.1, S_{base} denotes the complex power base of the test system. U_{HV} and U_{MV} denote the system high- and medium voltage levels. R, X_L and B denote the resistance, reactance and susceptance of the transmission lines. X_T denotes the transformer reactance and Z the impedance between the reference 'master' generator and bus-1.

7.5.1 Stand-alone master controller

The most simple way to overcome the non-linearity problem is to use a stand-alone master controller. In this approach only one basic controller is applied and connected to one of the buses of the system. In this case, the controller only regulates the voltage at one bus and lets the system come to balance using its own connectivity.

Figure 7.11 shows the implementation of the stand-alone master controller in the test system. The 'slack' generator represented by the controlled current source, is implemented at bus-1. In this controller scheme, only one 'slack' generator is implemented. The generator should handle the active power imbalance occuring in the system. Note that G_{Cj} refers to the controlled-power 'slack' generator (at bus-j): in this case G_{C1} at bus-1.

Table 7.1: Component parameters used in the 3-bus test system

Description	Parameter	Value	Unit
System base	S_{base}	100	MVA
System voltage	U_{HV}	100	kV
	U_{MV}	10	kV
Transmission lines:	R	0.0064	pu
$(T_{L12}, T_{L13}, T_{L23})$	X_L	0.0322	pu
	$\frac{B}{2}$	0.0306	pu
Transformer	X_T	0.1	pu
(T_1, T_2, T_3)			
Impedance	Z	1.0	pu

Table 7.2: Load flow settings and computed results in the 3-bus test system

Description	Parameters	Setting (MW)	Computed (MW)	Setting (Mvar)	Computed (Mvar)
Generation	Gref	0.0	-0.5	0.0	-6.5
	G_1	60.0	59.9	0.0	2.8
	G_2	60.0	60.4	0.0	2.8
	G_3	60.0	60.4	0.0	2.8
Load	$Load_1$	60.0	59.0	30.0	31.8
	$Load_2$	60.0	59.7	30.0	32.2
	$Load_3$	60.0	59.7	30.0	32.2
Shunt device	C_1	0.0	0.0	15.0	15.0
	C_2	0.0	0.0	15.0	15.3
	C_3	0.0	0.0	15.0	15.3

A load jump is applied by increasing the constant power load at bus-2, the load being modeled as a constant power of 30 MW. Figure 7.12 shows the transients of the active power where all the 30 MW power (of the load jump) is supplied by the 'slack' generator. The power balance is restored and all system parameters are back to stable, steady state values.

When the stand-alone master controller scheme is implemented, the problem of 'different signal' of voltages for the control input is eliminated by using only one controller at bus-1. In this way, the controller uses only one voltage as its reference signal. However, the challenge is that one generator should compensate for the power balance of the whole system. In the following sections, other proposals concentrate on dividing the 'slack' generator task.

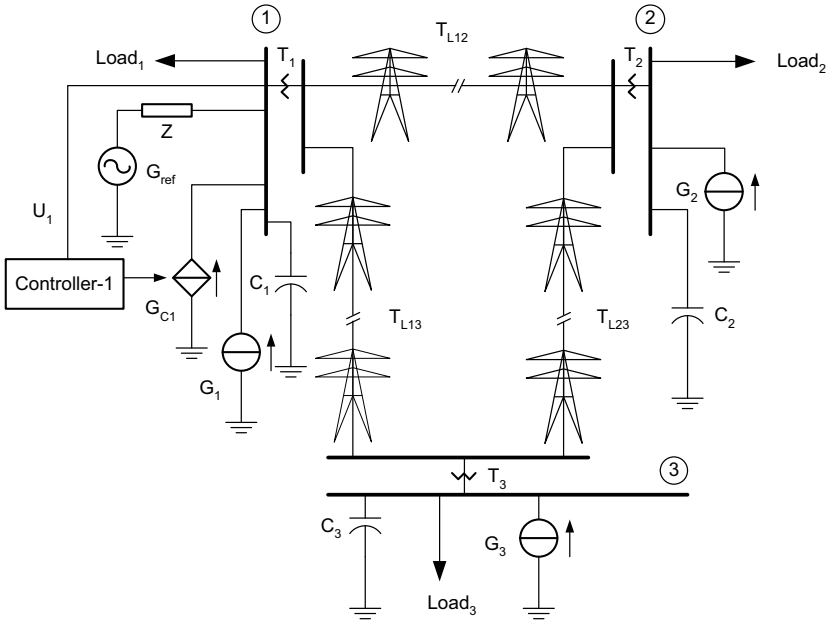

Figure 7.11: Implementation of the stand-alone master controller in the test system

7.5.2 Decentralized-controller with single reference

In practice, it is impossible to use one central generator to compensate for the whole system. Because of that, in this example three decentralized generators with their own controllers are applied. However, if these three controllers are applied 'as is' in the test system, even though the voltage can be regulated, the power balance of the generators is not achieved. It is already expected that the system is decoupled and the voltage at each bus is not exactly the same. Therefore, decentralized-controllers with single reference is proposed here. In this approach, the 'slack' generator at each bus has its own controller, but the reference signal is common to all of them and can be taken from any voltage point.

Figure 7.13 shows the implementation of the decentralized-controller with single reference in the test system. Each of the 'slack' generators, represented by the controlled current source is implemented at buses 1, 2 and 3. The generators altogether should take care of the active power imbalance that occurs in the system. One control signal is used by all generators, i.e. the voltage at bus-1 (U_1). Note that G_{Cj} refers to the controlled-power 'slack' generator at bus-j.

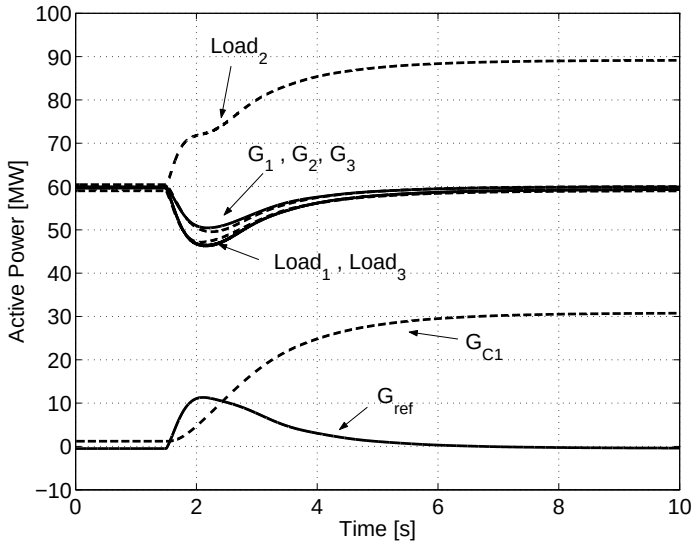

Figure 7.12: Transients of the active power when a 30 MW load jump is applied at bus-2 of the system shown in Figure 7.11

A load jump is applied by increasing the constant power load at bus-2, the load being modeled as constant power, of 30 MW. Figure 7.14 shows the transients of the active power. The 30 MW power of the load jump is supplied by the three 'slack' generators at buses 1, 2 and 3. Each generator supplies the required power into balance, i.e. 10 MW. Also, all system parameters are back to stable, steady state values.

In the same way as in the first approach, by implementing the decentralized-controller with a single reference, the problem of 'different signal' of voltages for the control input is eliminated by using only one controller at bus-1. The difference is that this control signal is used for all three controllers. With this approach the control generator is no longer centralized. However there is one aspect that should be considered. This approach needs a communication link between each controller to transfer the reference data signal. It might happen that not all system has this luxury.

In the next section, the third method that can be applied for the system without communication link between each controller is described.

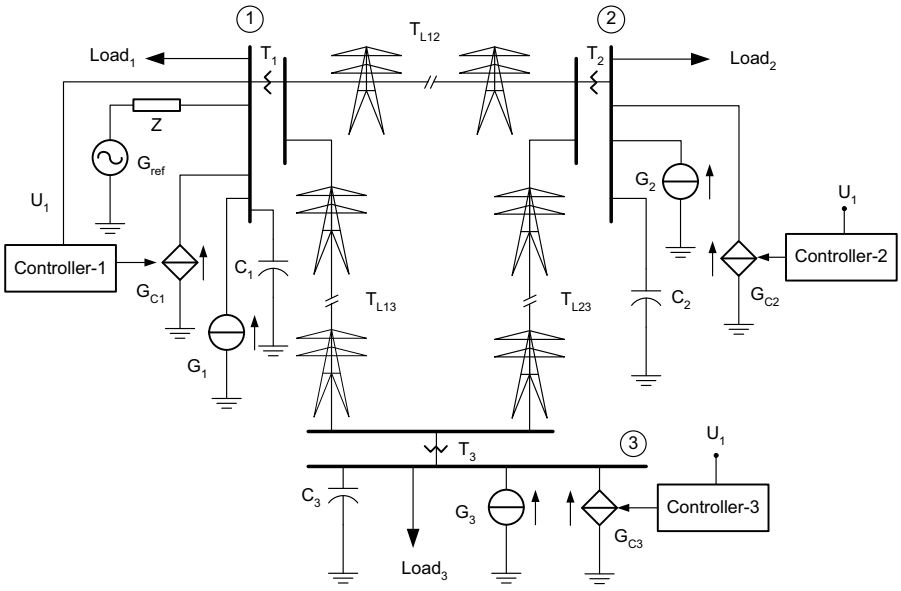

Figure 7.13: Implementation of the decentralized-controller with single reference in the test system

7.5.3 Decentralized controller with hysteresis

The third approach proposed uses three decentralized controllers, one applied at each bus. As discussed above, the linear controller cannot work perfectly in the non-linear decoupled system. The symptom that happens by applying the basic controller over the test system, is that in steady-state the controller oscillates as the system is decoupled and the reference signal is not exactly the same.

To prevent this symptom, hysteresis is applied in the controller input: the controller stops regulating the system whenever the value of the voltage lies within the hysteresis boundary. The use of hysteresis is allowed as long as the width of it is less or equal than the tolerance of the voltage, being 1% of the rated value.

Figure 7.15 shows the implementation of the decentralized controller with hysteresis. The 'slack' generators represented by the controlled current sources are implemented at buses 1, 2 and 3. One 'slack' generator is implemented at each bus. In this control scheme, each 'slack' generator uses the voltage where the generator is implemented. The generators altogether should take care of the active power imbalance occurring in the system. Note that G_{Cj} refers to the 'slack' generator at bus-j. The generator G_{Cj} is also linked to the control signal the voltage of bus-j (U_j).

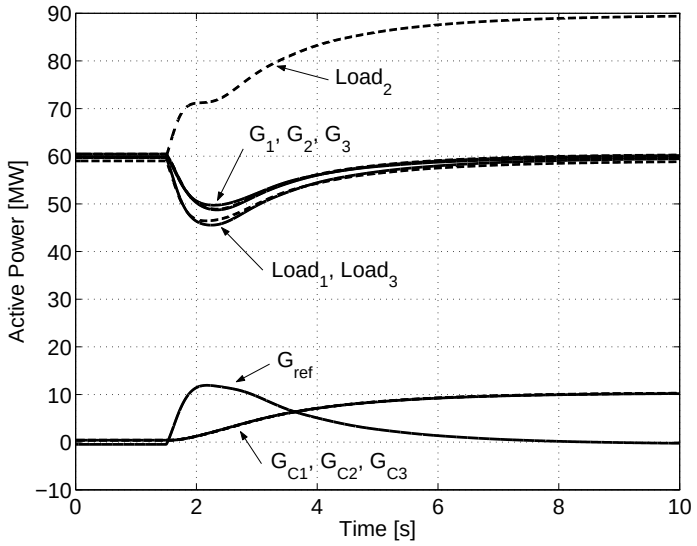

Figure 7.14: Transients of the active power when a 30 MW load jump is applied at bus-2 of the system shown in Figure 7.13

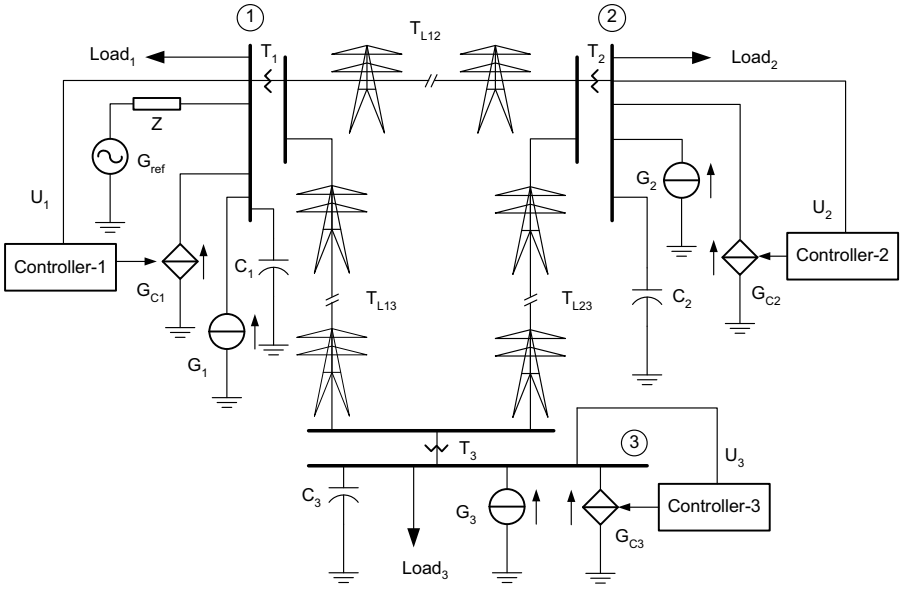

Figure 7.15: Implementation of the robust controller in the test system

A load jump is applied by increasing the load at bus-2, the load being modeled as constant power of 30 MW. Figure 7.16 shows the transients of the active power. The 30 MW power of the load jump is supplied by the three 'slack' generators at buses 1, 2 and 3, each generator supplying 10 MW. All system parameters are restored to stable, steady state values.

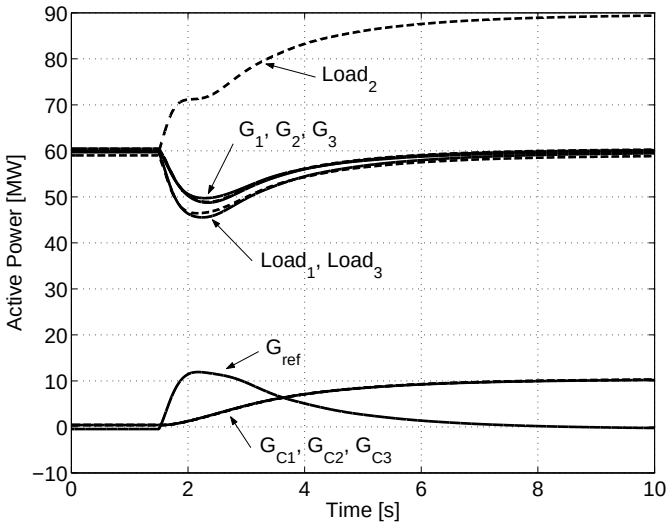

Figure 7.16: Transients of the active power when a 30 MW load jump is applied at bus-2 of the system shown in Figure 7.15

By applying this approach, the power balance of the system can be achieved. The effect of hysteresis is that there is a steady state error on the voltage, but while the steady state value is smaller than the tolerance of the voltage value, it can be accepted. Thus, the voltage regulation is maintained. It might be not the optimal solution, but the system still operates within the specifications. The main advantage of this approach is that the requirement of the communication link between controllers is eliminated.

7.6 Conclusions

This chapter presents models and control systems for maintaining the power balance in the power system with active distribution networks (ADS), where the DG units covering the total demand of the original power system are implemented within the ADS via power-electronic converters. Moreover, the ADS are connected to the transmission system via power-electronic interfaces.

Due to the power-electronic interfaces, the output power of the DG units and the ADS are decoupled from the grid frequency. As a result, the ADS cannot detect power imbalance as an altered system frequency such as in classical power systems [44], [43]. Therefore, in this chapter the idea is developed to use the voltage to detect and maintain the power balance.

Some assumptions are applied to the power system model to deal with the problem that the voltage magnitude at a bus is affected by the reactive power flow. Moreover, control systems are developed to deal with the problem that the voltages at the buses throughout the power system are not the same.

For this purpose, three possible control system concepts are adjusted and applied: stand-alone master controller, decentralized-controller with single reference, and decentralized controller with hysteresis. The simulation results show that by applying each of these three control systems, the power balance in the power system can be maintained by the ADS. In the first control system, the power imbalance is taken care of by one ADS unit while in the latter two, the power imbalance is taken care of by several ADS units. The simulation results show that when a load jump is applied in the power system to simulate the power imbalance, the power balance is restored by means of the ADS with each of the three control systems developed, and all system parameters return to stable, steady state values.

Each control approach proposed here has its own advantages and drawbacks. The stand-alone master controller is the most simple one, easy to implement and has a good performance. The main disadvantage is that it uses a single generator to supply the required power. The second approach, the decentralized-controller with single reference can overcome the single generator problem, at the price of requiring a communication link between controllers to transfer the reference signal data. The most interesting approach to be implemented is the third one, the decentralized controller with hysteresis, since this approach uses a split generator for each bus and in addition the three controllers are totally independent. Thus, the need of communication between controllers is eliminated.

It should be noted that the primary action is taken care of by a strong source which acts as frequency reference.

Chapter 8

Conclusions

8.1 Overview

Currently, concerns on environmental issues lead to an increasing implementation of environmentally-friendly generation in electrical power systems. Many of these generation technologies tend to be connected to the distribution systems, in which they are referred to as *distributed/decentralized/embedded generation* (DG). In literature, the technical impact of DG on the distribution systems have been studied often. Due to the small DG penetration level, the impact of DG on the transmission system has not been treated so often. However, when the penetration level of DG in a power system becomes higher, it can be expected that the impact is no longer restricted to the distribution systems, but influences the system as a whole.

In this work, we have investigated and discussed the impact of DG on power systems with a focus on the transmission system. Power system studies are usually based on computer simulations. This simulation-based approach is used in this work as well. For this purpose, we have introduced the concept of a 'vertical-to-horizontal' transformation of power systems. This transformation is the result of an increasing DG penetration level in the system. To study the DG impact on power systems, simulations have been performed on scenarios developed within the 'vertical-to-horizontal' transformation context.

DG technology and especially the way DG is connected to the grid determine DG characteristics influencing a power system. Dispatchable/non-dispatchable DG or direct/indirect grid-connected DG are included in these characteristics, and become the basis for the DG models used in the system simulation.

We have focused on the impacts of DG on the system transient stability, and more specifically on the rotor angle stability. By means of the *swing equation*, *power angle equation*, and *equal area criterion*, the transient behavior of the rotational dynamics of synchronous machines is studied. To assess the system transient stability, after a disturbance, we have used two indicators: maximum rotor speed deviation and oscillation duration, rather than the classical sys-

tem stability indicators: *critical clearing angle* and the corresponding *critical clearing time*. Due to the large number of scenarios to be simulated in combination with a relatively large power system, the use of the classical indicators is impractical.

Simulation have been performed on the well-known 39-bus New England transmission test system. This test system has several advantages: not only does it represents a relatively large power system, the system parameters are easily accessible and it has been widely used in literature.

Distribution systems, with DG incorporated, are represented in a simplified way according to models found in literature. The power system simulation software package PSS/E v.25.4 has been used to simulate the test system. DG based on classical rotating machines is modelled by means of the available models in the software package libraries. User-written models have been developed for DG based on power-electronic converters.

We have simulated the incorporation of DG in the test system with different increasing load scenarios, DG grid-connection strengths, DG technologies, and protection schemes of power-electronic interfaced DG. As expected, these factors influence the power system transient stability in a different way. There appears to be no significant stability problem up to about 30% DG penetration level. This 30% DG penetration is obtained when DG is implemented to cover a 50% load increase. Therefore, we consider this 30% DG penetration level to be a high DG penetration level in the system. In general, when DG, regardless the technology, is implemented to cover a load increase in the system, the transient stability is better than when only the centralized generation (CG) covers the increasing load. This makes sense as all centralized generators remain in the system - including their active and their reactive power controls and the energy stored in their rotating masses, along with the increasing DG penetration levels. In this way, implementing DG is a natural way of 'limiting' the power flows in the transmission lines. Therefore it *inherently* improves transient stability of the transmission system, since large power flows have a detrimental effect on the damping of the oscillations.

To simulate the 'vertical-to-horizontal' power system transformation, scenarios have been developed in which the DG penetration level is raised while the load is constant. This leads to an overcapacity in the system, and an economic dispatch is used in these simulations so that the most inefficient CG unit(s) is(are) taken out of service (efficiency considerations). DG has been implemented as power-electronic interfaced DG so that it does not contribute to the inertia (stored kinetic energy) of the system. In this way, the total inertia of the system reduces as CG units are taken out of service, and the system becomes more vulnerable in the face of a disturbance. However, the fact that the DG generates power close to the loads causes a reduction in the total real power flowing in the system, and through the faulty branch. This appears to counteract and compensate the tendency of the system to become more unstable. Therefore, by optimizing the load flow in the system (e.g. by rescheduling the output of the CG units), the transient stability of the system that goes through the 'vertical-to-horizontal' transformation can even be improved.

The simulation results within this 'vertical to horizontal' power system transformation framework also suggest that a DG penetration limit exists and this limit is influenced by the total kinetic energy remaining in the system, and the reactive power support scheme. Therefore, a straightforward remedy for instability problems that may occur due to the DG implementation could be advocated by assigning certain CG units as synchronous condensers, that provide inertia to the system and, in addition, the needed reactive power support.

The simulation of a power system reaching 100% DG implementation has been done where assumptions are taken that all DG units are implemented via power-electronic converters within active distribution systems (ADS). Moreover, the ADS are connected to the transmission system via power-electronic interfaces too. It has been modeled that the power system is connected to one source providing a constant 50 Hz voltage, that can be, for instance, a connection (tie line) to an external system. This source is meant only to gives a (system) frequency reference for the other generators and supplies no power at steady state. Since the the output power of all generators within the ADS are decoupled from the system frequency due to the power-electronic interfaces, the voltages have been used so that the ADS can detect and maintain the power balance in the power system.

8.2 Stochastic Stability Studies

The merit of stochastic stability studies is evident even in the case of a relatively simple example as studied in this thesis. The stochastic approach becomes a necessity when, for example, DG units are based on (highly) intermittent renewable energy sources e.g. wind and solar energy, or when the dependence between the renewable DG units (power generation) and the loads need to be taken into account.

8.3 Remarks and Future Works

8.3.1 'Inertia' Contribution

When a 'vertical-to-horizontal' transformation in the power system takes place, the inertia in the system decreases. DG units could provide/emulate 'inertia' to the system in order to confine the impact such as unwanted frequency deviations for a large-scale DG integration. For that purpose, some converter-connected DG technologies could be equipped with controllers enabling DG to contribute to the primary frequency control, for example by enabling the extraction of kinetic energy stored in the turbine blades of variable-speed wind turbines or by combining different types/technologies of DG units.

8.3.2 Reactive Power Control

The possibilities for reactive power control within the system are also reduced during the transformation. As DG is set to maximize the active power generation, providing reactive power to the system may become a problem. However, various solutions are available for providing reactive power to the system (e.g. capacitor banks, synchronous condensers, FACTS devices, etc).

When the passive distribution systems transform into active ones, i.e. both generation and consumption, the active distribution systems should take over some functions of the shutdown CG units to provide inertia and/or reactive power to the system.

Appendix A

List of Symbols and Abbreviations

Latin symbols

Upper case

$\%DG_{level}$	DG penetration level
A	Area [m^2]
B	(line) susceptance [S, pu]
C_p	power coefficient, the power coefficient of the device (turbine)
E	energy irradiance [Wm^{-2}] (Chapter 2), or transient internal voltages of machine [V, pu] (Chapter 5)
$E(t)$	error signal, difference between desired and real output;
G	conductance [S]
H	effective head of small hydro-power plants [m], or significant wave height [m] (Chapter 2), or per unit inertia constant [s] (Chapters 3-6)
I	current [A, pu]
J	moment of inertia [kgm^2]
K	constant term (in control blocks)
L	inductance [H, pu]
M	inertia constant [J/mech rad]
N	number of units
P	active power [W, pu], output power [W, pu]
P_r	Probability distribution (Chapter 6)
Q	flow rate [m^3s^{-1}] (Chapter 2), or reactive power [Var, pu]
R	(line) resistance [Ω, pu]

Upper case, continued

S	apparent power [VA]
T	torque [Nm]
U	voltage [V,pu]
$U(t)$	controller output signal (Chapter 7)
X	reactance [Ω, pu]
Y	admittance [S, pu]
Z	impedance [Ω, pu]

Lower case

a_i	constant corresponding to CG unit generation cost i
b_i	constant corresponding to CG unit generation cost i
c_i	constant corresponding to CG unit generation cost i
f	frequency [Hz]
f_i	energy generation cost of CG unit i (in cost unit)
g	gravitional constant [ms^{-2}]
j	complex identity ($\sqrt{-1}$)
n	generator rotational speed [rpm]
p	number of magnetic pole pairs of the field circuit of the generator (Chapter 3), or probability value (Chapter 6)
$par(P_{DG_i})$	integer proportional to the "size of DG_i", the active power generated by the aggregate DG at a particular load bus-i (Chapter 4)
s	slip of induction machine
t	time [s]
v	velocity [ms^{-1}]

Greek symbols

α	azimuth angle [rad] (Chapter 2), or constant corresponding to CG unit generation cost (Chapter 5)
β	altitude angle [rad] (Chapter 2), or constant corresponding to CG unit generation (Chapter 5)
δ	angular rotor displacement [rad]
Δ	simulation step [s], usually for time t
η	efficiency
ϕ	phase angle [rad]
ρ	density of fluid [kgm^{-3}]
σ	standard deviation
θ	angle [rad]
φ	current phase angle [rad]
ω	angular velocity [rads^{-1}]

List of Abbreviations

AC	Alternating Current
ADS	Active Distribution Systems
ASM	squirrel cage induction generator
CCA	Critical Clearing Angle
CCT	Critical Clearing Time
CG	Centralized Generator
CHP	Combined Heat and Power
DC	Direct Current
DG	Distributed Generation
DN	Distribution Network
EAC	Equal Area Criterion
EHV	Extra-High Voltage
FACTS	Flexible AC Transmission System
G	Generator (Chapter 7)
HV	High Voltage
IEEE	Institute of Electrical and Electronics Engineers
IGBT	Insulated Gate Bipolar Transistor
LV	Low Voltage
Max. dev.	Maximum rotor speed deviation
MCS	Monte Carlo Simulation
MV	Medium Voltage
OPF	Optimal Power Flow
Osc. dur.	Oscillation duration
PE	power electronic interfaced DG without grid voltage and frequency control
PEC	power electronic interfaced DG - with grid voltage and frequency control
PI	Proportional-Integral controller
PLL	Phase Locked Loop
PQ-source	constant active and reactive power generator
PSS/E	Power System Simulator for Engineering
PV	Photovoltaic
PWM	Pulse Width Modulation
RMS	Root-Mean-Square
RTDS	Real Time Digital Simulator
Sin Wave Gen	Sine-Wave Generator
SM	synchronous generator - without grid voltage and frequency control
SMC	synchronous generator - with grid voltage and frequency control

List of Abbreviations, continued

SMES	Superconducting Magnetic Energy Storage
T_L	Transmission Line (Chapter 7)
T	Transformer (Chapter 7)
TN	Transmission Network
UEP	Unstable Equilibrium Point
VSC	Voltage Source Converter

Appendix B

Test System Data

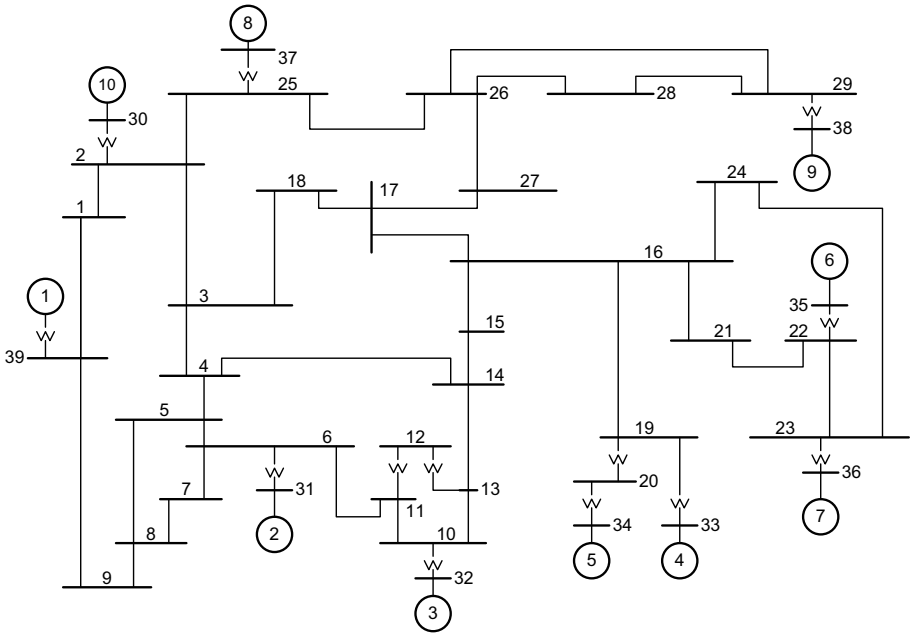

Figure B.1: Single line diagram of the 39-bus New England test system [49]

Table B.1: Bus Data of the New England 39 Bus Test System [49]

Bus (nr.)	Volts (pu)	Load (MW)	Load (MVAr)	Gen (MW)	Gen (MVAr)
1	-	0.0	0.0	-	-
2	-	0.0	0.0	-	-
3	-	322.0	2.4	-	-
4	-	500.0	184.0	-	-
5	-	0.0	0.0	-	-
6	-	0.0	0.0	-	-
7	-	233.8	84.0	-	-
8	-	522.0	176.0	-	-
9	-	0.0	0.0	-	-
10	-	0.0	0.0	-	-
11	-	0.0	0.0	-	-
12	-	7.5	88.0	-	-
13	-	0.0	0.0	-	-
14	-	0.0	0.0	-	-
15	-	320.0	153.0	-	-
16	-	329.0	32.3	-	-
17	-	0.0	0.0	-	-
18	-	158.0	30.0	-	-
19	-	0.0	0.0	-	-
20	-	628.0	103.0	-	-
21	-	274.0	115.0	-	-
22	-	0.0	0.0	-	-
23	-	247.5	84.6	-	-
24	-	308.6	-92.2	-	-
25	-	224.0	47.2	-	-
26	-	139.0	17.0	-	-
27	-	281.0	75.5	-	-
28	-	206.0	27.6	-	-
29	-	283.5	26.9	-	-
30	1.0475	0.0	0.0	250	-
31	0.982	9.2	4.6	-	-
32	0.9831	0.0	0.0	650	-
33	0.9972	0.0	0.0	632	-
34	1.0123	0.0	0.0	508	-
35	1.0493	0.0	0.0	650	-
36	1.0635	0.0	0.0	560	-
37	1.0278	0.0	0.0	540	-
38	1.0265	0.0	0.0	830	-
39	1.03	1104.0	250.0	1000	-

Table B.2: Line Data of the New England 39 Bus Test System [49]

Line Bus	Data Bus	Resistance	Reactance	Susceptance	Transformer Magnitude	Tap Angle
1	2	0.0035	0.0411	0.6987	0	0
1	39	0.0010	0.0250	0.7500	0	0
2	3	0.0013	0.0151	0.2572	0	0
2	25	0.0070	0.0086	0.1460	0	0
3	4	0.0013	0.0213	0.2214	0	0
3	18	0.0011	0.0133	0.2138	0	0
4	5	0.0008	0.0128	0.1342	0	0
4	14	0.0008	0.0129	0.1382	0	0
5	6	0.0002	0.0026	0.0434	0	0
5	8	0.0008	0.0112	0.1476	0	0
6	7	0.0006	0.0092	0.1130	0	0
6	11	0.0007	0.0082	0.1389	0	0
7	8	0.0004	0.0046	0.0780	0	0
8	9	0.0023	0.0363	0.3804	0	0
9	39	0.0010	0.0250	1.2000	0	0
10	11	0.0004	0.0043	0.0729	0	0
10	13	0.0004	0.0043	0.0729	0	0
13	14	0.0009	0.0101	0.1723	0	0
14	15	0.0018	0.0217	0.3660	0	0
15	16	0.0009	0.0094	0.1710	0	0
16	17	0.0007	0.0089	0.1342	0	0
16	19	0.0016	0.0195	0.3040	0	0
16	21	0.0008	0.0135	0.2548	0	0
16	24	0.0003	0.0059	0.0680	0	0
17	18	0.0007	0.0082	0.1319	0	0
17	27	0.0013	0.0173	0.3216	0	0
21	22	0.0008	0.0140	0.2565	0	0
22	23	0.0006	0.0096	0.1846	0	0
23	24	0.0022	0.0350	0.3610	0	0
25	26	0.0032	0.0323	0.5130	0	0
26	27	0.0014	0.0147	0.2396	0	0
26	28	0.0043	0.0474	0.7802	0	0
26	29	0.0057	0.0625	1.0290	0	0
28	29	0.0014	0.0151	0.2490	0	0
12	11	0.0016	0.0435	0.0000	1.006	0
12	13	0.0016	0.0435	0.0000	1.006	0
6	31	0.0000	0.0250	0.0000	1.07	0
10	32	0.0000	0.0200	0.0000	1.07	0
19	33	0.0007	0.0142	0.0000	1.07	0
20	34	0.0009	0.0180	0.0000	1.009	0
22	35	0.0000	0.0143	0.0000	1.025	0
23	36	0.0005	0.0272	0.0000	1	0
25	37	0.0006	0.0232	0.0000	1.025	0
2	30	0.0000	0.0181	0.0000	1.025	0
29	38	0.0008	0.0156	0.0000	1.025	0
19	20	0.0007	0.0138	0.0000	1.06	0

Appendix C

Generator, Governor and Excitation Systems Data

Table C.1: Detailed model unit data for a cylindrical synchronous generator (as CG or DG) [53]

Parameter	T_{do}	T_{do}	T_{qo}	T_{qo}	H	D	X_d
Value	5.0	0.05	1.0	0.04	4	0	1.75
Parameter	X_q	X_d	X_q	X_d	X_l	$S(1.0)$	$S(1.2)$
Value	1.65	0.30	0.75	0.20	0.175	0.2	0.4

Table C.2: Detailed model unit data for induction genrator (as DG) [53]

Parameter	T	T	H	X	X	X	X_l
Value	0.98	0	3.5	3.1	0.18	0	0.1
Parameter	E_1	$S(E_1)$	E_2	$S(E_2)$	0.	$SYN-POW*$	
Value	1	0	1.2	0	0	0	

*SYN-POW, Mechanical Power At Synchronous Speed (> 0). Used only to start machine, otherwise ignored.

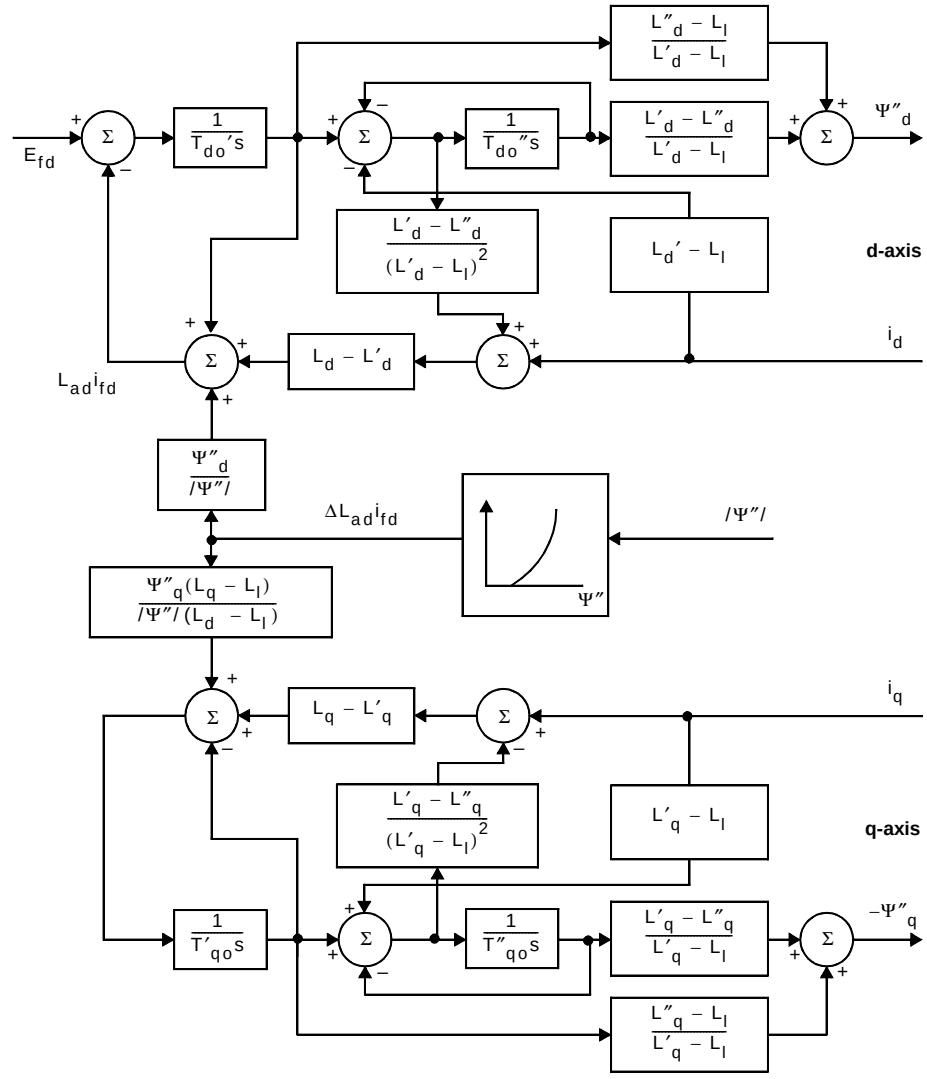

Figure C.1: Synchronous generator model block diagram [53]

Table C.3: Detailed model unit governing system data for synchronous machine [53]

Parameter	T_A/T_B	T_B	K	T_E	E_{MIN}	E_{MAX}
Value	0.1	10	300	0.05	0	5

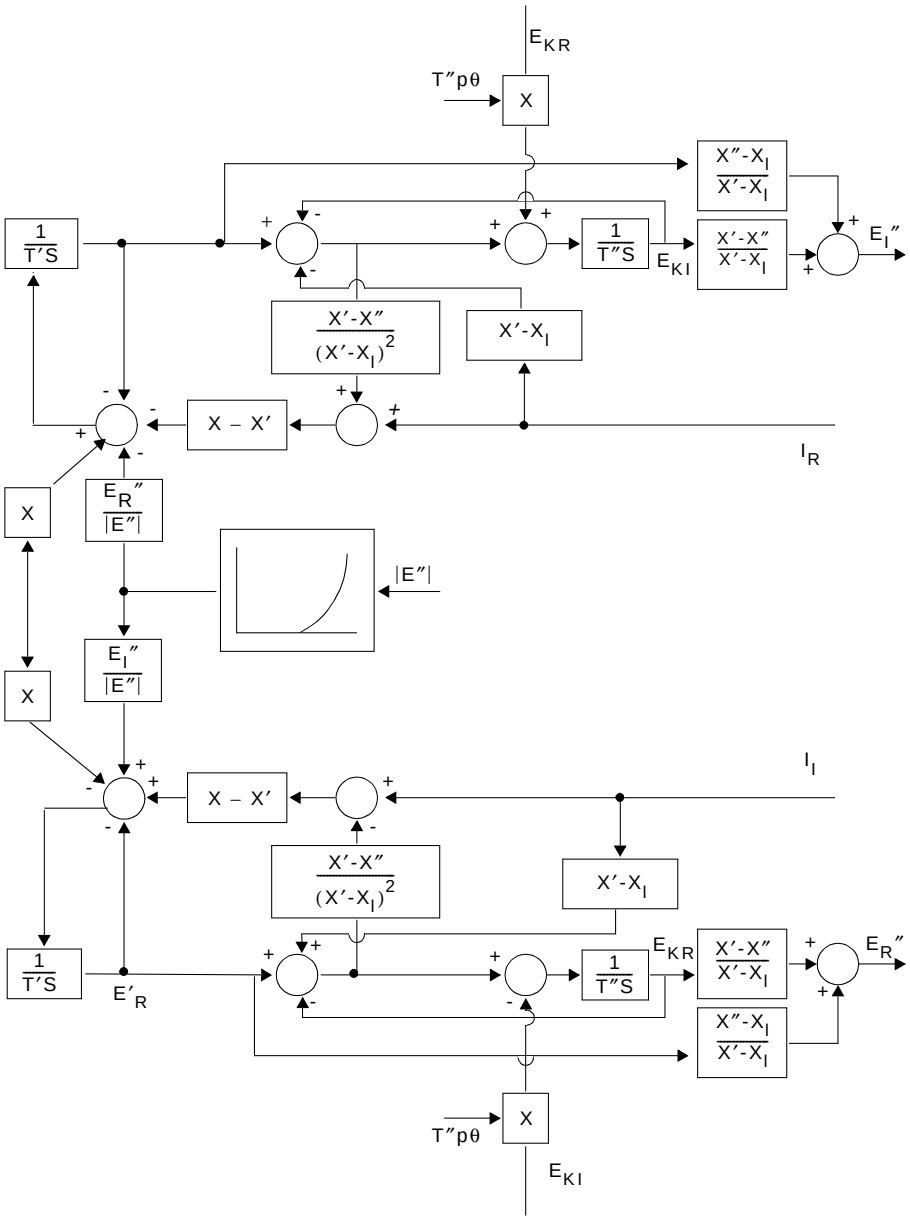

Figure C.2: Induction machine model block diagram [53]

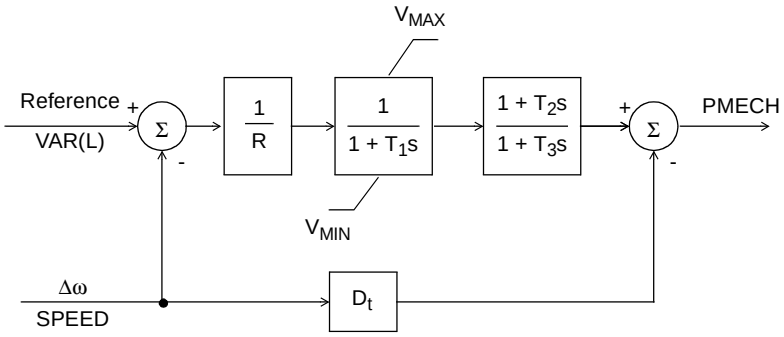

Figure C.3: Governor model block diagram [53]

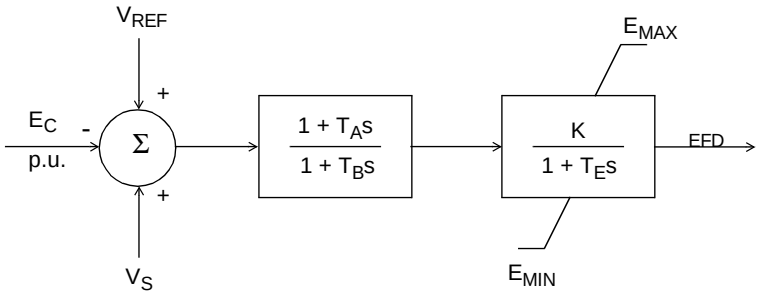

Figure C.4: Governor model block diagram [53]

Table C.4: Detailed model unit excitation system data for synchronous machine [53]

Parameter	R	T_1	V_{MAX}	V_{MIN}	T_2	T_3	D_t
Value	0.05	0.05	0.91	0	2.1	7	0

Appendix D

Power Flow Computation

D.1 Power Flow Problem

One of the most common studies in power systems is a load flow (or power flow) calculation. This computation provides insight in the state of a power system for a specific steady-state situation, as it computes, among others, the voltage (magnitude and phase angle) at each bus and the power flow (real and reactive) in each line [25].

In mathematical terms, solving a load flow problem is nothing more than solving a system of non-linear algebraic equations. Solving the load flow problem starts from obtaining the single-line diagram data of power systems [25], where the transmission lines – represented by the equivalent circuits and the numerical values for the series impedance Z and the total line-charging admittance Y – are used to determine all elements of the $N \times N$ bus admittance matrix of a system (with N buses), with the typical element Y_{ij} of this matrix given by

$$\begin{aligned} Y_{ij} &= |Y_{ij}|\angle\theta_{ij}, \\ &= |Y_{ij}|\cos\theta_{ij} + j|Y_{ij}|\sin\theta_{ij}, \\ &= Gij + \hat{j}B_{ij}. \end{aligned} \tag{D.1}$$

Y_{ij} is the admittance element between bus i and j, a complex identity represented in the polar coordinate by the magnitude $|Y_{ij}|$ and the angle θ_{ij} and in the cartesian coordinate by G_{ij} and B_{ij}, where G_{ij}, B_{ij} are the conductance and susceptance of the element Y_{ij}. The voltage U at a typical bus i of the system is

$$\begin{aligned} U_i &= |U_i|\angle\delta_i, \\ &= |U_i|\cos(\delta_i) + j\sin(\delta_i), \end{aligned} \tag{D.2}$$

while the current injected into the network at bus i in terms of the elements Y_{in} of $\mathbf{Y_{bus}}$ is

$$\begin{aligned} I_i &= Y_{i1}U_1 + Y_{i2}U_2 + \cdots + Y_{iN}U_N, \\ &= \sum_{n=1}^{N} Y_{in}U_n. \end{aligned} \tag{D.3}$$

According to this representation, the load flow equations can be written as

$$P_i = |U_i|^2 G_{ii} + \sum_{n=1, n\neq i}^{N} |U_i U_n Y_{in}| \cos(\theta_{in} + \delta_n - \delta_i), \tag{D.4}$$

$$Q_i = -|U_i|^2 B_{ii} + \sum_{n=1, n\neq i}^{N} |U_i U_n Y_{in}| \sin(\theta_{in} + \delta_n - \delta_i), \tag{D.5}$$

where P_i, Q_i are respectively the active and reactive power injections at node i. In the above equations, G_{ii}, B_{ii} are the conductance and susceptance of the element Y_{in} of the admittance matrix, respectively, and $|U_i|$ and δ_i the voltage magnitude and angle at node i, respectively.

Using (D.4) and (D.5), the *net* real P_i and reactive Q_i power entering the network at typical bus i can be computed. Denoting P_{gi} as the scheduled power generated at bus i and P_{di} as the scheduled power demand of the load at bus i, the *net* scheduled power being injected in the network at bus i, $P_{i,sch}$, can be defined as

$$P_{i,sch} = P_{gi} - P_{di}. \tag{D.6}$$

Now, let $P_{i,calc}$ be the calculated value of P_i, and

$$\begin{aligned} \Delta P_i &= P_{i,sch} - P_{i,calc}, \\ &= (P_{gi} - P_{di}) - P_{i,calc}, \end{aligned} \tag{D.7}$$

$$\begin{aligned} \Delta Q_i &= Q_{i,sch} - Q_{i,calc}, \\ &= (Q_{gi} - Q_{di}) - Q_{i,calc}. \end{aligned} \tag{D.8}$$

In reality, the calculated values do not always coincide with the scheduled ones. In this case, $\Delta P_i \neq 0$ or $\Delta Q_i \neq 0$, and it is said that a mismatch occurs. Suppose that mismatch does not occur. In this case $\Delta P_i = \Delta Q_i = 0$, and the *power-balance equations* (g_i' and g_i'') can be written as

$$\begin{aligned} g_i' &= P_i - P_{i,sch}, \\ &= P_i - (P_{gi} - P_{di}), \\ &= 0, \end{aligned} \tag{D.9}$$

$$\begin{aligned} g_i'' &= Q_i - Q_{i,sch}, \\ &= Q_i - (Q_{gi} - Q_{di}), \\ &= 0. \end{aligned} \tag{D.10}$$

Notice that the subscript i indicates that each bus of a power network has the above two equations. To this end, we can formulate the power flow problem as follows:

Find $|U_i|$, δ_i, P_i *and* Q_i, $i = 1, 2, \ldots$ *from* (D.4) *and* (D.5) *such that* (D.10) *and* (D.11) *are satisfied.*

Each bus i in a power system may be associated with four potentially unknown quantities P_i, Q_i, δ_i and $|U_i|$. Thus, the above stated problem is overdetermined and has an infinite number of solutions. In order to make the solutions uniquely determined, two of the four unknowns have to be specified. The remaining are computed. There exist three scenarios to choose the specified variables, related to three types of buses:

1. P_i and Q_i specified, *Load bus.*
2. P_i and $|U_i|$ specified, *Voltage-controlled bus.*
3. δ_i and $|U_i|$ specified, *Slack bus.*

In the power flow study, the unscheduled bus-voltage magnitudes and angles are called *state variables* or *dependent variables* since their values, describing the state of the system, depend on the quantities specified at all buses. The power-flow problem is to determine values for all state variables by solving an equal number of power-flow equations based on the input data specifications. As the functions P_i and Q_i are nonlinear with respect to δ_i and $|U_i|$, a power-flow calculation should employ iterative techniques.

D.2 Newton-Rhapson power flow solution

One method to solve a non-linear system of equations is the Newton-Rhapson method. This method is widely explained in standard numerical analysis books, and a basic tool within the PSS/E software [53]. Adaptation of this method to the power-flow problem is described in the following algorithm 5, [25]:

Remark D.2.1 *In Line 7, a linear system of type* $\mathbf{A}x = b$ *has to be solved for* x*. This in general requires inversion of* $\mathbf{A}$*. In our case,* $\mathbf{J} := \mathbf{A}$ *and so on. As* $\mathbf{J}$ *is a densely populated matrix, this inversion may become very time consuming for a large number of buses. In Line 8,* $\|\|\cdot\|\|_\infty = \max_i\{|\cdot_i|\}$*, the infinity norm. So, the Newton-Rhapson process is terminated if the maximum absolute value of the corrections is lower than* ϵ*.*

Remark D.2.2 *In line 4, note that* ΔP_1 *and* ΔQ_1 *of the slack bus are undefined when* P_1 *and* Q_1 *are not scheduled. Since the slack bus serves as reference for the angles of all other bus voltages, all terms involving* δ_1 *and* $\Delta|U_1|$ *are omitted from the equations because those corrections are both zero at the slack bus.*

Algorithm 5 Newton-Rhapson for power-flow problem

1: Guess the initial unknown voltages: $|U_i|^{(0)}$, $\delta_i^{(0)}$
2: Set tolerance ϵ
3: **for** $j = 1, 2, ...$ **do**
4: Compute $P_{i,calc}^{(j)}, Q_{i,calc}^{(j)}$ (from (D.4) and (D.5))
5: Compute the power mismatches (D.7), (D.8)
6: Compute the Jacobian $\mathbf{J}^{(j)}$

$$\mathbf{J}^{(j)} = \left[\begin{array}{ccc|ccc} \frac{\partial P_2}{\partial \delta_2} & \cdots & \frac{\partial P_2}{\partial \delta_N} & |U_2|\frac{\partial P_2}{\partial |U_2|} & \cdots & |U_2|\frac{\partial P_2}{\partial |U_N|} \\ \vdots & \mathbf{J_{11}} & \vdots & \vdots & \mathbf{J_{12}} & \vdots \\ \frac{\partial P_N}{\partial \delta_2} & \cdots & \frac{\partial P_N}{\partial \delta_N} & |U_2|\frac{\partial P_N}{\partial |U_2|} & \cdots & |U_N|\frac{\partial P_2}{\partial |U_N|} \\ \hline \frac{\partial Q_2}{\partial \delta_2} & \cdots & \frac{\partial Q_2}{\partial \delta_N} & |U_2|\frac{\partial Q_2}{\partial |U_2|} & \cdots & |U_2|\frac{\partial Q_2}{\partial |U_N|} \\ \vdots & \mathbf{J_{21}} & \vdots & \vdots & \mathbf{J_{22}} & \vdots \\ \frac{\partial Q_N}{\partial \delta_2} & \cdots & \frac{\partial Q_N}{\partial \delta_N} & |U_2|\frac{\partial Q_N}{\partial |U_2|} & \cdots & |U_N|\frac{\partial Q_2}{\partial |U_N|} \end{array}\right]^{(j)} \tag{D.11}$$

7: Compute the correction from the following system:

$$\mathbf{J}^{(j)} \left[\begin{array}{c} \Delta\delta_2 \\ \vdots \\ \Delta\delta_N \\ \hline \Delta|U_2| \\ \vdots \\ \Delta|U_N| \end{array}\right]^{(j)} = \left[\begin{array}{c} \Delta P_2 \\ \vdots \\ \Delta P_N \\ \hline \Delta Q_2 \\ \vdots \\ \Delta Q_N \end{array}\right]^{(j)} \tag{D.12}$$

8: **if** $\|\Delta\delta_i^{(j)}\|_\infty, \|\Delta|U_i|_i^{(j)}\|_\infty < \epsilon$ convergence is reached. **quit**
9: Add the correction to the previous value:

$$\delta_i^{(j+1)} = \delta_i^{(j)} + \Delta\delta_i^{(j)} \tag{D.13}$$

$$|U_i|^{(j+1)} = |U_i|^{(j)} + \Delta|U_i^{(j)}| \tag{D.14}$$

Bibliography

[1] T. Ackermann, G. Andersson, and L. Soder, *Distributed generation: a definition*, Electric Power Systems Research, 57 (2001), pp. 195–204.

[2] A. Al-Hinai and A. Feliachi, *Dynamic model of a microturbine used as distributed generator*, in 34^{th} Southeastern Symposium on System Theory, 18-19 March 2002, pp. 209–213.

[3] D. Audring and P. Balzer, *Operating stationary fuel cells on power systems and micro-grids*, in 2003 IEEE Bologna PowerTech Conference, Bologna, Italy, 23-26 June 2003, 6 pages.

[4] H. Barten and R. J. F. van Gerwen, *Flexibele elektriciteitsopslag*, Energietechniek, 79(12) (2001), pp. 601–605.

[5] M. Begovic, A. Pregeli, A. Rohatgi, and C. Honsberg, *Green power: Status and perspectives*, Proceedings of the IEEE, 89(12) (2001), pp. 1734–1743.

[6] L. B. Bernshtein, *Tidal power development - a realistic, justifiable and topical problem of today*, IEEE Transactions on Energy Conversion, 10 (3) (1995), pp. 591–599.

[7] A. M. Borbely and J. F. Kreider, *Distributed Generation the Power Paradigm for the New Millennium*, CRC Press LLC, 2001.

[8] R. E. Brown, *Electric Power Distribution Reliability*, Marcel Dekker Inc., New York, 2002.

[9] A. G. Bryans, B. Fox, P. A. Crossley, and M. O'Malley, *Impact of tidal generation on power system operation in ireland*, IEEE Transactions on Power Systems, 20(4) (2005), pp. 2034–2040.

[10] A. Burke, *Ultracapacitors: Why, how and where is the technology*, Journal of Power Sources, 91 (1) (2000), pp. 37–50.

[11] Cigre Technical Brochure TF 38.01.10, *Modeling new forms of generation and storage*, November 2000.

[12] Cigre Working Group 37.23, *Impact of increasing contribution of dispersed generation on the power system, Cigre Technical Brochure no. 137*, February 1999.

[13] B. Cook, *Introduction to fuel cells and hydrogen technology*, IEE Engineering Science and Education Journal, 11(6) (2002), pp. 205–216.

[14] A. Cooke, *personal communication on august 1*, OFGEM, (2003).

[15] M. W. Davis, *Microturbines - an economic and reliability evaluation for commercial, residential, and remote load applications*, IEEE Transactions on Power Systems, 14(4) (1999), pp. 1556–1562.

[16] D. N. Deokar, N. S. Lingayat, S. A. Khaparde, and S. P. Sukhatme, *Modelling tidal power plant at saphale*, in 1998 IEEE Region 10 International Conference on Global Connectivity in Energy, TENCON '98, vol. 2, 17-19 December 1008, pp. 544–547.

[17] R. Dettmer, *Wave energy gets seaworthy*, IEE Review, 48(5) (2002), pp. 14–19.

[18] M. K. Donnelly, J. E. Dagle, D. J. Trudnowski, and G. J. Rogers, *Impacts of the distributed utility on transmission system stability*, IEEE Transactions on Power Systems, 11(2) (1996), pp. 741–746.

[19] J. H. R. Enslin, *Interconnection of distributed power to the distribution network*, in IEEE Young Researcher Symposium: Intelligent Energy Conversions, Delft, the Netherlands, 18-19 March 2004.

[20] E.On Netz GmbH, Bayreuth, Germany, *E.On Netz, Grid Codem*, August 2003.

[21] L. M. Faulkenberry and W. Coffer, *Electrical Power Distribution and Transmission*, Prentice-Hall, New Jersey, 1996.

[22] J. P. Frau, *Tidel energy: Promising projects la rance, a successful industrial-scale experiment*, IEEE Transactions on Energy Conversion, 8(3) (1993), pp. 552–558.

[23] W. Gao, *Performance comparison of a fuel cell-battery hybrid powertrain and a fuel cell ultracapacitor hybrid powertrain*, in 2004 IEEE Power Electronics in Transportation, Detroit, Michigan, USA, 21-22 October 2004, pp. 143–150.

[24] F. M. Gatta, F. iliceto, S. Lauria, and P. Masato, *Modelling and computer simulation of dispersed generation in distribution networks. measures to prevent disconnection during system disturbances*, in 2003 IEEE Bologna PowerTech Conference, Bologna, Italy, 23-26 June 2003, 10 pages.

[25] J. J. Grainger and W. D. Stevenson, *Power System Analysis*, McGraw-Hill Inc., 1968.

[26] G. Grassi and A. V. Bridgwater, *European research in biomass energy*, in 25th Intersociety Energy Conversion Engineering Conference IECEC-90, 12-17 August 1990, pp. 126–130.

[27] S. W. Hadley and W. Short, *Electricity sector analysis in the clean energy futures study*, Energy Policy, 29(14) (2001), pp. 1285–1298.

[28] A. D. Hansen, F. Iov, P. Sorensen, and F. Blaabjerg, *Overall control strategy of variable speed doubly-fed induction generator wind turbine*, in Nordic Wind Power Conference, Gotheborg, Sweden, 1-2 March 2004, 7 pages.

[29] R. Hebner, J. Beno, and A. Walls, *Flywheel batteries come around again*, IEEE Spectrum, 39(4) (2002), pp. 46–51.

[30] J. W. Herzog, *Current and near-term emission control strategies for diesel powered generator sets*, in 24^{th} Annual International Telecommunication Energy Conference INTELEC, 2002, pp. 394–399.

[31] N. Janssens, *Impact of power flows on interarea oscillations and mitigation by means of svcs or qpss*, in 14^{th} Power Systems Computation Conference, 24-28 June 2002, 7 pages.

[32] N. Jenkins, *Impact of dispersed generation on power systems*, ELECTRA, 199 (1999), pp. 6–13.

[33] N. Jenkins, R. Allan, P. Crossley, D. Kirschen, and G. Strbac, *Embedded Generation*, no. 31 in Power Energy Series, IEE, 2000.

[34] P. Kundur, *Power System Stability and Control*, McGraw-Hill Inc., New York, first ed., 1994.

[35] P. Kundur, J. Paserba, and S. Vitet, *Overview on definition and classification of power system stability*, in CIGRE/IEEE PES International Symposium Quality and Security of Electric Power Delivery Systems, 2003, pp. 1–4.

[36] W. R. Lachs and D. Sutanto, *Battery storage plant within large load centres*, IEEE Transaction on Power Systems, 7 (1992), pp. 762–767.

[37] G. Lalor, A. Mullane, and M. O'Malley, *Frequency control and wind turbine technologies*, IEEE Transaction on Power Systems, 20 (2005), pp. 1905–1913.

[38] G. Lalor, J. Ritchie, S. Rourke, D. Flynn, and M. J. O'Malley, *Dynamic frequency control with increasing wind generation*, in 2004 IEEE Power Engineering Society General Meeting, Denver, Colorado, USA, vol. 2, 6-10 June 2004, pp. 1715–1720.

[39] M. A. Laughton, *Fuel cells*, IEE Engineering Science and Education Journal, 11 (2002), pp. 7–16.

[40] C. A. Luongo, *Superconducting storage systems: An overview*, IEEE Transactions on Magnetics, 32 (1996), pp. 2214–2223.

[41] A. P. S. Meliopoulos, *Challenges in simulation and design of μ grids*, in 2002 IEEE Power Engineering Society Winter Meeting, vol. 1, 2002, pp. 309–314.

[42] J. Morren, S. W. H. de Haan, and J. A. Ferreira, *Model reduction and control of electronic interfaces of voltage dip proof dg units*, in 2004 IEEE Power Engineering Society General Meeting, vol. 2, 6-10 June 2004, pp. 2168–2173.

[43] A. Mullane, G. Bryans, and M. O'Malley, *Kinetic energy and frequency response comparison for renewable generation systems*, in International Conference on Future Power Systems 2005, Amsterdam, the Netherlands, 16-18 November 2005, 6 pages.

[44] A. Mullane and M. O'Malley, *The inertial response of induction-machine-based wind turbines*, IEEE Transactions on Power Systems, 20 (2005), pp. 1496–1503.

[45] K. Nielsen, *Wave energy plants - the way forward*, in IEE Colloqium Wave Power: An Engineering and Commercial Perspective (Digest No: 1997/098), 13 March 1997, pp. 7/1–7/5.

[46] K. Ogata, *Modern control engineering*, Prentice-Hall, 4^{th} ed., 2002.

[47] I. T. F. on Load Representation for Dynamics Performance, *Load representation for dynamic analysis*, IEEE Transactions on Power Systems, 8(2) (1993), pp. 472–483.

[48] J. O'Sullivan, M. Power, M. Flynn, and M. O'Malley, *Modelling of frequency control in an island system*, in 1999 IEEE Power Engineering Society Winter Meeting, New York, New York, USA, vol. 1, 31 January-4 February 1999, pp. 574–579.

[49] M. A. Pai, *Energy Function Analysis for Power System Stability*, Kluwer Academic Publishers, Boston, 1989.

[50] G. Papaefthymiou, A. Tsanakas, M. Reza, P. H. Schavemaker, and L. van der Sluis, *Stochastic modelling and analysis of horizontally-operated power systems with a high wind energy penetration*, in 2005 IEEE St. Petersburg PowerTech Conference, St. Petersburg, Russia, 27-30 June 2005, 7 pages.

[51] M. R. Patel, *Wind and Solar Power Systems*, CRC Press LLC, 1999.

[52] G. Pepermans, J. Driesen, D. Haeseldonckx, R. Belmans, and W. D'Haeseleer, *Distributed generation: definition, benefits and issues*, Energy Policy, 33 (2005), pp. 787–798.

[53] Power Technologies, Inc., Schenectady, US, *PSS/E 25.4 On-line Documentation*, December 1997.

[54] A. Price, *Technologies for energy storage-present and future: Flow batteries*, in 2000 IEEE Power Engineering Society Summer Meeting, vol. 3, 16-20 July 2000, pp. 1541–1545.

[55] F. Provoost, A. Ishchenko, A. Jokic, J. M. A. Myrzik, and W. L. Kling, *Self controlling autonomous operating power networks*, in 18^{th} International Conference on Electricity Distribution, CIRED 2005, Turin, Italy, 6-9 June 2005, 5 pages.

[56] M. Rabinowitz, *Power systems of the future (part 4)*, IEEE Power Engineering Review, 20 (2000), pp. 4–6.

[57] S. Rahman, *Green power: What is it and where can we find it?*, IEEE Power and Energy Magazine, 1 (2003), pp. 30–37.

[58] M. Reza, J. Morren, P. H. Schavemaker, W. L. Kling, and L. van der Sluis, *Power electronic interfaced DG units: Impact of control strategy on power system transient stability*, in 2005 IEE 3^{rd} Reliability of Transmission and Distribution Networks, London, United Kingdom, 15-17 February 2005, 4 pages.

[59] M. Reza, P. H. Schavemaker, W. L. Kling, and L. van der Sluis, *A research program on intelligent power systems: Self controlling and self adapting power systems equipped to deal with the structural changes in the generation and the way of consumption*, in 17^{th} International Conference on Electricity Distribution, CIRED 2003, Barcelona, Spain, 12-15 May 2003, 6 pages.

[60] M. Reza, P. H. Schavemaker, J. G. Slootweg, W. L. Kling, and L. van der Sluis, *Impacts of distributed generation penetration levels on power systems transient stability*, in IEEE Young Researcher Symposium: Intelligent Energy Conversions, Delft, the Netherlands, 18-19 March 2004, 6 pages.

[61] M. Reza, A. M. van Voorden, P. H. Schavemaker, G. C. Paap, and L. van der Sluis, *Implementation of renewable electrical energy generation in an urban distribution network: Impacts of energy storage and demand growth*, in 17^{th} International Conference on Electricity Distribution, CIRED 2003, Barcelona, Spain, 12-15 May 2003, 6 pages.

[62] P. Robinson, *Microhydro in Papua New Guinea-the experiences of an electrical engineer*, IEE Power Engineering Journal, (1988), pp. 273–280.

[63] G. Rogers, *Demystifying power system oscillations*, IEEE Computer Applications in Power, 9 (1996), pp. 30–35.

[64] R. B. Schainker, *Executive overview: Energy storage options for a sustainable energy future*, in 2004 IEEE Power Engineering Society General Meeting, vol. 2, 6-10 June 2004, pp. 2309–2314.

[65] S. M. Schoenung and C. Burns, *Utility energy storage applications studies*, IEEE Transactions on Energy Conversion, 11 (1996), pp. 658–665.

[66] F. Schwartz, R. Pegallapati, and M. Shahidehpour, *Small hydro as green power*, in 2005 IEEE Power Engineering Society General Meeting, 12-16 June 2005, pp. 1883–1890.

[67] T. Sels, C. Dragu, T. V. Craenenbroeck, and R. Belmans, *Overview of new energy storage systems for an improved power quality and load managing on distribution level*, in 16^{th} International Conference and Exhibition on Electricity Distribution (IEE Conf. Publ No. 482), CIRED 2001, Amsterdam, the Netherlands, vol. 4, 18-21 June 2001, 5 pages.

[68] S. Sheth and M. Shahidehpour, *Geothermal energy in power systems*, in 2004 IEEE Power Engineering Society General Meeting, Denver, Colorado, USA, 6-10 June 2004, pp. 1972–1977.

[69] J. G. Slootweg, *Wind Power: Modelling and Impact on Power Systems Dynamics*, PhD Thesis, Delft University of Technology, 2003.

[70] J. G. Slootweg, S. W. H. de Haan, H. Polinder, and W. L. Kling, *Modeling new generation and storage technologies in power system dynamics simulations*, in 2002 IEEE Power Engineering Society Summer Meeting, Chicago, Illinois, USA, vol. 2, 21-25 July 2002, pp. 868–873.

[71] J. G. Slootweg and W. L. Kling, *Impacts of distributed generation on power system transient stability*, in 2002 IEEE Power Engineering Society Summer Meeting, Chicago, Illinois, USA, vol. 2, 21-25 July 2002, pp. 503–508.

[72] N. Sriram and M. Shahidehpour, *Renewable biomass energy*, in 2005 IEEE Power Engineering Society General Meeting, 12-16 June 2005, pp. 1910–1915.

[73] Tennet, Arnhem, the Netherlands, *Technische gegevens van componenten van het door TenneT beheerde 380 kV- en 220 kV-net situatie per 1 november 2003*, November 2003.

[74] A. M. Tuckey, D. J. Patterson, and J. Swenson, *A kinetic energy tidal generator in the Northern Territory Results*, in 23^{rd} International Conference on Industrial Electronics, Control and Instrumentation IECON 97, vol. 2, 9-14 November 1997, pp. 937–942.

[75] T. V. Van and R. Belmans, *Distributed generation overview: current status and challenges*, International Review of Electrical Engineering (IREE), 1 (2006), pp. 178–189.

[76] T. V. Van, J. Driesen, and R. Belmans, *Interconnection of distributed generators and their influences on power system*, International Energy Journal, 6 (2005), pp. 127–140.

[77] G. A. M. van Kuik, *Are wind turbines growing too fast?*, in 2001 European Wind Energy Conference and Exhibition, 2-6 July 2001, pp. 69–72.

[78] B. M. Weedy, *Electric Power Systems*, McGraw-Hill Inc., first ed., 1994.

[79] T. J. T. Whittaker, *The development of shoreline wavepower in the uk*, in International Conference on Renewable Energy - Clean Power 2001, 17-19 November 1993, pp. 117–120.

[80] K. H. Williamson, R. P. Gunderson, G. M. Hamblin, D. L. Gallup, and K. Kitz, *Geothermal power technology*, Proceedings of the IEEE, 89 (2001), pp. 1783–1792.

[81] A. Woyte, T. V. Van, R. Belmans, and J. Nijs, *Voltage fluctuations on distribution level introduced by photovoltaic systems*, IEEE Transactions on energy conversion, 21 (2006), pp. 202–209.

[82] Y. Xue, T. van Cutsem, and M. Ribbens-Pavella, *A simple direct method for fast transient stability assessment of large power systems*, IEEE Transactions on Power Systems, 3 (1988), pp. 400–412.

Scientific Contributions

Publications

1. M. Reza, A. O. Dominguez, P. H. Schavemaker, W. L. Kling. *Maintaining the power balance in an 'Empty Network'.* European Transactions on Electrical Power, Vol. 16, No. 5, September-October 2006, pp. 479-493.

2. M. Reza, D. Sudarmadi, F. A. Viawan, W. L. Kling, L. van der Sluis. *Dynamic Stability of Power Systems with Power Electronic Interfaced DG.* In Proceedings of IEEE Power Systems Conference and Exposition, Atlanta, Georgia, USA, 29 October-1 November 2006, 6 pages.

3. M. Reza, G. Papaefthymiou, W. L. Kling. *Investigating Transient Stability Impacts of a 'Vertical-to-Horizontal' Transformation of Power Systems.*In Proceedings of IEEE Young Researcher Symposium, Gent, Belgium, 27-28 April 2006, 6 pages.

4. M. Reza, A. O. Dominguez, P. H. Schavemaker, W. L. Kling. *Maintaining the power balance in an 'Empty Network'.* In Proceedings of International Conference on Future Power Systems (FPS) 2005, Amsterdam, The Netherlands, 16-18 November 2005, 8 pages.

5. M. Reza, C. P. Rodriguez, P. H. Schavemaker, W. L. Kling. *A Transient Stability Studies of a 'Vertical-to-Horizontal' Transformation of Power Systems on a Real Time Digital Simulator.* In Proceedings of International Conference on Future Power Systems (FPS) 2005, Amsterdam, The Netherlands, 16-18 November 2005, 6 pages.

6. M. Reza, M. Gibescu, P. H. Schavemaker, W. L. Kling, L. van der Sluis. *Transient Stability Impacts of a 'Vertical-to-Horizontal' Transformation of Power Systems.* In Proceedings of IEEE PowerTech Conference, St Petersburg, Russia, 23-27 June 2005, 6 pages.

7. M. Reza, G. Papaefthymiou, P. H. Schavemaker, W. L. Kling, L. van der Sluis. *Stochastic Transient Stability Analysis of Power Systems with Distributed Energy Systems.* In Proceedings of CIGRE Symposium, Athens, Greece, 15-16 April 2005, 8 pages.

8. M. Reza, J. Morren, P. H. Schavemaker, W. L. Kling, L. van der Sluis. *Power Electronic Interfaced DG Units: Impact of Control Strategy on Power System Transient Stability.* In Proceedings of 3^{rd} Reliability of Transmission and Distribution Networks (RTDN) 2005, London, United Kingdom, 15-17 February 2005, 4 pages.

9. M. Reza, G. Papaefthymiou, P. H. Schavemaker, W. L. Kling, L. van der Sluis. *Investigating Network Constraints (Congestions) of Horizontally-Operated Power Systems with Stochastic Distributed Generation.* In Proceedings of 3^{rd} Reliability of Transmission and Distribution Networks (RTDN) 2005, London, United Kingdom, 15-17 February 2005, 4 pages.

10. M. Reza, P. H. Schavemaker, J. G. Slootweg, W. L. Kling, L. van der Sluis. *Impact of Distributed Generation Grid Connection Strength on Power System Transient Stability.* In Proceedings of the 4^{th} IASTED International Conference on Power and Energy Systems (EuroPES) 2004, Rhodes, Greece, 28-30 June 2004, 6 pages.

11. M. Reza, J. G. Slootweg, P. H. Schavemaker, W. L. Kling, L. van der Sluis. *Impacts of Distributed Generation Penetration Levels on Power Systems Transient Stability.* In Proceedings of IEEE Power Engineering Society, General Meeting, Denver, Colorado, USA, 6-11 June 2004, 6 pages.

12. M. Reza, J. Morren, P. H. Schavemaker, J. G. Slootweg, W. L. Kling, L. van der Sluis. *Impacts of Converter Connected Distributed Generation on Power System Transient Stability.* In Proceedings of IEEE Young Researcher Symposium: Intelligent Energy Conversions, Delft, The Netherlands, 18-19 March 2004, 6 pages.

13. M. Reza, G. Papaefthymiou, P. H. Schavemaker, L. van der Sluis. *Potential for Transmission Lines Losses Reduction in Electrical Power System Operation with Distributed Generation.* In Proceedings of 8^{th} Indonesian Student Scientific Meeting 2003 Conference, Delft, The Netherlands, 9-10 October 2003, 4 pages.

14. M. Reza, J. G. Slootweg, P. H. Schavemaker, W. L. Kling, L. van der Sluis. *Investigating Impacts of Distributed Generation on Transmission System Stability.* In Proceedings of IEEE PowerTech Conference, Bologna, Italy, 23-26 June 2003, 7 pages.

15. M. Reza, P. H. Schavemaker, W. L. Kling, L. van der Sluis. *A Research Program on Intelligent Power Systems: Self Controlling and Self Adapting Power Systems Equipped to Deal with the Structural Changes in the Generation and the Way of Consumption.* In Proceedings of CIRED 2003 Conference, Barcelona, Spain, 12-15 May 2003, 6 pages.

16. M. Reza, A. M. van Voorden, P. H. Schavemaker, G. C. Paap, L. van der Sluis. *Implementation of Renewable Electrical Energy Generation in an Urban Distribution Network: Impacts of Energy Storage and Demand Growth.*

In Proceedings of CIRED 2003 Conference, Barcelona, Spain, 12-15 May 2003, 6 pages.

17. M. Reza, W. L. Kling. *Solving Network Constraints (Congestions) by Investigating Impact of Phase Shifters on the Flows.* In Proceedings of the 2^{nd} IASTED International Conference Power and Energy Systems (EuroPES) 2002, Crete, Grece, 25-28 June 2002, pp. 189-193.

18. D. Sudarmadi, M. Reza, G. C. Paap, L. van der Sluis. *DC Interconnection between Java and Sumatera, in Indonesia.* In Proceedings of IEEE Power Systems Conference and Exposition, Atlanta, Georgia, USA, 29 October-1 November 2006, 6 pages.

19. A. Mostavan, E. Joelianto, M. Reza, L. van der Sluis. *Discrete Event Controller Design of a Solar PV Water Pumping System using Signal Interpreted Petri Net.* In Proceedings of the 6^{th} Asian Control Conference, Bali, Indonesia, 18-21 July 2006, 6 pages.

20. E. Joelianto, A. Mostavan, M. Reza, L. van der Sluis. *A Discrete Event Controller for PV-Wind Hybrid Energy System using Signal Interpreted Petri Net.* In Proceedings of the 6^{th} Asian Control Conference, Bali, Indonesia, 18-21 July 2006, 8 pages.

21. F. A. Viawan, M. Reza, *The Impact of Distributed Generation on Voltage Dip and Overcurrent Protection Coordination.* In Proceedings of International Conference on Future Power Systems (FPS) 2005, Amsterdam, The Netherlands, 16-18 November 2005, 6 pages.

22. G. Papaefthymiou, A. Tsanakas, M. Reza, P. H. Schavemaker, L. van der Sluis. *Stochastic Modelling and Analysis of Horizontally Operated Power Systems with High Wind Energy Penetration.* In Proceedings of IEEE PowerTech Conference, St Petersburg, Russia, 23-27 June 2005, 7 pages.

23. G. Papaefthymiou, A. Tsanakas, M. Reza, P. H. Schavemaker, L. van der Sluis. *Reliability Assessment of HV/MV Transformer Links for Distributed Power Systems Planning.* In Proceedings of 3^{rd} Reliability of Transmission and Distribution Networks (RTDN) 2005, London, United Kingdom, 15-17 February 2005, 6 pages.

Talks

1. *Impacts of Distributed Generation and Distribution Systems on Power System Transient Stability*, ABB Corporate Research, Västerås, Sweden, May 18, 2006.

2. *'Empty Network'.* Panel Discussion on "Reliable Power - Europes Strength", Brussels, Belgium, May 10, 2006 (poster).

3. *Inherently Stable Transmission Systems on a Vertical-to-Horizontal Transformation of Power Systems with Distributed Generations*, Lunch Lecture KEMA, Arnhem, The Netherlands, February 16, 2006.

4. *Developing Indonesian Electricity with Distributed Generation.* International Conference on Indonesia Toward 2020, Hamburg, Germany, March 4-5, 2005.

5. *An Example of Utilizing a Stochastic Approach to Elaborate the Investigation of the Impacts of Distributed Generation on Power Systems.* The 3^{rd} Indonesian Applied Mathematics Society in The Netherlands (IAMS-N) Seminar on Applied Mathematics, Delft, The Netherlands, October 21, 2004.

6. *Potential of Renewable-Energy-Based Decentralized Generation in Power Network for Carbon Dioxide Emission Reduction.* The 9^{th} Indonesian Student Scientific Meeting, Aachen, Germany, October 7-9, 2004.

7. *Potential for Distributed Generation in Indonesian Electrical Power Systems.* The 8^{th} Indonesian Student Scientific Meeting, Delft, The Netherlands, October 9-10, 2003.

Acknowledgment

This thesis describes my work that was performed during my appointment at the Electrical Power System (EPS) Research Group, Faculty of Electrical Engineering, Mathematics and Computer Science, Delft University of Technology (TU Delft), the Netherlands.

Upon completion, I am indebted to a number of people for their direct or indirect contributions.

I would like to specially thank prof.ir. W. L. Kling (Wil) and prof.ir. L. van der Sluis (Lou) for being the promotor and the co-promotor of my PhD research, and especially for giving me a great opportunity to do research in the EPS Research Group. My special thanks also go to my daily supervisor dr.ir. P. H. Schavemaker (Pieter) and dr.ir. M. Gibescu (Madeleine) for fruitful discussions and encouragement during the research.

Many encouraging discussions were done during the appointment with highly experienced people in the field. In this respect, my appreciations should go to prof.dr.ir. J. A. Ferreira (TU Delft's Electrical Power Processing), prof.dr.ir. J. H. Blom (Technische Universiteit Eindhoven), prof.ir. M. Antal (Technische Universiteit Eindhoven, emeritus), prof.dr.ir R. Belmans (Katholieke Universiteit Leuven, Belgium) and prof.dr. M. J. O'Malley (University College Dublin, Ireland) of the promotion committee for their time to carefully read the manuscript.

This research has been performed within the framework of the research program 'intelligent power systems' of the IOP-EMVT (*Innovatiegerichte Onderzoeksprogramma's - ElektroMagnetische VermogensTechniek*) Program, financially supported by SenterNovem. SenterNovem is an agency of the Dutch ministry of Economic Affairs. The 'Intelligent Power Systems' research program is conducted by the Electrical Power Systems and the Electrical Power Processing Research Groups of the Delft University of Technology (TU Delft) and the Electrical Power Systems and Control System Research Groups of the Eindhoven University of Technology (TU Eindhoven), the Netherlands. For this, I would like to thank again prof.ir. M. Antal, the chairman of the IOP-EMVT program committee, ir. G. W. Boltje (SenterNovem), the program coordinator, and the leaders and supervisors of the project, prof. Kling, prof. van der Sluis, and dr. Schavemaker mentioned earlier and furthermore ir. S. W. H. de Haan (TU Delft's Electrical Power Processing), dr.ir. J. M. A. Myrzik (TU Eindhoven's Electrical Power Systems), prof.dr.ir P. van den Bosch (TU Eindoven's Control

Systems), and dr.ir. A. A. H. Damen (TU Eindhoven's Control Systems), for the scientific discussions and the technical feedback from the 'real world'. It was so often that these discussions paved the way to better understand many aspects that were and are still beyond my knowledge. My thanks are also to George Papaefthymiou, Johan Morren, Frans Provoost, Anton Ishchenko, Andrej Jokic, Roald de Graaff, Jody Verboomen, Cai Rong, and Sjef Cobben, the Ph.D. students, with whom I discussed scientific subjects and technical experiences we faced in the IOP-EMVT project.

Special thanks are also once more to George Papaefthymiou, my officemate, with whom I shared interests in many subjects from the very technical to the philosophical and spiritual ones, and Bob Paap, Marjan Popov, Tirza Drizi, Boukje Ypma, Ezra van Lanen, Arjan van Voorden, Johan Vijftigschild, Jan Heydeman, Barbara Slagter, Bart Ummels, Ralph Hendriks, Didik Sudarmadi, and I Made Ro Sakya, the EPS-mates, all in all, with whom I experienced a highly stimulating and pleasant working atmosphere during my stay at the EPS group. The initial part of this thesis is based to some extent on dr.ir. J. G. Slootweg's thesis, who was kind enough to share his knowledge and experience with me. The students Alejandro Dominguez and Cristovo Rodriguez are acknowledged for their contributions to this research.

Many thanks also go to those who support me with their hospitality and friendship during my stay in the Netherlands. I found it not easy to mention all their names, since the names would make a couple of pages! Nevertheless, I would like to acknowledge Yogi Erlangga, Dedy Wicaksono, Uly Nasution, Diah Chaerani and Anita Pharmatrisanti with whom I shared experiences as Indonesian Ph.D. students in Delft, and discussed our hopes and dreams in the future, and the younger Averrouz Mostavan, Zulfikar Dharmawan, Datuk Ary Samsura, Boy Fadhilah, Ikshan Rashad and Yusuf Maury who sincerely helped me with practical things from repairing bikes to reinstalling crashed computers, and also becoming nice friends for chatting during our interaction in Delft. I would like also to acknowledge Sheikh Sharief and the Sufi brothers and sisters in Rotterdam, with whom I shared colorful and enjoyable experiences on life and spirituality.

I wish to deeply thank my parents, my sister Mia Miranti and my brother Muhammad Lukman for their sincere support and prayers so that I could make my way up to where I am now. I am also grateful to my grand parents and my parents-in-law for their constant support and encouragement.

Special thanks should go to my wife Novi Ineke Cempaka Wangi for her endless support and encouragement throughout the difficulties I was facing in this work, as well as to my son Muhammad Rifqi Aulia Yahya, who can erase my problems just by smiling and laughing.

Most of all, I ultimately praise and thank Allah the Almighty, the Creator who creates all these nice people and the pleasant opportunities.

Muhamad Reza

Delft, Summer 2006

Biography

Muhamad Reza was born on November 4, 1974, in Bandung, the capital of the province of West Java, Indonesia. He finished the secondary school education at SMA Negeri 3 Bandung, Indonesia in 1993. In 1997, he obtained a B.Sc. degree in Electrical Engineering from Bandung Institute of Technology (ITB) with honor (*cum laude*). From 1998 until 2000 he attended Delft University of Technology (TU Delft), the Netherlands, from where he received an M.Sc. degree in Electrical Engineering with honor (*cum laude*). Since February 2002, he joined Electrical Power System Research Groups, chaired by Professor Lou van der Sluis, at the Faculty of Electrical Engineering, Mathematics and Computer Science as a PhD student within the framework of the research program 'Intelligent Power Systems' supported financially by SenterNovem, an agency of the Dutch Ministry of Economic Affairs.

From 1994-1997 he was awarded fellowship by Toyota-Astra Foundation, Indonesia for his B.Sc. study. In 1997 he was awarded *Ganesha Prize* as the best ITB student Year 1997 (highest in the university), and in 1998 he received a grant from *Bandoengsche Technische Hogeschool Fonds (BTHF)* where he used it for working on a research activity at the Electrical Power System Research Group (EPS), TU Delft, for three months. From 1998-2000 he was awarded a fellowship within the *Highly Talented Indonesian Student (Thalis)* Program for his M.Sc. study. In 2000 he was awarded the *Best Grade Average* of the Master of Science International Program 1998-2000, at TU Delft.

His work experience include student internships in Schlumberger Wireline, Manila, the Philippines (1996), and in PT Tesla Daya Elektrika, Bandung, Indonesia (1997). In 1997-1998 and 2000-2002 he was with the Electrical Power System and Distribution Laboratory, Department of Electrical Engineering, ITB, where he involved in some projects with PLN, Indonesia (2001), YPF Maxus, Indonesia (2001), and Pertamina, Indonesia (2001). He is currently working as a Research & Development scientist in power systems at ABB Corporate Research, Västerås, Sweden.

Muhamad Reza is married to Novi Ineke Cempaka Wangi and has a son, Muhammad Rifqi Aulia Yahya.